The Role of Temporal Frequency in Continuous Flash Suppression: A case for a unified framework

Shui'Er Han

A thesis submitted in fulfilment of the requirements for the degree of

Doctor of Philosophy (PhD)

Faculty of Science, School of Psychology

University of Sydney

2018

Contents

List of Main Text Figures

List of Tables

Statement of Originality

This is thesis is submitted to the University of Sydney in fulfilment of the requirements for the Degree of Doctor of Philosophy. It is submitted as a thesis by publications, which to my best knowledge, is the product of my own work. I certify that all the assistance received in preparing this thesis and sources have been acknowledged in the text. I hereby declare that I have not submitted this material, either in full or in part, for a degree at this or any other institution.

Shui'Er Han

SYDNEY, August 2018

Authorship Attribution Statement

Chapter 2 of this thesis is published as "*Han, S, Lunghi, C., & Alais, D. (2016). The temporal frequency tuning of continuous flash suppression reveals peak suppression at very low frequencies. Scientific reports, 6, 1-12,* doi: 10.1038/srep35723*"*. In this study, I programmed the experimental tasks and collected the data. I also designed the study and programmed the visual stimuli with my supervisor. Together with my co-authors, I analysed the data and wrote the paper.

Chapter 3 of this thesis is published as "*Han, S, Randolph, B., & Alais, D. (2016). Slow and steady, not fast and furious: slow modulations strengthen continuous flash suppression. Consciousness and Cognition, 58, 10-19,* doi: 10.1016/j.concog.2017.12.007". My contributions to this work were: programming the visual stimuli and experimental tasks, analysing and collecting the data. I also designed the study and wrote the paper with my co-authors.

Chapter 4 of this thesis is published as "*Han, S, & Alais, D. (2017). Strength of continuous flash suppression is optimal when target and masker modulation rates are matched. Journal of Vision, 18(3), 1-14,* doi: 1-/1167/18.3.3". My contributions to this work were: designing the study, programming the experimental tasks, analysing and collecting the data. I programmed the visual stimuli and wrote the paper with my supervisor, who is also a co-author on this paper. All work presented in Chapters 3-5 were performed with approval of the Human Research Ethics Committee, University of Sydney (Ref: 2016/662).

Attest to Authorship Attribution Statement

Student attestation:

I attest that the statements listed in the authorship attribution statement are, to the best of my knowledge, factual and correct.

Name: Shui'Er Han Date: 25/08/18

……

Supervisor attestation:

As supervisor for the candidature upon which this thesis is based, I can confirm that the authorship attribution statements are correct.

Name: Professor David Alais Date: 25/08/18

Acknowledgements

Firstly, I would like to thank my supervisor, Prof. David Alais for supporting my research and for providing guidance when I needed it. Thank you also for supporting my visits to labs overseas, those experiences were invaluable and the many learning opportunities. I learnt a lot from you and I am excited for what lies ahead! I will remember the fun and laughter, and the many Thai lunches in the lab.

Thank you to Prof. Eli Peli and Prof. Randolph Blake for hosting me at your respective labs in 2017! I have learnt a lot about vision prosthetics from Prof. Peli and had a lot of fun times with his lab at the Schepens Eye Research Institute. I am also grateful to Professor Randolph Blake for giving me the confidence to be bold and creative with my work. The camaraderie and support I experienced in Prof. Blake's lab at Vanderbilt University was unforgettable. All these would not be possible, had the University of Sydney not granted me a Grant-in-Aid.

Thank you to the past and present members of the Alais lab, including Emily, Jess, James, Sujin, Huihui, Axel, Tarryn, Raph, Rob, Garry, Jogi and Tam (to name a few!). It has been a fun few years studying sensory perception alongside you. Thank you also to Will, Charlie, Justine, and Aaron. You have been a source of great company and support in times of stress. I am also grateful to Professor Bart Anderson and Professor Alex Holocombe for their valuable feedback on my research!

A big thank-you to my two best friends, Mum and Fiona! Thank you for being a sounding board and a constant source of support throughout my arduous PhD journey. Thank you to Lance, Micheal and the ladies from Silverbelles for being good listeners and great friends! And last but not least, thank you Colin for believing in my crazy ideas. Your company and encouragement has made writing this thesis a lot more fun than it would have been.

Abstract

In continuous flash suppression (CFS), a rapidly changing Mondrian sequence is presented to one eye in order to suppress a static target presented to the other eye. Targets generally remain suppressed for several seconds at a time, contributing to the widespread use of CFS in studies of unconscious visual processes. Nevertheless, the mechanisms underlying CFS suppression remain unclear, complicating its use and the comprehension of results obtained with the technique. As a starting point, this thesis examined the role of temporal frequency in CFS suppression using carefully controlled stimuli generated by Fourier Transform techniques. A low-level stimulus attribute, the choice of temporal frequency allowed us to evaluate the contributions of early visual processes and test the general assumption that fast update rates drive CFS effectiveness. Three psychophysical studies are described in this thesis, starting with the temporal frequency tuning of CFS (Chapter 2), the relationship between the Mondrian pattern and temporal frequency content (Chapter 3), and finally the role of temporal frequency selectivity in CFS (Chapter 4). Contrary to conventional wisdom, the results showed that the suppression of static targets is largely driven by high spatial frequencies and low temporal frequencies. Faster masker rates, on the other hand, worked best with transient targets. Indicative of early, feature selective processes, these findings are reminiscent of binocular rivalry suppression, demonstrating the possible use of a unified framework.

(1556 characters including spaces)

Chapter 1

Introduction

Despite the rich incoming stimulation from the external environment, our daily conscious experience remains a subset of the information at any given time point. For example, numerous activities may occur in your surroundings as you walk down the street, but your attention and awareness may be limited to a few events. Since the unperceived stimuli may contain behaviourally relevant information, questions arise regarding the extent to which the unperceived stimuli are processed and whether or not do they influence behaviour. Over the past decades, scientists have adopted a wide variety of tools to address these questions, often resorting to methods that impair stimulus visibility. Methods include presenting stimuli of interest at far distances (Pillai, 1939), in close temporal arrangement with a masking stimulus (Fowler, Wolford, Slade and Tassinary, 1981) or using brief stimulus presentation times (Adams, 1957; Kunst-Wilson and Zajonc, 1980). Some studies tapped on the properties of visual neglect, presenting the stimulus of interest to neglected fields, where patients do not report awareness of the stimulus (Audet, Bub and Lecours, 1991; Driver and Mattingley, 1998; Vuilleumier et al., 2002).

Among the many methods employed to manipulate visual awareness is dichoptic stimulation. In this technique, a device such as a stereoscope (Carmel, Arcaro, Kastner and Hasson, 2010) is used to present dissimilar images to corresponding regions of the two eyes (Blake, 1995). Images are also typically presented to the central vision, though some studies have expanded the use of dichoptic stimulation into the visual periphery (Blake, O'Shea and Mueller, 1992; Ritchie, Bannerman and Sahraie, 2012). When dissimilar images such as orthogonally oriented gratings are viewed in this manner, one of them will be temporarily

suppressed from visual awareness (e.g., Blake and Logothetis, 2002). This characteristic of dichoptic stimulation has been used to examine the neural concomitants of visual awareness and unconscious visual processing (e.g., Haynes, Deichmann and Rees, 2005; Yuval-Greenberg and Heeger, 2013). Several variations of dichoptic stimulation have also been developed to prolong the period of suppression, one of them being continuous flash suppression (CFS).

Independently discovered by two research groups (Fang and He, 2005; Tsuchiya and Koch, 2005), CFS involves the presentation of a 10 Hz dynamic pattern sequence to one eye and a low contrast, static target to the other eye. Individual patterns could be noise images (as in Fang and He, 2005), but studies typically adopt the patterns used by Tsuchiya and Koch (2005), which are composed of coloured squares organised in a random spatial layout (otherwise known as "Mondrians"). As targets could remain suppressed for several seconds in CFS (Tsuchiya and Koch, 2005), it is no surprise that CFS is widely used in studies of unconscious visual processing (Yang, Brascamp, Kang and Blake, 2014). Using CFS, some studies found shorter suppression durations for native language alphabets, upright, fearful and familiar facial stimuli (Yang, Zald and Blake, 2007; Jiang, Costello and He, 2007; Stein, Sterzer and Peelen, 2012; Gobbini et al., 2013), leading them to conclude that these stimuli have preferential access to visual awareness. Others question the extent to which unperceived stimuli undergo semantic analysis, suggesting that low-level stimulus properties may offer an alternative explanation (Kang, Blake and Woodman, 2012; Moors, Wagemans and de-Wit, 2016; Sakuraba, Sakai, Yamanaka, Yokosawa and Hirayama, 2012; Hedger, Gray, Garner and Adams, 2016).

As with any newly developed technique, it is important to understand its limitations and refine its use. For instance, the strength of CFS suppression could be

comparable between upright and inverted facial stimuli, but the former might produce shorter suppression durations because it is more recognisable. To rule out this possibility, studies have used control tasks where the target stimulus was blended onto the Mondrian pattern sequence (Jiang et al., 2007). The assumption was that if certain target types were processed unconsciously, CFS would produce larger differences in reaction times than the control. This comparison was later found to be inadequate, as the two tasks appear to tap on different perceptual and cognitive processes (Stein, Hebart and Sterzer, 2011). Other outstanding methodological issues are the influence of participant decisional criteria in determining stimulus visibility (Yang et al., 2014), changes in perceptual sensitivity and response criteria over time (Purcell, Stewart and Stanovich, 1983; Yang et al., 2014), and individual differences in CFS effectiveness (e.g., up to 50% of participants were omitted from Sklar, et al. (2012) because of insufficient suppression strength).

Studying the underlying mechanisms of CFS would be the most straightforward manner to improve its use. Previous studies attributed CFS's effectiveness to the transient onsets and offsets of the dynamic pattern sequence (Tsuchiya and Koch, 2005; Tsuchiya, Koch, Gilroy and Blake, 2006), but little attention has been paid to test this assumption. To fill this gap, this thesis investigates the role of temporal frequency in CFS, as varying the temporal frequency content of the Mondrian sequence is an easy way of manipulating the amount of transients presented. To begin, the following sections provide an overview of the CFS technique and two other forms of dichoptic stimulation, namely, binocular rivalry (BR) and flash suppression (FS). Both FS and BR are often compared to CFS (e.g., Tsuchiya et al., 2006), and as will be discussed later in Section 1.5, these comparisons will help define the framework used in this research.

1.1 Binocular rivalry (BR) and its underlying mechanisms

In BR, each eye simultaneously receives an image sufficiently different from the other eye to prevent binocular fusion, e.g., dichoptically presenting a pair of orthogonally oriented gratings. As illustrated in Figure 1.1, both images are also presented in the corresponding spatial locations of each eye. Observations on BR go way back in history, starting from the 16th century when Porta (1953; as cited in Wade 1998) made the first unambiguous demonstration of such interocular competition. Upon presenting separate pages of text to each eye, he made the observation that only a page could be perceived, showing how the input to one eye could dominate perception and suppress the other. However, it was not until the 19th century that systematic studies on binocular rivalry grew in popularity. Using the mirror stereoscope he invented, Sir Charles Wheatstone (1838; cited by Blake, 2005) presented different English letters to each eye, noting that the perception of the letters generally alternated stochastically, although sometimes appeared as a mixture. He found that neither image could be willed into visual awareness, though later studies showed that the exertion of willpower through eye movements could influence the dominance durations of each image (Blake, 2005).

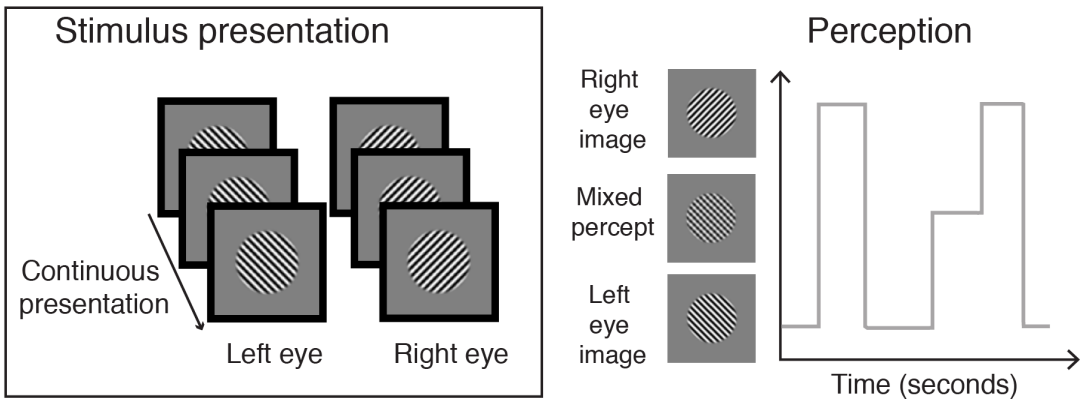

Figure 1.1: Schematic diagram of binocular rivalry (BR). In BR, each eye receives an image dissimilar from the other eye so that binocular fusion is prevented. Images are typically static and presented

continuously throughout the course of an experimental trial. The resulting percept involves an irregular alternation between the two images with occasional mixtures of both images.

Competition between monocular neurons was thought to produce BR. For example, Blake (1989) argued that the primary goal of binocular vision is fusion, in which the slightly disparate images from the two eyes undergo a matching process to form the percept of a single object. Under this view, a successful binocular match results in the stable percept of a single binocular object, whereas mismatches result in reciprocal periods of dominance and suppression of dissimilar features. The competition was thought to depend on the eye of origin; neural activity elicited by the image presented to one eye competed with activity associated with the image presented in the other eye at early visual processing stages such as V1 (e.g., Polonsky, Blake, Braun and Heeger, 2000; Haynes et al., 2005), not between the *concepts, identities or semantic meanings* of the presented images. In support of this account, studies showed that when the images were swapped between the eyes, changes in the resulting percept tended to occur and were typically of the image presented to the dominant eye (Blake, Westendorf, and Overton, 1980; Lee and Blake, 2004). Suppression was also found to operate in local spatial zones; when radial gratings are presented to each eye, focal contrast increments give rise to a rapid perceptual dominance change at the locus of the increment that spreads gradually of perceptual dominance change (Wilson, Blake, Lee, 2001).

Other studies demonstrated competition between two concepts or stimulus identities (i.e., stimulus rivalry). For example, Diaz-Caneja (1928; translated by Alais et al., 2000) divided an image of concentric circles and an image of parallel lines into halves and created composite images from the half of each form. These images were presented in opposite eyes to provoke BR. Instead of perceiving rivalry only between the two composite images, perceptual alternations sometimes occurred between the

whole forms of concentric circles and parallel lines. Similarly, Whittle, Bloor, and Pocock (1968) showed that matching contours could combine across the eyes in BR. These observations also applied to dichoptic patchwork stimuli. Instead of perceiving alternations between dichoptic patchwork stimuli, Kovács, Papathomas, Yang and Fehér (1996) found that perception alternated between coherent patterns. Further demonstrating that the occurrence of rivalry alternations was not limited by the eye of origin, swapping orthogonal gratings at 3 Hz between the eyes did not always lead to rapid perceived changes in orientation, sometimes producing instead similar perceptual alternations as static, fixed presentations of dichoptic stimuli (Logothetis, Leopold and Sheinberg, 1996). Furthermore, studies have found that form and motion were also able to rival or fuse independently of each other (Alais and Parker, 2006; Andrews and Blakemore, 2002).

These observations of stimulus rivalry contradicted previous assumptions of an early, low-level mechanism in BR (Blake, 1989; Blake, 2001; Blake and Wilson, 2011). However, Lee and Blake (1999) found that stimulus rivalry occurred within a limited parameter space. The authors found that swapping sinusoidal gratings between the eyes could only produce stimulus rivalry if the gratings were low contrast, high spatial frequency (> 5 cycles per degree), flickering and swapped between the eyes at rapid rates (e.g., 6 Hz). Later in a 2004 study, the same authors evaluated Kovács et al. (1996)'s findings. They discovered that rivalry between local, eye-based spatial zones occurred during interocular grouping between patchwork dichoptic stimuli. The authors also pointed out that because participants are typically asked to make a binary judgment on the perceptual dominance of rival stimuli, the incidence of reported interocular grouping in patchwork dichoptic stimuli might have depended on the proportion of local spatial zones favouring one image over the other. Thus, the

incidence of stimulus rivalry did not necessarily preclude of influence early visual processes. In fact, stimulus and eye rivalry have been shown to co-exist (Bonneh et al., 2001; Silver and Logothetis, 2007), and it is now agreed that rivalry suppression could involve neural events distributed across multiple levels of visual processing (Blake and Wilson, 2011).

While other studies were focussed on the extent of eye-specific and stimulus-specific influences in BR, some researchers busied themselves with the influence of stimulus properties on rivalry dynamics. As it turns out, this was a necessary line of investigation that would provide information pertinent to the visual pathways involved during rivalry suppression. The early visual system consists of two prominent subcortical parallel pathways, namely the magnocellular (M) and parvocellular (P) pathways, which then form the primary inputs to the cortical dorsal and ventral pathways respectively (Liu et al., 2006). The M/dorsal pathway has a higher contrast sensitivity (Purpura, Kaplan, and Shapley, 1988) and is more responsive to low spatial frequencies, dim illumination and higher temporal frequencies (Derrington and Lennie, 1984; Purpura et al., 1988). This contrasts with the Parvo/ventral pathway (P/ventral), which has a higher spatial resolution, is colour sensitive and more responsive to lower temporal frequencies (Derrington and Lennie, 1984; Hicks, Lee, and Vidyasagar, 1983). As a result of these differences, the Magno/dorsal (M/dorsal) pathway is more suited for global motion perception (Chapman, Hoag, and Giaschi, 2004) whereas the P/ventral pathway is more suited for form, spatial detail and colour discrimination (Livingstone and Hubel, 1988). These differences have also led to the formulation of the dual-stream theory, which associates P/ventral stream with visual awareness and the M/dorsal stream with the

computation of consciously inaccessible information for action preparation (Milner and Goodale, 2008).

Given that BR is frequently used to manipulate visual awareness, it seemed intuitive that the P/ventral pathway would be primarily involved in rivalry suppression. Consistent with this idea, previous research showed that transient dichoptic images (Bower and Haley, 1964) and images of low contrast (Burke, Alais, and Wenderoth, 1999; Liu, Tyler and Schor, 1992) were more likely to fuse. Higher contrast images, on the other hand, were likely to enhance suppression by promoting exclusive perceptual dominance (Hollins, 1980). Rivalry between motion stimuli was found to be due to spatial conflict in the motion stimuli rather than motion conflict *per se*; when each eye was adapted to opposing motion stimuli, no incidence of motion or motion rivalry was observed when both eyes were later presented with the same static grating (Ramachandran, 1991). Raising the temporal frequency of motion stimuli was also linked to a lower incidence of motion rivalry (Carlson and He, 2000), and this was yet again support for a P/ventral bias given the greater M responses to higher temporal frequencies (Derrington and Lennie, 1984). Support on spatial frequency content, however, was less conclusive. For example, Baker and Graf (2009a) found that images with naturalistic properties, e.g., 1/f spatial frequency spectrum and phase aligned high spatial frequencies, dominated over images with less naturalistic properties. These observations contradicted the idea of P/ventral bias in BR, as one would predict that images with greater higher spatial frequency content would dominate in BR.

Another puzzling property of BR is its stochastic perceptual transitions, and several attempts have been made to explain the processes triggering these alternations. One popular theory identifies neural adaptation as the key-contributing

factor. By this view, neurons encoding each image are engaged in reciprocal inhibition, such that processes elicited by one image inhibits processes elicited by the other image. Over time, the neural activity associated with the perceptually dominant image wanes due to adaptation, eventually reversing the balance of activity associated with the other image and triggering a perceptual switch (e.g., Lehky, 1988; McDougall, 1901; Sugie, 1982). Indeed, adaptation has been implicated in several aspects of rivalry dynamics, such as the initial rivalry period (Carter and Cavanagh, 2007) and the respective changes in the contrast sensitivity of rivalling images over time (Alais, Cass, O'Shea, and Blake, 2010). It even accords with both eye-based and stimulus-based accounts, as the adaptation process could arise anywhere along the visual processing hierarchy (Lago-Fernández and Deco, 2002). Nevertheless, despite the bulk of supporting evidence, the explanation does fall short in accounting for the influence of perceptual meaning on rivalry incidence (Andrews and Lotto, 2004) and the effect of emotional valence on perceptual dominance (Alpers and Gerdes, 2007; Alpers and Pauli, 2006; Alpers, Ruhleder, Walz, Muhlberger, and Pauli, 2005).

A more recent idea proposed by Leopold and Logothetis (1999) draws from the notion that visual perception is an inference-like process (Helmholtz, 1924; Knill and Pouget, 2004). Under this theory, alternations in multi-stable stimuli such as BR are not a mere consequence of passive sensory responses such as neural adaptation and reciprocal inhibition. Instead, perceptual alternations result from evaluations and inferences made on the incoming sensory information conflict, also taking into account information from higher order and non-sensory influences. As the evaluation processes could span multiple-levels of the visual hierarchy (Tong, Meng and Blake, 2006), this idea has been successful in accounting for the frontal cortical activations during BR (Knapen, Pearson, Brascamp, van Ee, and Blake, 2008; Lumer, Friston,

and Rees, 1998) and the correlation between mood disorders and perceptual alternations (Pettigrew and Miller, 1998). The idea also does not preclude the effects of neural adaptation (Blake and Wilson, 2011), showing promise as a model for interpreting BR dynamics.

Another explanation attributes BR alternations to neural oscillations. Proposed by Pettigrew (2001), perceptual transitions in rivalry are viewed as a product of clock-like, neural oscillators located in subcortical regions. These oscillators are believed to be susceptible to fluctuations in serotonin levels (Carter et al., 2005; Carter and Pettigrew, 2003) and may even underlie other forms of perceptual bi-stability (Carter and Pettigrew, 2003). For example, these oscillators may underlie bi-stability obtained with optically superimposed monocular stimuli (O'Shea, Parker, La Rooy and Alais, 2009), ambiguous stimuli such as the Necker Cube (Necker, 1832) and so-called "motion-induced blindness", where static stimuli are presented with a moving background (Bonneh, Cooperman, and Sagi, 2001). Suggestive evidence for this account includes positive correlations in alternation rates for various forms of perceptual multi-stability (Carter and Pettigrew, 2003), and behavioural oscillations in several aspects of visual perception (Drewes, Zhu, Wutz, and Melcher, 2015; Tomassini, Spinelli, Jacono, Sandini, and Morrone, 2015). However, more research is needed to confirm its validity and its relation to adaptation and perceptual inference models.

1.2 The Laws of Rivalry

As the research on rivalry mechanisms mushroomed, it became increasingly necessary to summarise the key characteristics of BR. In 1965, Levelt published a seminal monograph describing four governing tenets of BR, which would come to guide later developments and interpretations of empirical research. The goal of this

section is to introduce these propositions in their original characterisation and to provide an update on these key principles. I begin by defining some key terms used in the description of rivalry dynamics (e.g., *alternation rate* and *predominance*). Familiarity with these concepts is important, for they are not only frequently used as dependent measures in most empirical research, but also used in the formulation of BR principles.

To reiterate the perceptual experience during BR, each image of a dissimilar dichoptic pair would be perceived exclusively for a temporary period of time, such as 1-2 seconds, before the other image becomes visible, in an on-going and irregular perceptual alternation between the two images. One way of characterising the competition is to record the *dominance duration,* the period in which an image dominates exclusively (Brascamp, Klink, and Levelt, 2015). Over the course of the viewing time, the image percepts will alternate stochastically, and the histogram of individual dominance periods for a given image can be described by a gamma distribution (Blake and Logothetis, 2002; Logothetis et al., 1996). The *average dominance duration* can be used to represent the characteristics of the distribution (Kang, 2009; Brascamp et al., 2015), though some studies do report the median (e.g., Patel, Stuit, and Blake, 2015). Another way of representing the perceptual dominance of an image is to compute the total proportion of exclusive visibility over the total rivalry viewing time, that is, the *predominance* of an image (Brascamp et al., 2015). Finally, rivalry dynamics are also described by the rate at which the image percepts switch, i.e., the *alternation rate* (Brascamp et al., 2015).

In his original work, Levelt (1965) sought to understand why non-corresponding contours in the eyes produced BR. Defining *stimulus strength* in terms of the contrast and density of pattern contours, Levelt (1965) manipulated luminance

and pattern differences between the eyes and recorded equibrightness judgments. In the first set of experiments, participants were presented with a pair of white disks that contained a concentric circle in both or one of the images. They were asked to adjust the luminance of either the left or right disk, till both disks were of equal brightness. Using the best-fitting curves of the recorded data, Levelt (1965) then computed the relative weights or stimulus strengths of each eye. The results showed that, when only one eye contained a concentric circle, there was a shift in weight or stimulus strength towards the eye. The total sum of weights, however, remained constant. In later experiments, Levelt (1965) presented a homogenous luminance field to one eye and a test disk to the other eye. He varied the size of the test disk and found that although smaller test disks increased in relative stimulus strength, the perceived brightness of the disk remained comparable across different disk sizes. Using these findings, Levelt (1965) then built an account of the perceptual conflict experienced in binocular rivalry, giving rise to the four propositions summarised below:

Table 1: Levelt's Original Propositions

Proposition I	When the stimulus strength is increased in one eye (i.e., increased relative luminance or presence of contour), the predominance of the corresponding image will increase.
Proposition II	Increased stimulus strength in one eye, however, does not affect the average dominance duration of the same eye.
Proposition III	Increasing the stimulus strength in one eye increases the rate of perceptual alternation between the two images.
Proposition IV	The perceptual alternation between the two images also occurs at a faster rate when the stimulus strengths in both eyes are increased.

In a recent review, Brascamp et al. (2015) evaluated these four propositions were evaluated and suggested modifications. To give a brief overview, the first

proposition of Levelt's (1965) monograph has remained largely unchallenged, though a proper conceptualisation of stimulus strength is required. This is because properties that appear to prolong the perceptual dominance in one study may not have the same effect in another. For example, Baker and Graf (2009a) found that images with naturalistic phase spectra dominated over images with randomised phase information. This would suggest that the naturalistic organisation of image contours contributed to stimulus strength, but randomised phase information was found to be more perceptually dominant in multi-Gabor arrangements (Bonneh and Sagi, 1999; Hunt, Mattingley, and Goodhill, 2012).

Unlike the first proposition, the second proposition has been met with mixed results. In its original formulation, the second proposition assumed that only the contralateral stimulus could effect change in an image's dominance duration. This counterintuitive proposal has found support in some studies, which showed no effect on dominance durations when the stimulus strength of the same eye is varied, but significant changes in dominance durations for the contralateral eye (Blake, 1977; Fox and Rasche, 1969; Leopold and Logothetis, 1996; Logothetis et al., 1996; Meng and Tong, 2004). Other studies disputed the claim, demonstrating modest but significant changes in dominance durations when the stimulus strength of the same eye is varied (Bossink et al., 1993; Shiraishi, 1977; Mueller and Blake, 1989; Brascamp et al., 2006). Kang (2009) showed that the discrepancy in results could be partly attributed to stimulus size, as larger stimulus pairs (i.e., 0.8° by 3.2° visual angle) tended to conform to the second proposition whereas smaller stimuli (i.e., 0.8° by 0.8° visual angle) generally increased in average dominance durations with stimulus strength. The reliance on stimulus size could be partly driven by interactions among local spatial zones, as rivalry alternations have been found to synchronise

between two separate spatial zones with similar orientations (Alais, Lorenceau, Arrighi, and Cass, 2006). Another limitation of the original formulation was that it did not consider pairings where one of the stimuli was fixed at a relatively low strength compared to the other. True enough, under these conditions, large changes in dominance durations were found when the strength of the stronger stimulus was varied (Brascamp et al., 2006; Moreno-Bote, Shpiro, Rinzel and Rubin, 2010; Platonov and Goossens, 2013**).** This prompted the revision by Brascamp et al. (2015), who proposed that increasing the relative difference in strengths between the two eyes would primarily serve to increase the average dominance duration of the stronger stimulus.

According to Levelt's third proposition, a larger difference in relative stimulus strength would result in faster perceptual alternations. Assuming that there would be more perceptual switches towards the stronger stimulus, the third proposition offered an explanation of how changes in the predominance of a stimulus (Proposition I) could co-exist with unaffected average dominance durations (Proposition II). However, in light of the revisions to the second proposition, i.e., the stronger stimulus would produce longer dominance durations, Brascamp et al. (2015) suggested that raising the difference in stimulus strength between the two eyes would slow down perceptual alternations. This modification to the third proposition would predict peak alternation rates when both stimuli are matched in strength, which has been corroborated empirically (Moreno-Bote et al., 2010). Note, however, that the incidence of mixed percepts may produce a deviation in results, producing no change in alternation rate despite larger interocular differences in stimulus strength. The same issue applies to the fourth proposition. Although it is currently well supported by many studies (e.g., Brascamp et al., 2006; Buckthought et al., 2008; Kang, 2009;

Meng and Tong, 2004; Platonov and Goossens, 2013), the neglect of mixed percepts is problematic, given its relevance to rivalry dynamics. Brascamp et al. (2015) thus recommends including the incidence of mixed percepts in future computations of alternation rates, and it is encouraging that investigative work on mixed percepts has already begun (e.g., see the effect of shared stimulus complexity on rivalry coherence in Alais and Melcher, 2007). Further study would only reveal better ways to evaluate alternation rates, and further improve the predictive power of the third and fourth propositions. Another potential limitation to the fourth proposition is the possibility of a reverse relationship at very low stimulus strengths. Predicted by computational models (Brascamp et al., 2015; Seely and Chow, 2011), there is some support for this prediction (e.g., Platonov and Goossens, 2013) that calls for further research. The following presents the four propositions again. Modifications by Brascamp et al. (2015) are indicated with an asterisk (*).

Table 2: Modified Propositions

Proposition I	Remains the same as the Levelt (1965) formulation.
Proposition II*	Increasing the difference in stimulus strengths between the two eyes increases the average dominance duration of the stronger stimulus.
Proposition III*	Raising the difference in strengths between the two eyes slows the alternation rate.
Proposition IV*	Increasing the strength of stimuli in both eyes while keeping them equivalent to each other increases the alternation rate, but the trend may operate in a reverse direction at near-threshold stimulus strengths.

1.3 FS and its underlying mechanisms

Similar to BR, FS involves the presentation of dichoptic images. Discovered by McDougall in 1901, the FS procedure begins with the monocular presentation of one image in the pair of dichoptic images for a brief period of time e.g., 1 second (Wolfe, 1984), and is replaced by a short interval where no stimuli are presented to

both eyes. The first and second images are then abruptly introduced, leading to the forced dominance of the second image (Tsuchiya et al., 2006; Wolfe, 1984). This guarantees that the first percept experienced in the dichoptic period would be of the new image, allowing finer control over the perceived image than BR, in which the initially dominant image is usually unpredictable. However, the forced dominance does not last long; the stochastic alternations observed in BR resume over a second or so (Kreiman, Fried, and Koch, 2005).

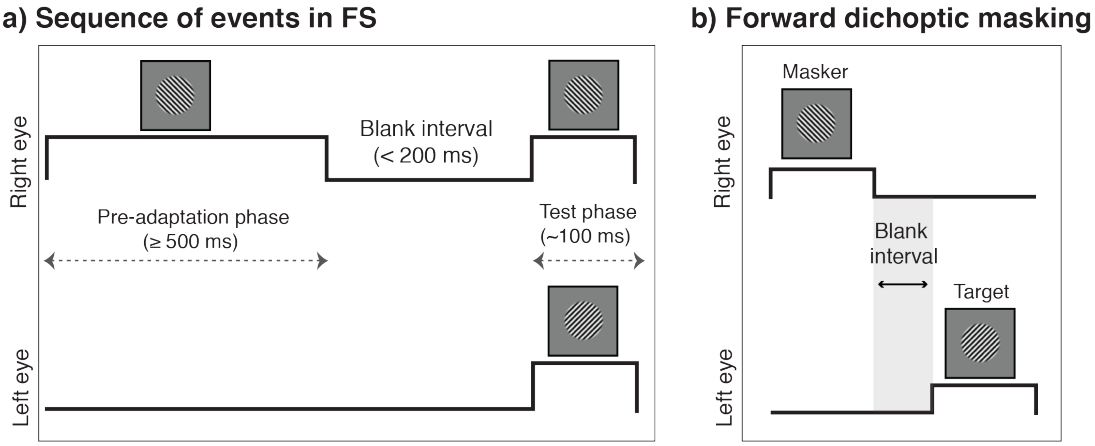

Figure 1.2: Schematic diagrams of flash suppression (FS) and forward dichoptic masking. (a) In FS, one eye receives an image for a brief period of time (e.g., 1 second) before the second image is abruptly introduced to the other eye in the test phase. This causes the pre-adapted image to be suppressed from visual awareness. In some instances, FS may be conducted with a blank interval between the pre-adaptation and test phase (as shown), but it is not necessary. Figure produced using the findings of Wolfe (1984). (b) Unlike FS, dichoptic masking does not require a pre-adaptation phase. This is illustrated in the sequence of events in forward dichoptic masking, where the masker briefly precedes and impairs the visibility of the target image. Short intervals between the masker and target are typically used to suppress the target effectively (Enns and Di Lollo, 2000).

In dichoptic masking, the sensitivity to a transient, monocular image is impaired by briefly presenting an incompatible image to the contralateral eye (Legge, 1979). Given the presentation schedule of FS, it is tempting to classify it as a form of dichoptic masking. However, three key differences between these two methods argue against this assumption. Firstly, FS requires at least 150 ms of monocular presentation

to be effective (Wolfe, 1984), but this is not required in dichoptic masking (Figure 1.2). Secondly, although the effectiveness of dichoptic masking and FS both vary with temporal parameters such as target duration and inter-stimulus interval (Brussell and Favreau, 1977; Enns and Di Lollo, 2000; Hellige, Walsh, Lawrence, and Prasse, 1979; Wolfe, 1984), there is more flexibility in FS. For example, prolonged target durations would impair masking effectiveness (Brussell and Favreau, 1977), but FS is still effective between 500 ms and 1000 ms dichoptic image presentations after the onset of the second image (Wolfe, 1984). Finally, FS is not dependent on the luminance, orientation, or spatial frequency of the monocular image (Wolfe, 1984), meaning that light adaptation and other forms of masking (e.g., forward masking, pattern masking) cannot solely account for FS. In contrast, the effect of masking is enhanced by spatial edges (Macknik, Martinez-conde, and Haglund, 2000).

Instead, some properties of FS are reminiscent of rivalry suppression. For example, Wolfe (1984) showed that the minimum monocular presentation period (i.e., 150 ms) required for effective FS coincided with the minimum presentation duration required for a pair of dichoptic images to engage in BR. In addition, although FS has a greater depth of suppression than BR (Tsuchiya et al., 2006), its suppression effectiveness could be explained by BR observations. In FS, the monocular presentation of the first image needs to sufficiently long, which accords with neural adaptation accounts of BR (e.g., Lehky, 1988). Being presented for a substantial amount of time, activity corresponding to the first image might have started waning due to adaptation, allowing the second image to dominate perceptually. This advantage could be further bolstered by the subsequent brief presentations of the first and second images, as transients have been shown to promote perceptual dominance in BR (Blake, Westendorf, and Fox, 1980). The similarities between FS and BR have

also been observed at physiological and behavioural levels. Not only do both paradigms elicit similar patterns of neuronal responses in the inferotemporal visual cortex of the macaque brain (Sheinberg and Logothetis, 1997), but they also implicate early visual processing (e.g., Tong and Engel, 2001; Wilke, Logothetis and Leopold, 2006). Psychophysically, Wilke, Logothetis and Leopold (2003) found an effect of target surround in a form of FS (i.e., generalised flash suppression), which accords with observations in BR (Paffen, Alais and Verstraten, 2006; Paffen, Alais and Verstraten, 2005; Paffen, te Pas, Kanai, van der Smagt and Verstraten, 2004).

1.4 CFS and its underlying mechanisms

As aforementioned, CFS is generally produced when a high contrast, dynamic Mondrian pattern sequence (the masker) and a static low contrast target are simultaneously presented to different eyes (Tsuchiya and Koch, 2005; see also Figure 1.3). It is an effective form of interocular suppression that combines the benefits of both FS and BR. Like FS, CFS reduces the uncertainty of the first percept, but its effectiveness does not depend on the pre-adaptation of the image to-be-suppressed. Little is known about the underlying mechanisms of CFS, though previous studies often attribute its effectiveness to the rapid pattern changes in the Mondrian sequence (Tsuchiya and Koch, 2005; Tsuchiya et al., 2006; Yang and Blake, 2012). For example, Tsuchiya and Koch (2005) viewed CFS as a combination of BR and FS processes, proposing that each pattern change resets the Mondrian's period of dominance. The authors also argued against the proposition that CFS is a form of potent BR, pointing out that CFS violates Levelt's (1965) second proposition of BR. In a later study, Tsuchiya et al. (2006) thought that CFS is an accumulation of FS processes (Tsuchiya et al., 2006). The authors argued further against a pure BR account, citing the disproportionately large depth of suppression compared to BR, and

the correspondence between the peak Mondrian update rates (i.e., around 3-10 Hz; Tsuchiya and Koch, 2005) and required pre-adaptation period in FS (i.e., ~ 150 ms; Wolfe, 1984).

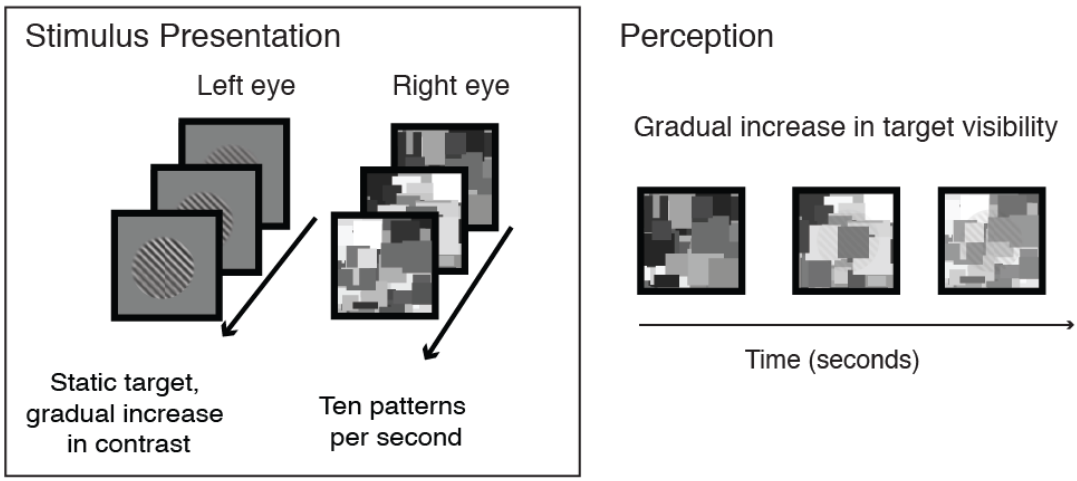

Figure 1.3: Schematic diagram of Continuous Flash Suppression (CFS). In CFS, a static target of lower visual contrast is typically presented with a dynamic sequence of Mondrian patterns. This produces an effective and long lasting suppression where the target gradually increases in visibility over several seconds. Unlike BR, the first percept is always of the Mondrian sequence. CFS also contrasts from FS, as it does not require pre-adaptation of the target.

Whilst there might be common processes between CFS and FS, the arguments against a BR account remain inadequate. First, the effectiveness of FS depends critically on the pre-adaptation phase (Wolfe, 1984), whereas CFS is typically conducted *without* pre-adaptation. It is therefore difficult to imagine how FS processes could be accumulated in CFS, and how optimal Mondrian refresh rates could relate to FS pre-adaptation periods. Second, the violation of Levelt's (1965) second proposition does not serve as a strong argument against a BR account, as it has been challenged by recent studies (e.g., Brascamp et al., 2006; Kang, 2009; see also Section 2.3.1 for more details). The more recent, revised proposition is that the stronger stimulus of a dichoptic pair would produce longer average dominance durations as its strength increases (Brascamp et al., 2015). This has been observed in

CFS, where raising the visual contrast of the mask increased suppression durations (Tsuchiya and Koch, 2005). Lastly, given the similarities between FS and BR (e.g., Sheinberg and Logothetis, 1997; see also Section 2.4), it is difficult to justify the substantial involvement of FS processes while rejecting a BR account. In fact, recent evidence revealed several similarities between CFS and BR. Studies show that both paradigms are feature selective (Moors, Wagemans, and De-Wit, 2014; Stuit, Cass, Paffem and Alais, 2009; Yang and Blake, 2012), work better with spatial edges (Baker and Graf, 2009a; Maehara, Huang, and Hess, 2009) and higher visual contrast (Hollins, 1980; Tsuchiya and Koch, 2005), and have a small but significant serial dependency effect (van Ee, 2009; Moors, Stein, Wagemans, and van Ee, 2015a).

1.5 The framework of this research

Testing the importance of transients in CFS, as is the goal of this thesis, could provide insight into the relationship among CFS, BR and FS. However, due to the scope of this thesis, I will only focus on the mechanisms of CFS and how it relates to BR. This is because, compared to FS, BR has a longer and better-documented body of work that could provide a framework for evaluating CFS mechanisms. In addition, given the similarities between BR and CFS, it would be interesting to see if observations in CFS could be explained by BR mechanisms. Table 3 below summarises some stimulus properties that affect BR and CFS suppression. In sum, high spatial frequencies and high contrast appear to enhance CFS and BR suppression, suggesting a P/ventral pathway bias (Derrington and Lennie, 1984; Shapley, 1990; Green et al., 2009). However, this preference is less consistent in CFS, as the nominal 10 Hz Mondrian refresh rate is more likely to elicit responses from the M/dorsal pathway than the P/ventral pathway (Derrington and Lennie, 1984). I will

evaluate this discrepancy with our empirical findings on temporal frequency in the General Discussion (Chapter 5).

Table 3: Some factors that influence BR and CFS suppression

Factors	BR	CFS
Spatial frequency	Enhanced by phase-aligned high spatial frequency, e.g., images with naturalistic edges have a greater predominance (e.g., Baker and Graf, 2009).	Image contours are capable of cross-channel suppression (Maehara et al. 2009).
Temporal frequency	Lower incidence of rivalry at high frequencies (Wolfe, 1983), but transients reset perceptual dominance temporarily (Blake et al., 1990).	10 Hz nominal refresh rate, but optimal rates do vary with target type (Kaunitz et al., 2014).
Relative visual contrast	Enhanced by higher contrast, e.g., average dominance durations increase with contrast when the stimuli are small (Kang, 2009).	Not systematically studied, but suppression durations tend to increase with contrast (Tsuchiya and Koch, 2005).
Feature selectivity	Enhanced when rivalling stimuli share similar features e.g., higher contrast thresholds when rivalling stimuli share similar orientations (Stuit et al., 2009).	Stronger suppression with similar spatial frequencies (Yang and Blake, 2012) and speeds (Moors et al., 2014).

1.6 Manipulating temporal frequency

Manipulating temporal frequency is a straightforward way to evaluate the importance of transients in CFS. Strictly speaking, temporal frequency is defined as the number of events occurring per second. I arrive at two possible methods of manipulating temporal frequency. The first has been examined by previous studies, and it involves varying the number of Mondrian patterns per second (Tsuchiya and Koch, 2005; Zhu, Drewes, and Melcher, 2016). The second method manipulates temporal frequency in terms of periodic luminance changes per second, and has not been systematically studied in the CFS literature. This is surprising, as varying the number of pattern changes could be a coarse method of varying retinal illumination. Since each pattern is randomly sampled, not all pixels will be subjected to the same magnitude of luminance change per pattern update and there may not even be luminance alternations from one image to the next. This makes it difficult to equate the same Mondrian refresh rate across studies and different pattern sampling methods.

Using temporal frequency affords much greater control, and therefore more accurate inference of underlying mechanisms.

In this thesis I adopted the second method of manipulating of temporal frequency, as a periodic modulation. Although the magnitude of luminance change between patterns might not matter in a randomly sampled stimulus like the Mondrian masker, both methods cannot be equated without a proof of concept. Another motivation for adopting the second method was that it allowed us to understand refresh rate choices in CFS. As shown in Table 3, the nominal 10 Hz refresh rate in CFS contrasted with the low temporal frequency preference in BR, which was curious given the similarities between the two paradigms (e.g., Moors et al., 2014; Stuit et al., 2009; Yang and Blake, 2012). Using a different method of temporal frequency manipulation was a straightforward way of verifying the existence of this discrepancy between CFS and BR.

1.7 Thesis outline

Three empirical studies are presented in this thesis, each presented in their published formats. To preview, Chapter 2 examined the temporal frequency tuning of CFS using temporally narrowband filtered noise maskers. This revealed a low temporal frequency peak in suppression durations, which was evaluated and replicated by Chapter 3 using temporally filtered Mondrian maskers. Since static targets were used in Chapters 2-3, Chapter 4 asked if the enhanced CFS suppression observed with lower temporal frequency maskers was a consequence of temporal frequency selectivity. This hypothesis was tested with temporally narrowband filtered noise targets and maskers and indeed, CFS suppression was found to be temporally selective. The implications of these results were discussed in the General Discussion (Chapter 5) and all Supplementary materials were presented in Chapter 6.

Chapter 2

The temporal frequency tuning of continuous flash suppression reveals peak suppression at very low frequencies

The work in this chapter is published as:
Han, S, Lunghi, C., & Alais, D. (2016). The temporal frequency tuning of continuous flash suppression reveals peak suppression at very low frequencies. *Scientific reports*, 6, 1-12, doi: 10.1038/srep35723.

Individual data are accessible at: https://doi.org/10.17605/OSF.IO/R5JEV

Abstract

Continuous flash suppression (CFS) is a psychophysical technique where a rapidly changing Mondrian pattern viewed by one eye suppresses the target in the other eye for several seconds. Despite the widespread use of CFS to study unconscious visual processes, the temporal tuning of CFS suppression is currently unknown. In the present study we used spatiotemporally filtered dynamic noise as masking stimuli to probe the temporal characteristics of CFS. Surprisingly, we find that suppression in CFS peaks very prominently at approximately 1 Hz, well below the rates typically used in CFS studies (10 Hz or more). As well as a strong bias to low temporal frequencies, CFS suppression is greater for high spatial frequencies and increases with increasing masker contrast, indicating involvement of parvocellular/ventral mechanisms in the suppression process. These results are reminiscent of binocular rivalry, and unifies two phenomenon previously thought to require different explanations.

2.1 Introduction

The recent couple of decades has seen a great deal of research activity aimed at elucidating the extent to which visual processing can occur outside of conscious awareness. Several approaches have been used including binocular rivalry (Alais and Blake, 2005; Arnold and Quinn, 2010) and various kinds of masking (Kim and Blake, 2005). More recently a new approach known as continuous flash suppression (CFS) has become very popular since it first appeared (Tsuchiya and Koch, 2005; Yang and Blake, 2012; Yang et al., 2014). Like binocular rivalry, it involves presentation of irreconcilable images to each eye which prevents binocular fusion and triggers suppression of one eye's image. In the case of CFS, one eye receives a sequence of dynamic 'Mondrian' images updated typically at a rate of 10 Hz which reliably suppresses a target image of low to moderate contrast in the other eye (Fig 1a). The main appeal of CFS is that it provides a very strong and long-lasting suppression and the initial percept is reliably the dynamic masker. In contrast, binocular rivalry typically involves two dichoptic static images, which perceptually alternate in a stochastic manner. This allows easy study of visual processing in the suppressed eye and has seen CFS rapidly become the standard tool for investigating visual processing outside of awareness (Tsuchiya et al., 2006; Yang et al., 2007; Yang and Blake, 2012).

The mechanisms underlying CFS are not well understood and it is not clear why the dynamic Mondrian pattern provides such strong masking. This has not stopped many CFS studies from publishing bold claims about what kinds of information are processed in the absence of conscious awareness, including: preferential access to awareness for alphabets from native languages, upright, fearful and familiar facial stimuli, and reduced aftereffects specific to early stimulus properties (Tsuchiya and

Koch, 2005; Yang et al., 2007; Jiang et al., 2007; Stein et al., 2012; Gobbini et al., 2013). Nevertheless, these findings have not been found to be robust (Hedger, Adams and Garner, 2015; Hesselmann, Darcy, Sterzer and Knops, 2015; Moors, Wagemans and de-Wit, 2016) and differ from those obtained using binocular rivalry which generally show that images presented to the suppressed eye undergo very little processing (Zimba and Blake, 1983; Cave, Blake and McNamara, 1998; Blake and Logothetis, 2002; Kang et al., 2012). This difference is curious given that CFS is often presumed to be a form of interocular suppression, like binocular rivalry.

A better understanding of the mechanisms of CFS suppression is needed to clarify the role of interocular suppression and possible links between CFS and binocular rivalry. This is all the more important because of the strong theoretical implications of claims about images that are imperceptible nonetheless undergoing visual processing and reaching awareness. A clear understanding of the suppressive mechanisms involved and appropriate stimulus control are critically important in validly drawing such conclusions. As a starting point, we investigate the temporal frequency tuning of CFS using temporally narrow-band maskers, a dimension that has not been systematically studied previously. Although previous studies have examined the effect of varying Mondrian refresh rates (Tsuchiya and Koch, 2005; Zhu et al., 2016), frequency analyses show that the spectrum is consistently broadband and low-pass (Figure 2.1 c-d). Consistent with these observations, we find that masker suppression – when tested with narrowband temporal modulations – peaks very prominently at approximately 1 Hz, well below the 10–15 Hz refresh rates typically used in CFS studies (Xu, Zhang and Geng, 2011; Kaunitz, Fracasso, Skujevskis and Melcher, 2014; Faivre and Koch, 2014).

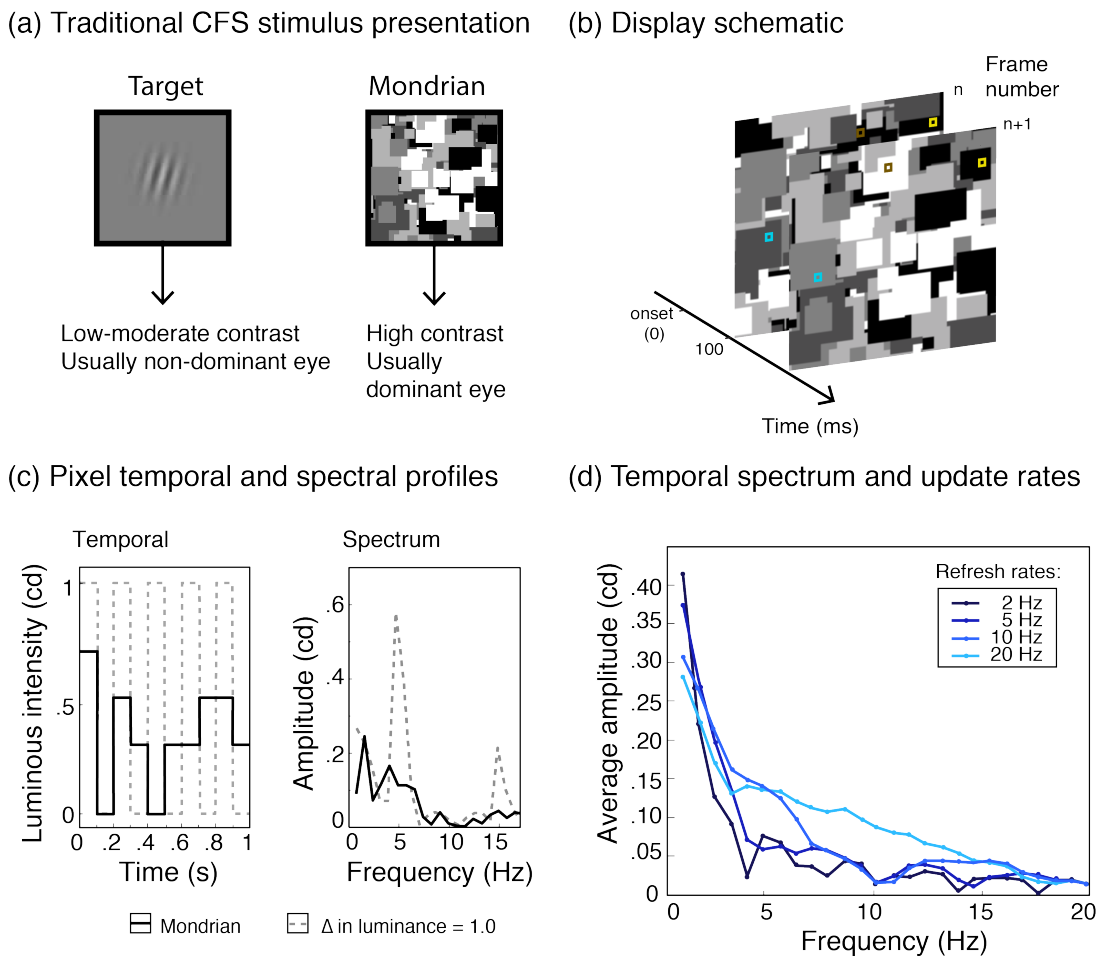

Figure 2.1. (a) Traditional CFS involves a dynamic Mondrian composed of randomly positioned shapes varying in size and luminance presented usually to the dominant eye and a smaller target to the other. Targets may be natural images or simple stimuli. (b) Dynamic Mondrians are commonly updated at 10 Hz by presenting new patterns every 100 ms. Because the grey levels of the Mondrian shapes vary randomly, some undergo large luminance changes between patterns (brown squares) whereas others change little or not at all (blue and yellow squares, respectively). Statistically, over a sequence of frames, the latter is much more likely, and this lengthens the period of the modulation and thus lowers the frequency. (c) Even if strong alternations did occur between the extreme luminance values, a 10 Hz Mondrian update rate would produce a 5 Hz square-wave modulation (grey dashed line, left) with a peak at 5 Hz and lesser peaks at the odd harmonics (grey dashed line, right). The actual waveform, however, is inevitably complex with low frequency components due the presence of multiple grey levels (here, $n = 5$) and non-uniform changes over time (black solid line, left). Consequently, the temporal spectrum is broader with a concentration of energy at frequencies much lower than the intended update rate (black solid line, right). (d) To demonstrate the low-frequency bias, we tracked the pixel timelines of 70 grayscale Mondrian patterns updated at 2, 5, 10 and 20 Hz (randomly sampling from 5 grey levels, 200 pixels each refresh rate), then Fourier transformed the data. The resultant amplitude spectra for all refresh rates have a very strong low-pass profile. For the typical 10 Hz Mondrian, only 1.3 % of total stimulus energy occurs at 10 Hz and the peak frequency occurs at 1 Hz, which has more than 20 times the energy (31 %) of the 10 Hz component. Raising the Mondrian update rate does little to boost high-frequency content and the strongly lowpass profile remains. Indeed, as the functions decline with frequency, they could be well described as temporal “pink noise”.

2.2 Results

2.2.1 Experiment 1

We examined the effect of temporal frequency in narrowband maskers (1 octave full-width at half-height; see also Figure 2.2b) on CFS suppression duration. Temporal frequencies were centred at rates of 0, 0.375, 0.75, 1.5, 3, 6.25, 12.5 and 25 Hz. Data were analysed in a one-way (masker temporal frequency) repeated-measures ANOVA. The effect of masker frequency was highly significant, with $F(6, 72)=17.5$, $p< .0001$, $\eta_p^2=0.59$, and results are plotted in Figure 2.3a as normalized suppression duration in a semilog plot. Consistent with the frequency spectrum of the Mondrian, suppression was much stronger at low than at high frequencies, yet the pattern follows a bandpass tuning that was well described by a Gaussian normal function. The Gaussian was fitted using a maximum likelihood routine with three free parameters: mean, standard deviation and vertical offset. Amplitude was not a free parameter and was defined as the maximum normalised suppression duration minus the baseline. The best-fitting Gaussians had the following parameters: mean = 0.97 Hz (SD = 0.48), standard deviation = 1.42 octaves (SD = 0.63), baseline = 0.44 (SD= 0.20) and amplitude = 1.52 (SD = 0.59).

To contrast the effect of masking temporal frequency with the static masker we binned the temporal frequency data into two categories of low and high frequency maskers. From Figure 2.3a, it is clear that 0.375, 0.75, 1.5 and 3 Hz fall within the same passband whereas the remaining frequencies, 6.25, 12.5 and 25 Hz, do not. This accords with previous research that estimated a broad, lowpass channel below 5 Hz and bandpass channel (>6 to 20 Hz) in human vision (Anderson and Burr, 1985; Cass and Alais, 2006). We therefore binned 0.375, 0.75, 1.5 and 3 Hz together as 'low frequency' and the remaining masker frequencies were defined as 'high frequency'.

Figure 2.3b shows the mean normalised suppression durations for the low and high masker temporal frequencies and the static control. A two-tailed paired *t*-test revealed that slow modulating maskers produced significantly larger normalised suppression durations than the static control, $t(12)= 3.38$, $p<.01$, confirming what is clear from the tuning function plotted in Figure 2.3a. Interestingly, fast modulating maskers were less effective than a static mask, producing shorter suppression durations than the static control, $t(12)= 3.53$, $p<.01$.

To validate the relevance of these trends to the CFS literature, we compared the peak raw suppression durations with that of a standard 10 Hz Mondrian masker (Stein et al., 2011). To obtain the peak suppression duration of each participant, a Gaussian normal function was first fitted to the raw data with amplitude as an additional free parameter. Peak suppression duration was then computed by summating the fitted amplitude and baseline. As depicted in Figure 2.3c, two tailed independent t-tests revealed that the most effective low frequency masker was comparable to the 10 Hz Mondrian masker, $t(23)= -0.28$, $p =.78$, $d = 0.12$. To further assess the performance of the filtered noise maskers, we computed the within-subject variability in raw suppression durations for low and high frequency bins and compared the results with that of the 10 Hz Mondrian. Two tailed independent t-tests revealed less variable raw durations for the low and high frequency noise maskers, $t(23)= 2.26$, $p<.05$, $d = 0.94$ and $t(23) = 4.35$, $p<.001$, $d = 1.81$ respectively, demonstrating a methodological advantage with filtered noise maskers.

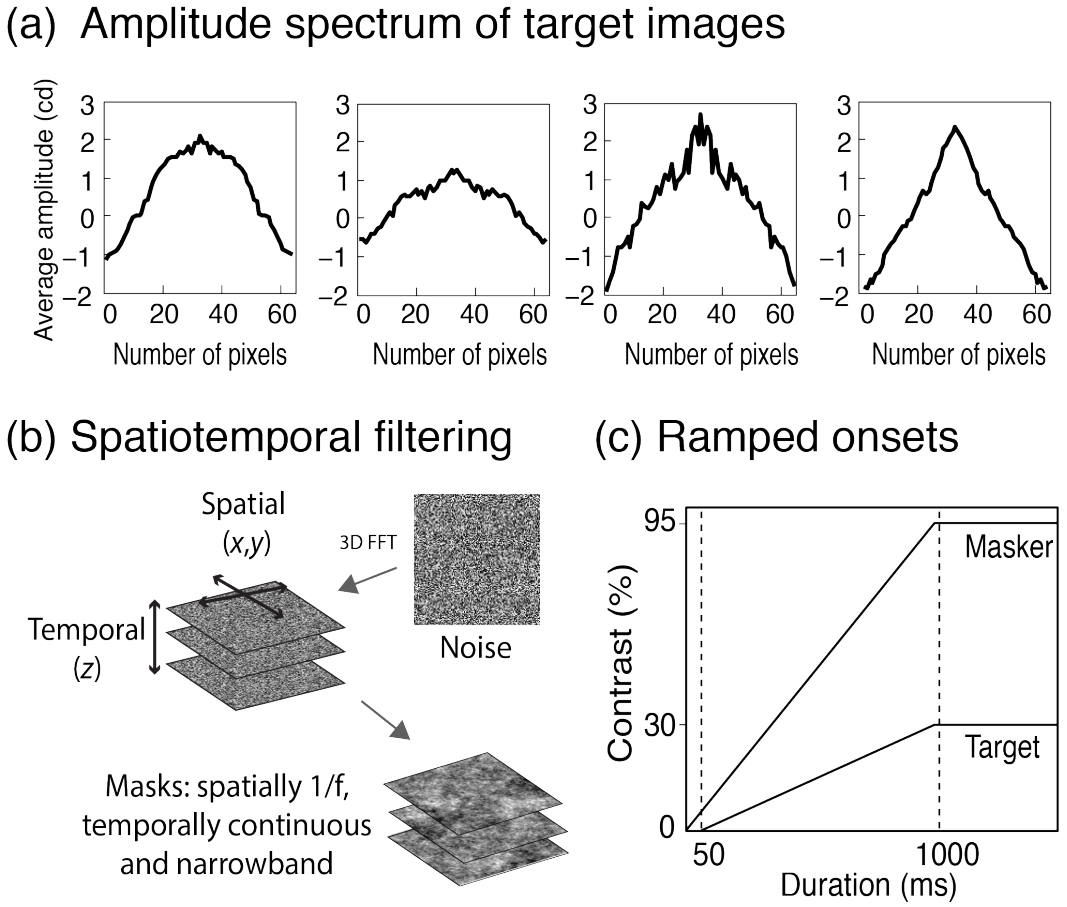

Figure 2.2. (a) Amplitude spectrum of target images: For comparability with previous studies, we used four greyscale natural images in Experiment 1. To select an appropriate masker, these images were first analysed with a two-dimensional FFT. The results reveal a 1/f spatial profile for each of the target images, thus maskers were given a 1/f amplitude spectrum. (b) Spatiotemporal filtering: A three-dimensional FFT was first computed for a stack of 205 randomly generated noise images. Filtering the z-axis with a log-Gaussian filter controlled masker temporal frequency, whereas individual noise images (x and y axes) were convolved with a circularly symmetric inverse frequency filter for spatial frequency. The resultant stimulus was temporally narrowband, continuously modulating pink noise. (c) Ramped onsets: To avoid abrupt transients, both masker and targets were ramped up to their maximum contrast over a period of 1000 ms and the masker preceded the target by 50 ms to allow cumulative suppressive effects.

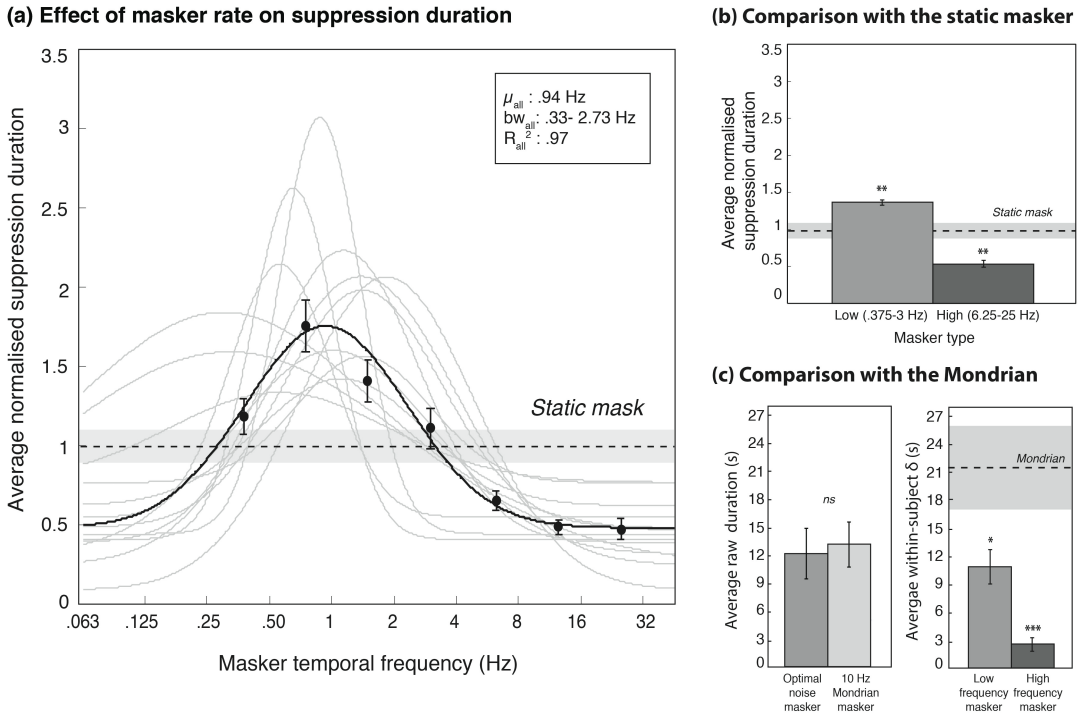

Figure 2.3. (a) Data from Experiment 1 showing suppression duration as a function of masker temporal frequency, with frequency plotted on a base 2 logarithmic scale. Maskers were dynamic noise stimuli filtered in the time dimension into narrow temporal frequency passbands. The data show CFS suppression duration is strongly dependent on temporal frequency, with maximum suppression for low temporal frequency maskers. The data pattern is consistent across all observers (grey traces) and is distinctly bandpass, not lowpass. With temporal frequency plotted on an octave scale (i.e., base 2 logarithm), the pattern is very well described by a Gaussian normal function. The best fit to the group data (solid black line: $R^2 = 0.97$) has a peak at 0.94 Hz and a standard deviation of 1.42 octaves. Peak suppression frequency for individual participants ranged from 0.30–1.85 Hz. (b) The data binned into low (0.375, 0.75, 1.5, 3 Hz) and high (6.25, 12.5 25 Hz) temporal frequencies, contrasted against a static noise masker (dashed line with shaded error bar) shows faster maskers resulted in significantly lower suppression durations than the static condition. (c) Raw data analyses comparing group averages and standard deviations for filtered noise maskers with a standard 10 Hz Mondrian. Peak suppression durations estimated from fitted Gaussian functions ('optimal noise masker') were comparable to the Mondrian, with the added advantage of lower within-subject variability, as demonstrated by the significantly lower variance in low and high frequency maskers compared to the Mondrian. These results demonstrate the applicability of narrowband filtered noise maskers for studying CFS temporal frequency processes. Asterisks denote statistical significance (*: $p < .05$, **: $p < .01$, ***: $p < .001$) after Holm-Bonferonni correction for multiple comparisons. Error bars represent ±1 standard error of the mean.

2.2.2 Experiment 2

We measured the temporal contrast sensitivity function for our temporally filtered masking stimuli to determine whether the peak suppression at low temporal frequencies was simply a manifestation of the tuning towards low temporal frequencies in human vision. Human contrast sensitivity to temporal frequency shows

a lowpass bias (Kelly, 1979) and is in general more sensitive to contrast changes at lower temporal frequencies with a corner frequency at around 8–10 Hz (Tolhurst and Movshon, 1975; Merigan and Maunsell, 1993). As these observations were made with narrow-band (sinusoidal) modulations of sinusoidal gratings, we wanted to establish the temporal contrast sensitivity function for our masker stimuli, which differ considerably to these classical stimuli in being spatially broadband noise patterns with an inverse frequency spectrum and having a temporal modulation bandwidth of one octave.

Absolute and increment contrast thresholds were measured for our masker stimuli and performance was compared using a Wilcoxon Signed-Ranks test. This revealed the resulting temporal contrast sensitivities for the two measures did not differ significantly (Z= 1.26, p= .21) and thus the sensitivity curves were combined and averaged for each participant. The group-averaged temporal sensitivity function is plotted in Figure 2.4. A one-way, repeated-measures ANOVA and revealed a significant effect of temporal frequency, $F(6, 54)= 37.4$, $p< .0001$, $\eta_p^2= 0.81$. The data were further explored using trend analyses up to third order and were found to exhibit a strong quadratic and a significant cubic trend, $F(1, 9)= 228.6$, $p< .0001$, $\eta_p^2= 0.96$, $F(1, 9)= 45.7$, $p< .001$, $\eta_p^2= 0.84$, respectively, but no significant linear trend, $p > 0.05$.

To compare the temporal contrast sensitivity function with the temporal frequency suppression tuning observed in Experiment 1, we conducted a two-way ANOVA with the factors being temporal frequency and task type (normalised suppression durations vs. normalised contrast sensitivity values). The main effect of temporal frequency was significant, $F(6, 126)= 25.2$, $p< .0001$, $\eta_p^2= 0.55$ as was the main effect of task type, $F(1, 21)= 146$, $p< .0001$, $\eta_p^2= 0.87$. The important result was

that temporal frequency interacted significantly with task, $F(6, 126)=21$, $p< .001$, $\eta_p^2= 0.5$, showing that temporal contrast sensitivity does not explain the temporal tuning in Experiment 1. As indicated in Figure 2.4, pairwise contrasts (Holm-Bonferroni corrected) showed the significant interaction was due to lower CFS suppression durations at 6.25 and 12.5 Hz, *average difference* = -1.66, and -1.07, t =-10.3 and -11 respectively, $p < 0.001$, and higher suppression durations at 0.375 and .75 Hz, *average difference* = .22, $t= 1.55$, $p< .01$ and *average difference* = .28, $t= 1.47$, $p< .05$ respectively.

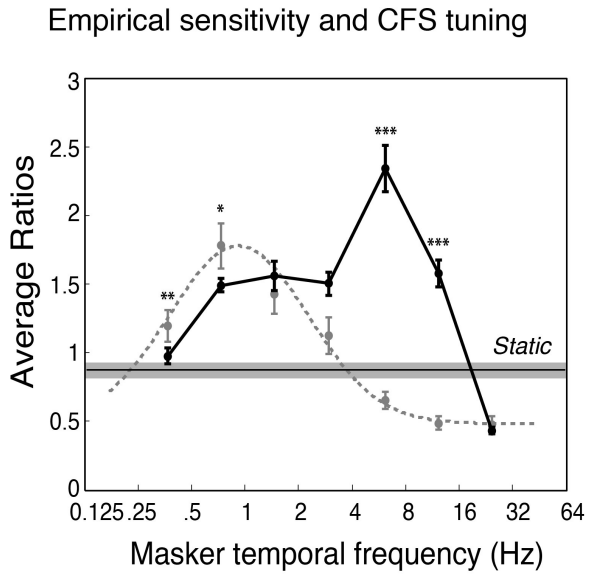

Figure 2.4. Data from Experiment 2. The solid black line shows temporal frequency sensitivity as measured in Experiment 2 to modulating noise patterns with a 1/f spatial frequency spectrum. For comparison, the suppression duration data from Experiment 1 together with the best-fitting function are replotted (dashed line). Temporal frequency is plotted on a base 2 logarithmic scale. The two datasets exhibit very different patterns and indicate that temporal contrast sensitivity cannot explain the temporal tuning of CFS suppression. Asterisks denote statistically significant differences between contrast sensitivity and suppression duration trends using independent samples t-tests, after Holm-Bonferonni correction (* = $p< .05$, **= $p< .01$, ***= $p< .001$). Error bars show ±1 standard errors of the mean.

2.2.3 Experiment 3

The confirmation that CFS suppression peaks at a very low temporal frequency is very informative as it suggests the involvement of the parvocellular pathway (Mishkin and Ungerleider and Macko, 1983; Ungerleider and Haxby, 1994)

in CFS suppression. Neurons in this pathway are most sensitive to low temporal frequencies (Derrington and Lennie, 1984; Livingstone and Hubel, 1988; Solomon, White and Martin, 1999) and high spatial frequencies, peaking around 6–10 cpd (Derrington and Lennie, 1984; Merigan and Maunsell, 1993). Interocular suppression in binocular rivalry is also thought to have a parvocellular basis (Livingstone and Hubel, 1988; Ramachandran, 1991; He, Carlson and Chen, 2005). Experiment 3 tested whether CFS suppression exhibits a bias for high spatial frequencies by comparing suppression durations for targets of low (1 cpd) and high (10 cpd) spatial frequency using the same masking stimuli as in Experiment 1. As these maskers have a 1/f spatial frequency profile, they produce equivalent neural response to all spatial frequencies which ensures the two spatial frequency conditions are comparable.

The results of Experiment 3 are plotted in Figure 2.5 and were analysed in a within-subjects, two-way (masker temporal frequency x spatial frequency) repeated-measures ANOVA. There were significant main effects for masker temporal frequency, $F(6, 66)=14.2$, $p< .0001$, $\eta_p^2= 0.56$, and target spatial frequency, $F(1, 66)=39.3$, $p< .0001$, $\eta_p^2= 0.78$. As expected, there was a significant interaction between masker temporal frequency and target spatial frequency, $F(6, 66)=8.4$, $p< .01$, $\eta_p^2= 0.43$. Pairwise comparisons with Holm-Bonferroni corrections demonstrated greater suppression durations for high spatial frequency targets at every level of temporal frequency (see Table 4 for statistical details).

As in Experiment 1, Gaussian distributions were fitted to the group mean data (Figure 2.5a) and to individual subjects' data. Two participants' data were excluded because all suppression times were uniform for the low spatial frequency condition and the Gaussian could not be meaningfully fitted. For the 10 remaining participants the parameters for the best-fitting individual Gaussians were compared across the two

levels of spatial frequency using Holm-Bonferroni corrected paired t-tests (see Table 2 for details). No significant differences were found for the Gaussian mean, standard deviation or baseline elevation, but a large and significant difference was obtained for amplitude, with high spatial frequency targets exhibiting longer suppression durations, $t(9) = 4.57$, $p < .01$, consistent with high spatial frequencies selectively activating CFS suppression mechanisms.

To contrast temporally modulating and static maskers, we binned temporal frequency into low and high frequency groups (as in Experiment 1) and compared them against the static masker, for both levels of spatial frequency (Figure 2.5b). The data for high spatial frequencies replicated the pattern observed in Experiment 1 (Figure 2.3b): slow modulating maskers produced significantly higher suppression durations than a static masker, $t(11) = 2.88$, $p < .05$ and fast modulating maskers produced significantly lower suppression durations, $t(11) = 3.98$, $p < .01$. For low spatial frequency targets, suppression duration was significantly lower with fast modulating maskers compared to static maskers, $t(11) = 4.13$, $p < .01$, but there was no significant difference between static and slow modulating maskers, $t(11) = .03$, $p = .98$. These comparisons are summarised in Figures 2.5b.

Table 4: Holm-Bonferroni corrected paired-sample tests in Experiment 3

Masker frequency (Hz)	1 cpd	10 cpd	t-statistic	*df*	*p* value
.375	0.66 (*SD*=0.28)	1.65 (*SD*=0.76)	3.63	11	< .05
.75	.78 (*SD*=0.30)	2.27 (*SD* =0.80)	5.87	11	< .0001
1.5	.70 (*SD*= 0.26)	2.29 (*SD*= 1.38)	3.61	11	< .01
3	0.63 (*SD*=0.17)	1.51 (*SD*=0.65)	4.15	11	< .05
6.25	0.54 (*SD*=0.26)	0.84 (*SD*= 0.30)	4.42	11	< .01
12.5	0.47 (*SD*=0.20)	0.65 (*SD*=0.26)	3.87	11	< .05
25	0.47 (*SD*=0.18)	0.55 (*SD*= 0.18)	3.20	11	< .01

Table 5: Parameter estimates for Experiment 3

Parameter	1 cpd	10 cpd	t-statistic	*df*	*p* value
Amplitude	0.38 (*SD*=0.19)	2.38 (*SD*=1.35)	4.46	9	< .01
Peak frequency (Hz)	.99 (*SD*=0.50)	.95 (*SD* =0.42)	.99	9	.86
Width (octaves)	1.33 (*SD*= 0.90)	1.53 (*SD*= 0.54)	.86	9	1.0
Baseline	0.43 (*SD*=0.20)	0.50 (*SD*=0.25)	2.05	9	.67
R^2	0.85 (*SD*=0.18)	0.92 (*SD*= 0.09)	1.21	9	.40

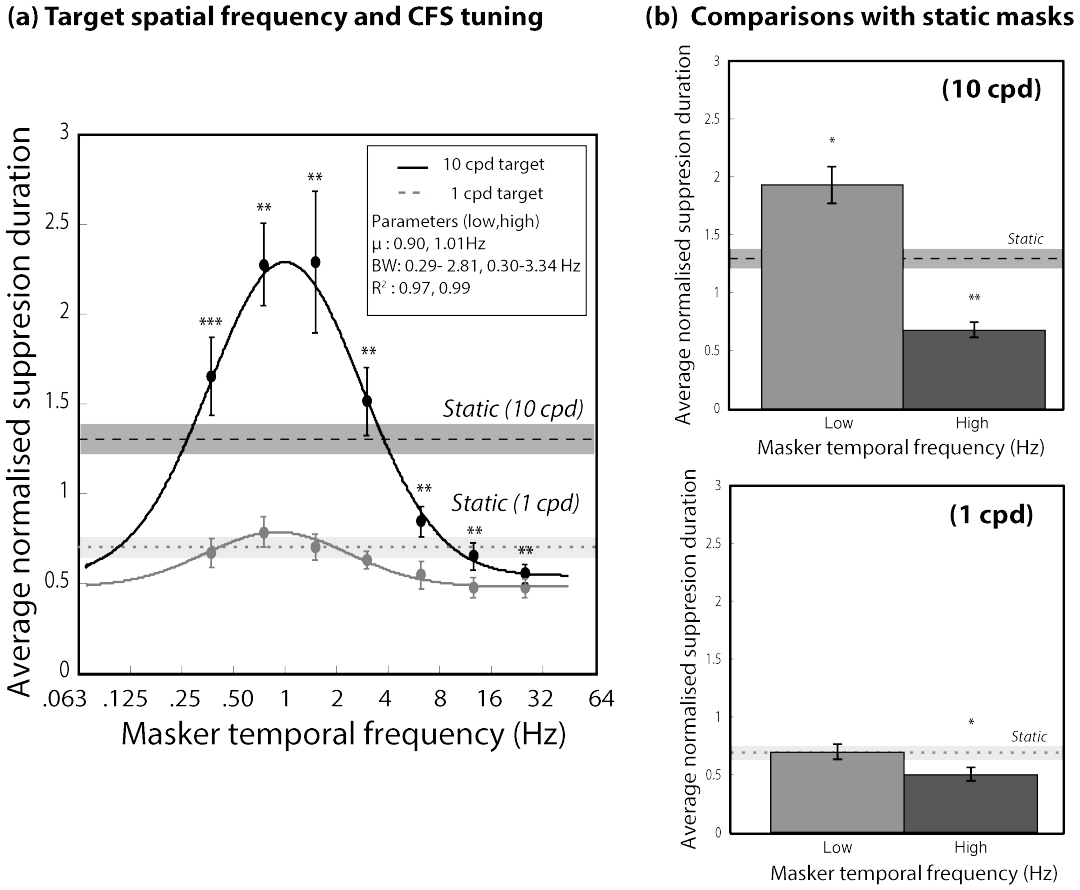

Figure 2.5. Data from Experiment 3. (a) Suppression duration as a function of masker temporal frequency and target spatial frequency. The suppressed target was either high spatial frequency (10 cpd, black line) or low spatial frequency (1 cpd, grey dashed line). Targets of 10 cpd were very strongly suppressed and showed a clear bandpass relationship over masker temporal frequency. Targets of 1 cpd showed significantly less suppression and were almost uniform over temporal frequency. The best-fitting Gaussians had similar peak frequencies and standard deviations for both low and high spatial frequencies: mean = 0.77 and 1.08 Hz, and standard deviation = 1.16 and 1.17 octaves, respectively. (b) Results for 10 and 1 cpd targets (upper and lower plots respectively), with low and high temporal frequencies contrasted against a static noise masker. Similar to Experiment 1, low frequency maskers suppressed 10 cpd targets for longer periods, and high frequency maskers for shorter periods, than the static condition. In contrast, low frequency maskers did not effectively suppress low spatial frequencies relative to a static masker, although faster maskers were found again to produce shorter suppression durations than the static condition. Asterisks denote statistical significance (*: $p < .05$, **: $p < .01$, ***: $p < .001$) after Holm-Bonferroni correction. Error bars represent ±1 standard errors of the mean.

2.2.4 Experiment 4

As well as being tuned to low temporal and high spatial frequencies, another characteristic of parvocellular processes is their contrast sensitivity. While the magnocellular contrast response function rises steeply but saturates early at around

20–30 % contrast, the parvocellular contrast response function exhibits a steady and non-saturating increase (Shapley, 1990; Green et al., 2009). Experiment 4 tested the effect of masker contrast at three levels (30, 50 and 90 %) on suppression duration, for masker modulation rates of 2 and 10 Hz. If the low temporal frequency bias in suppression durations seen in Experiment 1 is due to the involvement of parvocellular mechanisms in CFS suppression, a slow modulating masker should produce gradually increasing suppression durations as masker contrast increases, with no saturating plateau. A two-way (masker temporal frequency x masker contrast), repeated-measures ANOVA was run on the normalized data. Masker temporal frequency and masker contrast interacted significantly, $F(2,22)= 7.06$, $p< .05$ $\eta_p^2= 0.39$. The interaction was due to significantly greater suppression durations for the 2 Hz masker compared to 10 Hz across different contrast levels (Figure 2.6b). The differences between masker rates were compared with Holm-Bonferroni corrected t-tests and were significant across all contrast levels, $t(11) = 7.05$, $p<.001$, $t(11) = 3.30$, $p<.01$, $t(11) = 3.71$, $p<.01$, in ascending order of contrast. Separate analyses for each masker frequency showed a significant main effect of masker contrast for the 2 Hz masker, $F(2,22) = 10.85$, $p<.001$, $\eta_p^2= 0.50$, but not for the 10 Hz masker, $F(2,22) = 0.81$, $p= .41$, $\eta_p^2= 0.07$. For the slow modulating masker, suppression durations followed a significant increasing linear trend, $F(1,11)=15.7$, $p<.01$, $\eta_p^2= 0.59$.

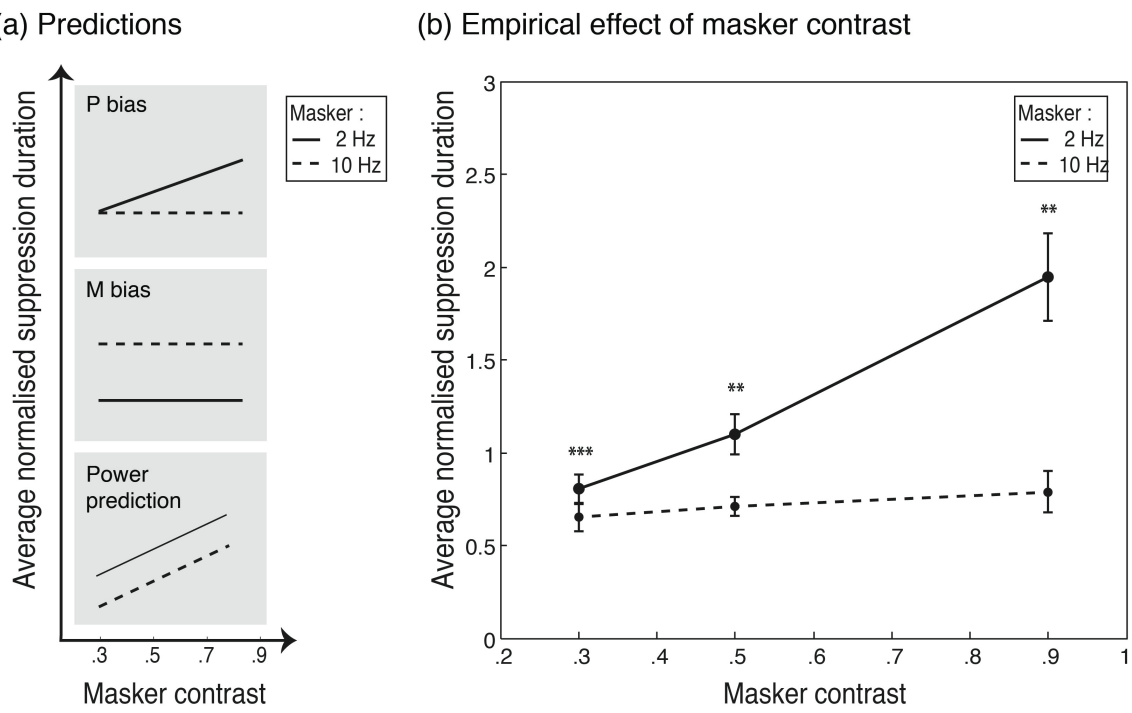

Figure 2.6. Predictions of contrast effect and results from Experiment 4. (a) If CFS is parvocellular biased, we predict no increase in suppression duration across contrast for 10 Hz maskers as they elicit magnocellular responses which saturate by 30 % contrast. By contrast, suppression duration should rise gradually for 2 Hz maskers as parvocellular responses rise monotonically with contrast. A magnocellular bias will show no contrast effect, with 10 Hz consistently a more effective masker than 2 Hz. If CFS suppression shows neither bias, increasing contrast should increase masker power and monotonically increase suppression durations for both masker rates, with low more effective than high frequency. (b) Suppression duration as a function of masker contrast and temporal frequency. Consistent with a parvocellular bias, increasing masker contrast increased suppression duration, but only for the 2 Hz maskers. Paired-samples t-tests show significantly greater suppression for 2 Hz relative to 10 Hz maskers across all contrast levels. Asterisks denote statistical significance (**: $p < .01$, ***: $p < .001$) after Holm-Bonferroni correction. Error bars represent ±1 standard errors of the mean.

2.3 Discussion

CFS is widely used to study unconscious processing of visual images suppressed from awareness yet little is known about the suppression process and appropriate stimulus control is lacking. We used spatiotemporally filtered dynamic noise sequences to reveal the temporal frequency tuning of CFS. Surprisingly, given the widespread use of Mondrian flicker rates in the range of 10–15 Hz, the temporal tuning peaks at about 1 Hz and is clearly bandpass, with suppression declining on either side of the peak – particularly on upper side. Indeed, maskers modulating at a typical CFS rate of 12.5

Hz provided very weak suppression and were less effective than a static noise image. Complementing the observed low-temporal-frequency bias, CFS suppression was stronger for high-spatial-frequency targets and increased monotonically with masker contrast.

The key to our stimulus is that it is narrowband. Even though a modulation of 1 Hz is quite slow, our stimulus modulated smoothly to provide uniform masking over time, in contrast to the discrete modulation of a dynamic Mondrian which is intermittently updated. Some studies have compared various Mondrian update rates (Tsuchiya and Koch, 2005; Zhu et al., 2016) but this is not equivalent to manipulating temporal frequency in a pattern that varies randomly in luminance between updates. The reason is simply that the typical presentation time of each Mondrian pattern i.e., 100 ms lengthens the period of modulation, producing a slower alternating waveform than intended. Moreover, given that the probability of maximal luminance alternations between successive updates is very low (i.e., n^{-10} for ten successive patterns with n fixed grey levels), power inevitably concentrates at lower temporal frequencies. This is illustrated in Figure 2.1c-d, where several very different flicker rates produce very similar frequency profiles, all concentrated at very low frequencies, with only a small fraction of the temporal energy present at the nominal flicker frequency. Even in the unlikely case that the stimulus alternated between the extreme luminance values from frame to frame, for example at a typical Mondrian rate of 10 Hz, this would create a square-wave modulation with a peak frequency at half the nominal flicker rate, that is, at 5 Hz. Here, by using spatiotemporally filtered noise as maskers we gain full and independent control over the spatial and temporal dimensions, without significant loss of suppressive strength despite the loss of contours and edges (Maehara et al., 2009; Baker and Graf, 2009a) (Figure 2.3c). This

accords with evidence showing effective suppression in CFS by low-pass filtered Mondrians[5], broad tuning functions for Mondrian refresh rates (Zhu et al., 2016) and robust suppression in binocular rivalry with filtered noise (Ling and Blake, 2010; Lunghi, Morrone and Alais, 2014). Moreover, our results advance previous work with broadband stimuli (Yang and Blake, 2012; Maehara et al., 2009) in characterising the nature of the mechanisms underlying CFS.

The stimulus tunings we report for CFS are consistent with a suppression process dominated by input from the parvocellular/ventral pathway. The parvocellular and the magnocelluar pathways are the two major paths from retina to cortex. They are well segregated up to V1 and after some interaction in early cortex, these subcortical paths project with a bias to the two major cortical pathways: parvo to the ventral stream and magno to the dorsal stream (DeYoe and Van Essen, 1988). Consistent with the selectivity we report for CFS suppression, parvo/ventral neurons are tuned to low temporal frequency, high spatial frequency (Merigan and Maunsell, 1993; Derrington and Lennie, 1984) and the contrast response function has a steady and non-saturating increase with contrast (Shapely, 1990; Green et al., 2009). By contrast, magno/dorsal neurons are tuned to high temporal and low spatial frequency stimuli, rising steeply with contrast but saturating early at around 20–30 % contrast (Mishkin et al., 1983; Ungerleider and Haxby, 1994). The finding that CFS suppression has a bandpass temporal tuning centred at a very low frequency, tuned to high spatial frequency and gains steadily in strength with increasing contrast suggests the involvement of the parvocellular pathway.

Our findings help clarify the CFS literature, which has been overly concerned with the rapid flicker in CFS maskers when seeking to explain CFS suppression. CFS suppression with flickering Mondrians has been described as driven by a continued

barrage of transients (Tsuchiya et al., 2006), which may also reduce the retinotopic neural adaptation in the masking eye (Tsuchiya and Koch, 2005; Yang and Blake, 2012). According to this interpretation, higher Mondrian refresh rates are therefore required to generate more transients and to reduce retinotopic adaptation. While flicker will certainly generate transients, and might attenuate retinotopic adaptation, this is clearly secondary. By far the biggest component of CFS suppression comes from low temporal frequencies, which are overwhelmingly the largest components in the temporal frequency spectrum of a flickering Mondrian (Figure 2.1d). This analysis alone suggests that CFS suppression is likely driven most strongly by maskers modulating at low temporal frequency, a observation that tallies with evidence showing the dominance of natural stimulus properties in rivalry (Alais and Melcher, 2007; Baker and Graf, 2009a). Our results confirm this, and together with the spatial frequency and contrast findings, suggest that the parvocellular/ventral pathway will be critical for an explanation of CFS suppression.

The likely involvement of parvocellular/ventral mechanisms in CFS links suppression in CFS more closely with binocular rivalry suppression – which is also thought to have a parvocellular/ventral bias (Tolhurst and Movshon, 1975; Kelly, 1979; Mishkin et al., 1983; Derrington and Lennie, 1984; Anderson and Burr, 1985; Livingstone and Hubel, 1988; Ramachandran, 1991; Merigan and Maunsell, 1993; Ungerleider and Haxby, 1994; Solomon et al., 1999). Binocular rivalry studies have shown that motion information can be integrated across two eyes even while they engage in colour and form rivalry (Carney, Shadlen and Switkes, 1987; Carlson and He, 2000; Andrews and Blakemore, 2002; Moors et al., 2014), suggesting no suppression of conflicting monocular motion signals. Thus both CFS and binocular rivalry suppression likely involve parvocellular/ventral mechanisms. This is

parsimonious at a theoretical level as both involve interocular suppression and unifies two phenomenon previously thought to require different explanations[7]. Moreover, it provides a possible framework for studying CFS, a proposition that is also supported by similar contributing factors (e.g., feature selectivity) (Maehara et al., 2009; Yang and Blake, 2012; Moors et al., 2014) to both types of suppression. The one obvious difference is that CFS and binocular rivalry produce vastly different perceptual experiences, as unlike binocular rivalry, perception in CFS does not alternate between the competing images[4]. A straightforward explanation of this could simply be that CFS involves a great imbalance of stimulus strength between the two eyes and perception follows the strongest image. This is true in binocular rivalry, where a contrast imbalance between the images will bias dominance to the stronger image and, notably, CFS studies invariably use a high-contrast masker and a target of low-to-moderate contrast. Consistent with this idea, we showed in Experiment 4 that raising CFS masker contrast did prolong masker dominance (Figure 2.6).

The current study mapped the temporal tuning of CFS suppression with temporally narrowband maskers. Our results revealed a low, bandpass temporal frequency tuning function that becomes more pronounced for high target spatial frequencies and increasing masker contrast. Similar to binocular rivalry (Livingstone and Hubel, 1988; Solomon et al., 1999; Ramachandran, 1991; He et al., 2005), these results indicate a parvocellular/ventral pathway involvement in CFS, opening up explanatory accounts of CFS to the more widely modelled phenomenon of binocular rivalry (Lehky, 1988; Blake, 1989; Mueller, 1990; Laing and Chow, 2002; Freeman, 2005; Alais et al., 2010). Our results also show that CFS is not simply a convenient method for suppressing visual awareness. Instead, it is a paradigm highly sensitive to the spatiotemporal properties of a stimulus and inappropriate stimulus control could

weaken suppression, increase the impact of response biases and demand characteristics and complicates the type of conclusions that can be drawn from it (Blake, Brascamp and Heeger, 2014; Hesselmann and Moors, 2015; Hedger et al., 2016). The use of spatiotemporally filtered noise is one way to provide proper stimulus control, and thus possesses a methodological advantage in uncovering the characteristics of CFS suppression. Future psychophysical and imaging studies using spatiotemporally filtered dynamic noise will further elucidate the neuronal processes underlying CFS.

2.4 Methods

2.4.1 Participants

All participants were drawn from a pool of undergraduate students at the University of Sydney studying second or third year psychology courses and were reimbursed $AU20 per hour for their participation. All had normal or corrected-to-normal eyesight. Participants also had normal stereovision, assessed using the Fly Stereo Acuity test. Experiments accorded with the Declaration of Helsinki and were approved by the University's Human Research Ethics Committee. Informed consent was also obtained from all participants. Samples were as follows:- Experiment 1: Author SH plus twelve naive observers (age range: 18–30 years, *SD*=4.19 years, 10 females) completed the task with filtered noise maskers whereas twelve naive observers (range: 19–30 years of age, *SD*= 4.33 years of age, 9 females) were presented with the Mondrian; Experiment 2: Author SH plus nine naive observers (range: 19–29 years of age, *SD*= 4.28 years of age, 8 females); Experiment 3: Twelve naive observers (range: 19–30 years of age, *SD*= 3.75 years of age, 8 females); Experiment 4: Twelve naive observers (range: 19–30 years of age, *SD*= 4.33 years of age, 9 females).

2.4.2 Experiment 1

Masker stimuli: Masking stimuli were spatiotemporally narrowband, created by filtering 205 randomly generated noise images (each 128 x 128 pixels, approximately 5.4° by 5.4°). The stack of noise images was first converted to the frequency domain using a three-dimensional Fast Fourier Transform (FFT), before applying spatial and temporal filters. Spatially, each noise image was given a 1/f amplitude spectrum since our targets were natural images that have a 1/f amplitude spectrum[57] (see also spatial spectrum of target images in Figure 2.2a). In the temporal dimension, a log-Gaussian filter with a full bandwidth of one octave was used to sample temporal frequency into narrow passbands. The peak frequency was varied to sample temporal passbands of 0.375, 0.75, 1.5, 3, 6.25, 12.5 and 25 Hz. The filtered three-dimensional spectrum was then inversed transformed, resulting in a temporally narrowband, continuously varying pink noise stimulus as opposed to the discrete presentation of the Mondrian. As a control, static maskers were also used (a single noise image with 1/f spatial spectrum, randomly sampled every trial from the stack of 205 noise images). All noise images were normalised to maximum contrast (15 % RMS) and a mean luminance spatial average. As an additional validation control, a standard 10 Hz Mondrian masker[38] was used. Each pattern contained 265 squares of 0, 30, 50, 70 or 100 % luminance that also varied in size from 0.52° to 1.30° in length. The Mondrian masker was presented in a similar fashion as the noise maskers and had the same dimensions (i.e., 5.4° by 5.4°), with the exception that the patterns were updated every 100 ms. All maskers were presented at 95% of maximum contrast.

Target stimuli: For compatibility with previous studies, we used static natural images as targets (a total of four, including two images of man-made objects). Image categories were chosen to be as inclusive as possible, only excluding categories that

are reportedly preferentially processed (e.g., faces) (Yang et al., 2007; Sakuraba et al., 2012). Without deeper understanding of preferential processing in CFS, this approach allowed us to keep the categories simple and task difficulty at a reasonable level. Image boundaries were smoothed with a two-dimensional Gaussian kernel with a standard deviation of 1.5 pixels. Targets were 2° by 2° in size and were presented at 30 % of maximum contrast in one of four quadrants within a 5.4° by 5.4° area to the suppressed area. Target location within each quadrant was jittered with 1° steps from trial to trial to reduce predictability and local adaptation.

To ensure stable fusion of the left- and right-eye images, dichoptic targets and maskers were each surrounded by a checkerboard frame 0.5° thick measuring 5.9° by 5.9° externally and 5.4° by 5.4° internally. To avoid abrupt transients, the contrast of the maskers and targets gradually ramped up to the specified magnitude during the initial 1000 ms of each trial (Fig. 2c). The masker was presented 50 ms before the target to allow for the accumulation of suppressive effects from successive flashes (Yang et al., 2014). All visual stimuli were presented via a DATAPixx video processor on a Mitsubishi Diamond Pro 2070SB CRT monitor with linearised luminance output at a screen refresh rate of 100 Hz and with 16-bit contrast resolution.

Procedure: Participants viewed the dichoptic stimuli through a mirror stereoscope, which was individually adjusted to achieve stable fusion. During a trial, participants fixated a central cross while the target and masker ramped up over 1 s to their specified contrast and waited until the target emerged. Their task was to indicate, as accurate as possible, the quadrant where the target was located. After each trial, the time required for the target to reach visibility (suppression duration) was recorded, followed by 5 seconds of binocularly presented white noise to mitigate afterimages

and adaptation effects. Each participant completed an average of 20 trials (10 trials per eye) for each masker temporal frequency, the order of which was randomised across participants. Presentation of target and masker was also randomised across dominant and non-dominant eyes to mitigate adaptation effects. To familiarise participants with the task demands, targets were presented at 60 % of maximum contrast before the experimental task. For each masker frequency, suppression durations were computed by averaging the suppression durations for which the target quadrant was correctly identified. Any outliers larger than three times the median absolute deviation from the median were excluded. Each participant's data were then normalised to their respective average durations across all masker temporal frequencies. The grand average per temporal frequency was then computed across all participants.

2.4.3 Experiment 2

Stimuli: Contrast detection and increment thresholds over temporal frequency were measured using the same masker patterns used in Experiment 1 except they were spatially windowed by a two-dimensional Gaussian function (SD_{xy}= 10 pixels), reducing the patterns to approximately 2° by 2° in size. These were monocularly presented (counterbalanced across eyes) 1.3° to the left or right of a central fixation cross within the same checkerboard frame as in Experiment 1. Targets were presented for 1 second, followed by 300 ms of visual white noise.

Procedure: Participants first completed the detection threshold task followed by incremental thresholds measured with the standard stimuli presented at 2.5 times the absolute threshold. Their task was to indicate target location (left or right of fixation) in the detection task or the target with the higher contrast in the discrimination task. Each participant completed 32 trials per masker temporal

frequency (16 per eye) with the order counterbalanced across participants. An adaptive staircase was used to vary contrast (QUEST) and thresholds were defined as the contrast at which responses were 75 % accurate. To obtain a detection sensitivity curve, each participant's thresholds were normalised to the respective average and then converted to the reciprocal value. Sensitivity curves for the increment task were computed from the just noticeable difference (JND) for each temporal frequency which were normalised to each participant's average and converted to the reciprocal.

2.4.4 Experiment 3

Stimuli: As for Experiment 1 except that target stimuli were filtered into low spatial frequency (1 cpd) and high spatial frequency (10 cpd) components by convolving the target images with a log-Gaussian spatial filter with a 1-octave bandwidth.

Procedure: As for Experiment 1 except that participants completed 16 trials per masker temporal frequency (8 trials per eye) in each spatial frequency condition, indicating the quadrant containing the target as soon as it became visible.

2.4.5 Experiment 4

Stimuli: Maskers were generated as in the previous experiments but only 2 levels of temporal frequency were compared: 2 and 10 Hz. Target stimuli were as in Experiment 1, presented at 25 % of the maximum contrast while three levels of masker contrast were compared: 30, 50 and 90 % of the maximum.

Procedure: Sixteen trials per masker temporal frequency (8 trials per eye) were presented, the frequency order and eye of presentation were counterbalanced across participants. Task and data analysis as in Experiments 1 and 3.

2.5 Chapter review

The effectiveness of CFS is typically attributed to the rapid pattern changes in the Mondrian masker. This widespread opinion is surprising, as little attention has been paid to examine its validity. In Chapter 2, I evaluated the importance of transients in CFS by varying the temporal frequency of CFS maskers. Temporal frequency was defined as periodic changes in luminance per second, as opposed to the more common definition, the number of patterns per second. Narrowband filtered noise maskers were used to control for the spatiotemporal content, and the results revealed a low temporal frequency bias. In addition, the peak at low temporal frequencies was further enhanced when high spatial frequency targets were used, suggesting a parvocellular bias reminiscent of BR. Thus, the results argued against the overarching importance of transients in CFS and demonstrated that the two definitions of temporal frequency were not equivalent. However, as CFS is usually conducted with contour-rich Mondrian patterns, the noise maskers used in this study might not provide an accurate reflection of CFS's temporal tuning. In the following study, I tested the hypothesis that a similar low temporal frequency bias could be observed in manipulations with intact Mondrian pattern structures.

Chapter 3

Slow and steady, not fast and furious: slow modulations strengthen continuous flash suppression

The work in this chapter is published as:
Han, S, Randolph, B., & Alais, D. (2016). Slow and steady, not fast and furious: slow modulations strengthen continuous flash suppression. *Consciousness and Cognition*, 58, 10-19, doi: 10.1016/j.concog.2017.12.007.

Individual data are accessible at: https://data.mendeley.com/datasets/29ygc3jzw6/1

Abstract

Continuous flash suppression (CFS) involves the presentation of a rapidly changing Mondrian sequence to one eye and a static target in the other eye. Targets presented in this manner remain suppressed for several seconds at a time, and this has seen the prevalent use of CFS in studies of unconscious visual processes. However, the mechanisms behind CFS remain unclear, complicating its use and the comprehension of results obtained with the paradigm. For example, some studies report observations indicative of faster, visual masking processes whereas others suggest slower, rivalry processes. To reconcile this discrepancy, this study investigates the effect of temporal frequency content and Mondrian pattern structure on CFS suppression. Our results show predominant influences of spatial edges and low temporal-frequency content, which are similar to binocular rivalry, affording a parsimonious alternative in unifying the two paradigms.

3.1 Introduction

Understanding the extent to which visual stimuli falling outside of conscious awareness remain effective in visual processing constitutes a key theme in psychology

and neuroscience research. Among the wide variety of tools used to suppress images from visual awareness (Alais and Blake, 2005; Breitmeyer, 2014; Kim and Blake, 2005), continuous flash suppression (CFS) has emerged as one of the most effective. In CFS, a dynamic sequence of complex, geometric images presented to one eye at a typical rate of 10 Hz can suppress a static target viewed by the other eye for many seconds at a time (Tsuchiya and Koch, 2005; Tsuchiya et al., 2006). Similar to binocular rivalry, CFS relies on neural inhibition, triggered when irreconcilable monocular images are viewed dichoptically. Yet, unlike rivalry, the dissimilar monocular images employed to create CFS tend not to alternate frequently, and the initial percept is reliably the dynamic masking pattern which can remain exclusively dominant for remarkably long durations. The reliability and potency of CFS enable easy study of unconscious visual processes, resulting in the frequent use of these Mondrian masking patterns in evaluating the potency of cross-modal and higher-order influences on processing of unconscious stimuli (Fang and He, 2005; Jiang et al., 2007; Kido and Makioka, 2013; Lunghi et al., 2017; Moors et al., 2015b).

Whilst these developments in unconscious perception research are intriguing, the stimulus factors governing the Mondrian masker's potency remain poorly understood. This is concerning, because conclusions drawn from CFS may be driven by factors such as insufficiently rigorous awareness measures and poorly masked stimulus features (Hedger et al., 2016). Indeed, studies report that the reliability of CFS suppression varies with feature similarity between the dichoptic images, increasing in strength when similar spatial frequencies and speeds are used (Moors et al., 2014; Yang and Blake, 2012). Han, Lunghi and Alais (2016) recently measured the temporal frequency tuning of CFS using temporally narrowband, filtered noise maskers. To control for spatial frequency differences, their noise maskers were spatially filtered to have a 1/f profile to resemble the spatial frequency profile of the target stimuli which, themselves, were natural images. Results from that study revealed a low temporal frequency peak in CFS suppression, which not only corresponded to the low-biased temporal frequency spectrum of the Mondrian

masker, but also became more pronounced with high spatial frequency and high contrast. These observations are reminiscent of a parvocellular bias in binocular rivalry (Bossink et al., 1993; Carlson and He, 2000; Mueller and Blake, 1989), suggesting a parsimonious interpretation of rivalry and CFS in terms of common interocular suppression mechanisms.

Whilst the temporally filtered noise maskers used in Han et al. (2016) are ideal for examining the temporal frequency tuning of CFS, and the low frequency bias corresponded to the Mondrian's temporal frequency spectrum (see Fig. 1d of Han et al., 2016), noise maskers are spatially random in phase. Consequently, they do not contain coherent spatial patterns and lack the rapidly changing shapes and contours that are the hallmark of dynamic Mondrian maskers. This may be an important difference as coherent spatial phase is known to enhance rivalry suppression (Alais and Melcher, 2007; Baker and Graf, 2009a) and the repeating pattern of transient onsets and offsets of shapes and contours in CFS does appear to enhance suppression (Tsuchiya et al., 2006). It is also not uncommon for studies to adapt the spatial form of Mondrian patterns to enhance suppressive strength, e.g., using ellipses instead of rectangles when suppression of face images is required (Stein et al., 2011; Sweeny et al., 2011). Akin to forms of masking such as the "standing wave of invisibility" (Macknik and Livingstone, 1998) and pattern structure masking (Breitmeyer, 1984; Enns and Di Lollo, 2000), these characteristics pose a paradox in which faster, visual masking processes and slower, rivalry processes both appear to play significant roles in CFS suppression. Thus, the goal of this study is to investigate more closely the low-frequency bias reported by Han et al. (2016) examining how the spatial integrity of the Mondrian pattern interacts with temporal frequency content.

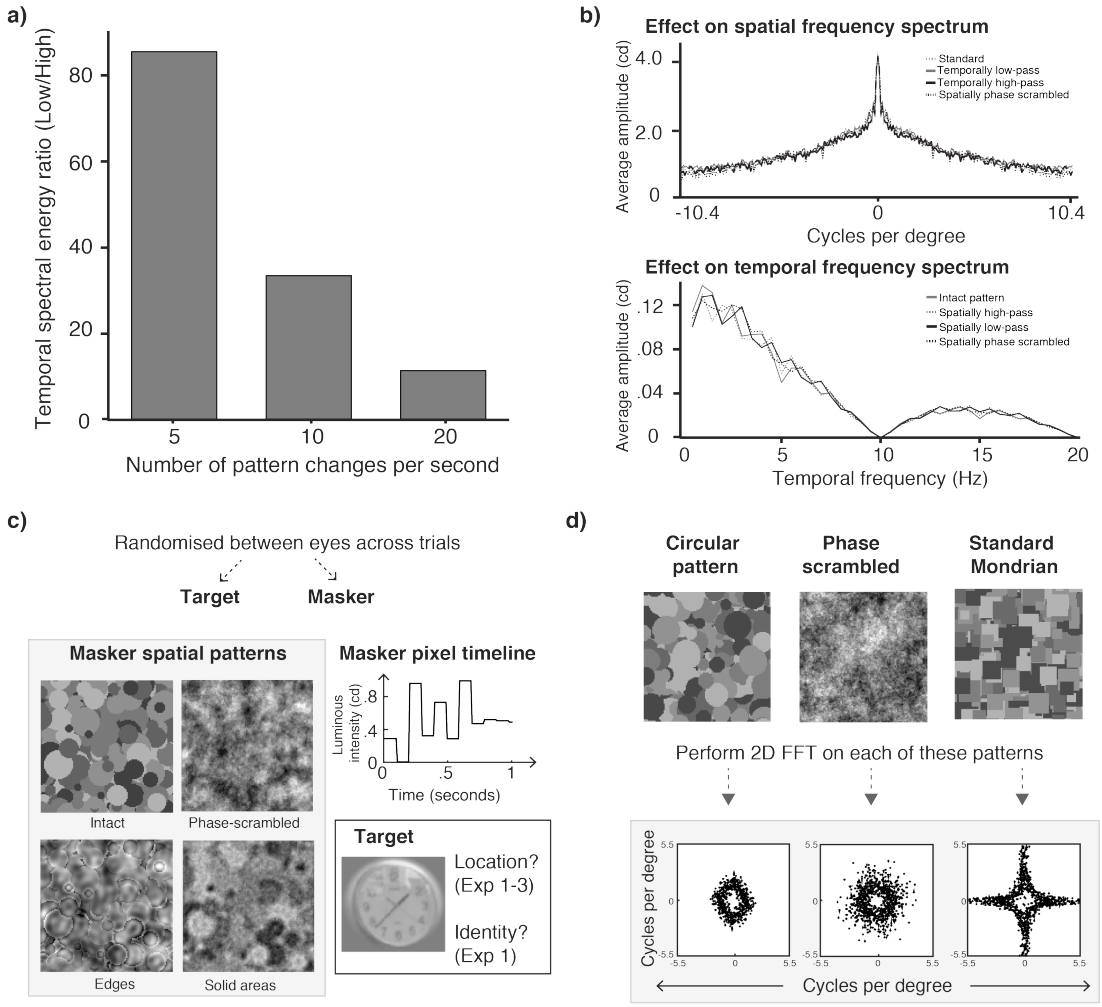

Figure 3.1. (a) The effect of varying Mondrian refresh rates on the proportions of by varying the number of pattern changes per second, but this approach also produces changes in temporal frequency content. The relationship between temporal frequency content and pattern update rate was quantified by computing the power spectral densities of low (< 4 Hz) and high (≥ 4 Hz) temporal frequencies, and then calculating the ratios of low-to-high energy for refresh rates of 5, 10 and 20 Hz. Overall, increasing the number of pattern changes per second results in decreasing ratios. (b) Temporal and spatial amplitude spectra for different stimulus manipulations. The amplitude spectra for spatial frequency were highly correlated among intact patterns, phase-scrambled patterns, and temporally high- and low-pass filtered Mondrian maskers. These stimuli also produced similar temporal frequency amplitude spectrum, demonstrating the feasibility of Fourier Transform techniques in stimulus control. Amplitude spectra shown were obtained by conducting two-dimensional Fourier Transforms (FFTs) on patterns measuring 12.4° by 12.4° (256 by 256 pixels), twice the size of that used in this study for a finer FFT frequency resolution. (c) Stimulus presentation and description. To reduce retinotopic neural adaptation and the predictability of the eye to which the target was presented, targets and maskers were randomized between eyes across trials. Examples of spatially manipulated Mondrian pattern types are presented along with the intact Mondrian pattern. Similar to the standard Mondrian, these patterns had a stepped temporal profile, with the exception of temporally filtered patterns. Targets were grey scale natural images windowed by a soft-edged circular mask. During the experiment, participants were asked to locate the quadrant containing the target or identify the type of target presented ('man-made or natural'). (d) Spatial frequency and orientation power spectrum of circular, phase-scrambled and standard Mondrian patterns. The top panel provides examples for each type of pattern, whereas the bottom panel describes the two-level contour plots of the two-dimensional FFTs of the respective patterns. Circular and phase-scrambled patterns have an isotropic spatial frequency spectrum, whereas the standard Mondrian pattern shows spectral energy peaks at the cardinal orientations.

In a bid to thoroughly understand the relationship between the Mondrian pattern and temporal frequency, we first addressed the roles of the Mondrian pattern and its components in Experiments 1–2. In Experiment 1, we asked if the Mondrian pattern acts on the level of target recognition. This was because studies frequently adapt the spatial form of the Mondrian pattern to resemble that of the target (Stein et al., 2011), raising the possibility that any resulting enhancement may be driven by impaired target recognition. Spatially phase-scrambled Mondrian sequences were compared to intact Mondrian patterns, and two judgment types (i.e., location and identity) were collected. Following that, we examined the effects of pattern edges and solid areas in Experiment 2. Spatial edges are known to influence both binocular rivalry (Levelt, 1965; Baker and Graf, 2009; Hunt et al., 2012) and masking (Macknik and Martinez-Conde, 2007; Macknik et al., 2000; Schiller and Smith, 1966), and it would be interesting to see if these features have a significant contribution to CFS suppression. We assessed the contributions of the individual pattern components by selectively preserving edges and solid areas, and then studied the relationship between these components by varying the extent to which each component was preserved.

Having revealed keynote features of the Mondrian pattern and its components, we then examined the effects of temporal frequency content and spatial pattern integrity in Experiment 3. We compared temporally low- and high-pass filtered maskers (i.e. <4 Hz and >4 Hz respectively), and then evaluated these maskers against unfiltered maskers in Experiment 3. Here is the reasoning behind this approach: matched in RMS contrast, the high-pass filtered masker reveals the suppressive strength of predominant masking influences whereas the low-pass filtered masker would reveal the importance of transients in CFS. Conducting these comparisons would demonstrate the suppressive strength of each of these processes and give us an idea of the dominant process in CFS. We also conducted these comparisons with phase-scrambled and intact Mondrian patterns, thereby allowing us to compare the size of pattern effects for each type of temporal frequency content. To ensure that the low-pass filtered and high-pass filtered maskers fall on either side of the crossover

point between low and high temporal frequency channels (~4 Hz), respectively (Cass and Alais, 2006), we used a cut-off temporal frequency of 4 Hz. This approach extended the work of Yang and Blake (2012), and provided a suitable comparison to Han et al. (2016). Our results corroborated and extended the findings of Han et al. (2016): we found that suppression was mainly driven by pattern edges and low temporal frequency content. High temporal frequency maskers, on the other hand, provided weak suppression regardless of pattern structure.

3.2 Materials and Methods

3.2.1 Participants

All participants were drawn from a pool of second or third year undergraduate students studying psychology courses at the University of Sydney. All had normal or corrected-to-normal eyesight, and tested normal for stereovision with the Fly Stereo Acuity test. Experiments accorded with the Declaration of Helsinki and were approved by the University's Human Research Ethics Committee. Informed consent was also obtained from all participants, and participants were reimbursed $AU20 per hour for their participation. Samples were as follows:- Experiment 1: Eleven naïve participants (age range: 19-30 years, *SD* = 3.67 years, 7 females); Experiment 2: Eleven naïve participants (age range: 20-29 years, *SD* = 3.11 years, 6 females) were presented with Mondrian patterns with intact, phase-scrambled structures, preserved edges and solid areas. An additional ten naïve participants (age range: 19 –30 years, *SD* = 4.29 years, 5 females) completed the interaction task; Experiment 3: Twelve naïve participants (age range: 20-38 years, *SD* = 5.47 years, 8 females).

3.2.2 Masker stimuli

Dynamic Mondrian patterns used in this study were updated at a rate of 10 Hz and randomly sampled for each and every trial from a set of ten such sequences. Each sequence lasted for 2.8s (280 frames in total) and contained twenty 5.5° visual angle

by 5.5° visual angle (114 by 114 pixels: 20.7 pixels per degree) Mondrian patterns composed of 265 circles measuring 0.26° visual angle to 0.65° visual angle in radius. A three-dimensional Fourier Transform was first performed on each of the ten dynamic Mondrian sequences, yielding amplitude and phase spectra that could be independently manipulated spatially and temporally. To generate phase-scrambled patterns (used in Experiment 1-3), random values, sampled from a uniform distribution between -2π to 2π, were summed with phase spectrum elements along the same timeline (z-dimension). The phase and amplitude spectra were then convolved and back-transformed (i.e., 2D inverse Fourier transform).

To selectively preserve solid areas and edges (Experiment 2), spectral amplitudes associated with lower spatial frequencies (< 3 cpd) were first separated from higher frequencies with low- and high-pass filters. Solid areas were then preserved by phase scrambling high spatial frequencies and edges were preserved by phase scrambling low frequencies. To vary the degree of phase scrambling, we multiplied a factor (.20 or .60) to random values before summating the result with the phase spectrum elements. Finally, the manipulated phase spectra were convolved with the corresponding amplitude spectra, and both low and high spatial frequency components were summed and back-transformed. To manipulate the temporal frequency content in Experiment 3, high- and low-pass temporal filters (> 4 Hz and < 4 Hz respectively) were also applied to the 3D spectra in addition to the spatial manipulations. All Mondrian sequences were set to 15 % RMS contrast and normalised to mean luminance.

3.2.3 Target stimuli

Target stimuli were eight grey scale, natural images (four man-made objects). Each image was extracted from the background using a soft-edged circular mask,

generated by computing a two-dimensional raised cosine measuring approximately 2.6° visual angle wide with .5° thick edges. As the Mondrian pattern consisted of circular shapes, this served to increase target/masker similarity. During the experiment, each target image was sampled randomly for each trial and jittered with 1° steps from trial to trial to reduce predictability. All target stimuli were normalised to mean luminance and presented at 5 % RMS contrast.

3.2.4 Apparatus

All visual stimuli were presented via a DATAPixx video processor on a 100 Hz Mitsubishi Diamond Pro 2070SB CRT monitor with linearised luminance output and 16-bit contrast resolution. The spatial resolution of the monitor was approximately 21 pixels per visual degree angle. Participants viewed the stimuli with a mirror stereoscope, which was adjusted to achieve stable fusion for each participant.

3.2.5 Procedure

During each trial, participants maintained fixation on a central cross and reported the quadrant containing the target, guessing if necessary (Experiments 1-3), or reported the category of the object (i.e. 'man-made or natural', Experiment 1). In total, 32 trials (16 trials for each eye) were collected for each masker type in Experiment 1, and a total of 24 trials (12 trials per eye) were completed for each masker type in Experiments 2-3. In all of these experiments, the time to visibility (suppression duration) was recorded for each trial. To avoid abrupt transients, targets were ramped up in contrast for the initial 800 ms whereas maskers were always presented immediately at full contrast. Presentation of target and masker was randomised across dominant and non-dominant eyes to mitigate retinotopic neural adaptation. Presenting two seconds of visual white noise to both eyes at the end of each trial precluded the experience of afterimages.

3.2.6. Data analysis

Each participant's data were first screened for inaccurate responses, which were excluded from the analysis. We then computed the median suppression duration of each masker type for each participant. Trials with durations that were longer than three times the median absolute deviation from the median duration were regarded as outlier trials and excluded from the analysis. Each participant had, on average, 38% of the trials (*SD* = 9%) excluded from each condition in Experiment 1, 23.2% (*SD* = 10%) in Experiment 2 and 33% (*SD* = 11%) in Experiment 3. Outliers made up 16% (*SD* = 9%) of the trials of each condition in Experiment 1, 17% (*SD* =6.6%) in Experiment 2 and 8.3% (*SD* = 3.4%) in Experiment 3. The suppression duration for each masker type was then estimated by averaging the remaining trials. As the b-CFS paradigm requires participants to make responses based on the visibility of the target, the magnitude of the time to visibility is affected by factors such as individual differences in interocular suppression durations, response times and subjective criteria (Gayet, Van der Stigchel and Paffen, 2014; Yang et al. 2014). Normalizing suppression duration data is therefore recommended for the b-CFS paradigm, as it reduces between-subject variability and increases statistical power (Gayet et al., 2014). To do so, we isolated individual data trends by normalizing the estimated durations for each masker type to the respective average across all masker types.

To preclude concern about the sample size used in this study, we assessed all effects of interest with the permutation test, a nonparametric method that evaluates a test statistic against an empirical distribution obtained by all of its possible permutations (Chong, 2008). The p-value would then be equivalent to the proportion of permutated values greater than the test statistic. Using this approach, mean differences between conditions were tested against empirical distributions computed

with 10 000 permutations. To ensure that the observed trends and resultant p-values were not driven by a particular individual's data, we evaluated our results by performing the jackknife procedure on the permutation test. This involved performing the permutation test repeatedly with one participant's data removed each time, thus reflecting the effect of individual data. Thus, if our results were driven by a single participant's data, then the removal of that participant from the dataset should yield a very different result with the permutation test. To quantify this information, we calculated the bias of the jackknife-estimated p-values using the following formula:

$$Bias = (n-1)\times(\widehat{\theta_{(.)}} - \hat{\theta})$$

where $\hat{\theta}_{(.)}$ was the average jackknife-estimated p-value and $\hat{\theta}$ the p-value obtained with the complete dataset. The bias reflected how well the jackknife results corresponded to that obtained without removing participants, and a relatively large number would suggest biases in the data. These computed values were used to evaluate the results obtained with the permutation test.

3.3. Results

3.3.1 Experiment 1

Given that Mondrian patterns are often tailored to maximise target/masker similarity (Stein et al., 2011), we asked if the Mondrian pattern acts at the level of target recognition. We measured suppression durations for two types of masker (intact versus phase-scrambled Mondrian patterns) with separate measurements for location and identity judgments. To assess the effect of masker pattern structure, we collapsed normalised durations across judgment type and then computed the mean differences between the pattern types. The data was collapsed across pattern types for the effect of judgment type. To test for the interaction between both factors, we computed the

difference in durations between intact and phase-scrambled patterns for each level of judgment type, and then compared the resultant differences.

Using the permutation test, we found a significant effect of masker pattern structure, Bias = 0.02, p = .001. Specifically, phase scrambling resulted in a two-fold reduction in normalised suppression durations (Figure 3.2; see also S1 for individual data), consistent with reduced rivalry suppression when one image was phase-scrambled (Alais and Melcher, 2007). Collapsed across pattern types, identity judgments required significantly longer durations than location judgments, Bias = 0.002, p = .002. Judgment type, however, did not interact significantly with pattern type, Bias = 0.18, p = .51. Holm-Bonferroni corrected, pairwise comparisons showed that the participants generally took longer to make identity judgments regardless of pattern type, but the differences were only significant in phase-scrambled patterns, Bias = 0.12, p = .048, and not intact patterns, Bias = 0.33, p = .20.

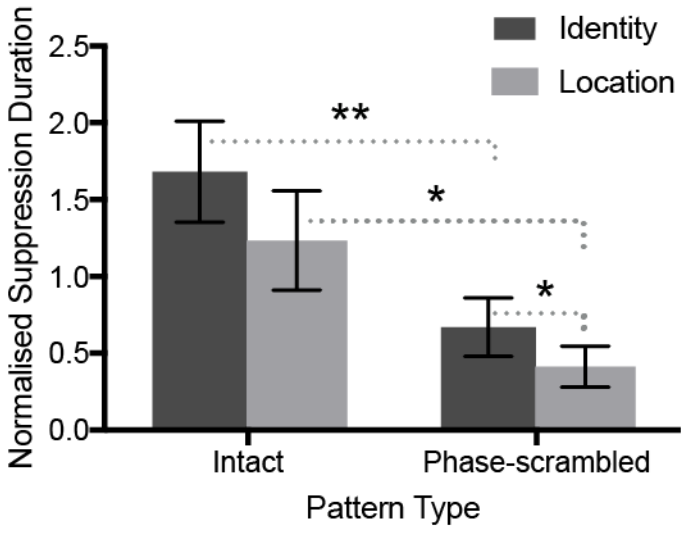

Figure 3.2. Data from Experiment 1 demonstrating the effect of Mondrian pattern structure on normalised suppression durations. To assess the role of the Mondrian pattern in CFS, participants were instructed to either identify the target or report the location of the target ('which quadrant?') for each trial. Suppression durations were measured and correct responses were then normalised to each individual's average. Overall, the presence of coherent pattern structure resulted in longer suppression, and this was true for identity and location judgments. Participants also took longer to make accurate identity judgments, but this was only

applicable to phase-scrambled patterns. Hence the coherent spatial form of the Mondrian pattern does not selectively impair target recognition. Instead, these patterns contribute to suppression strength. Asterisks denote statistical significance (*: p< .05, **: p< .01) after Holm-Bonferroni correction. Error bars represent 95 % confidence intervals of the mean.

3.3.2. Experiment 2

Having demonstrated that the pattern structure of the masker enhances suppression, we decomposed the sources of influence in Experiment 2. Edges and solid areas were preserved by phase scrambling high (≥ 3 cpd) and low (< 3 cpd) spatial frequencies, respectively, and the performance of these masks was evaluated against intact and phase-scrambled patterns using Holm-Bonferroni corrected pairwise comparisons. As pattern structure clearly contributed to suppression and did not have a significant interaction with judgment type in Experiment 1, location judgments were recorded in this experiment. Figure 3.3a illustrated the normalised durations produced by each pattern component (see also S2a for individual data). The performance of phase-scrambled patterns was statistically comparable to solid areas, Bias= 0.11, p = .30, but was weaker than edges, Bias = 0.01, p = .005. And although edges were more effective than solid areas, Bias = 0.03, p = .004, these were still weaker than intact patterns, which produced significantly longer suppression than solid areas and edges, Bias = -0.004, p = .006 and Bias = -0.08, p = .028 respectively. The suppressive advantage of intact patterns remained even after the effects of edges and solid areas were considered collectively (computed by summating the respective normalised durations before subtracting that of phase-scrambled patterns), Bias = 0.10, p = .006. This pattern of results was further supported by Bayes factors (see details in the Supplementary material).

This difference could be explained by an interaction between low and high spatial frequency pattern components, which we tested by varying the degree of phase

scrambling applied to each feature (i.e., 20 % or 60 %) in a separate task. Collapsed across the different levels of structural integrity in solid areas, patterns with more intact edge information produced longer suppression, Bias < .001, p = .001. Similarly, patterns with more intact solid areas produced longer normalised durations than patterns without, Bias = -0.01, p = .002. The structural integrity of solid areas and edges also interacted significantly, Bias = 0.13, p = .01. As described in Figure 3.3b, reducing the structural integrity of solid areas significantly reduced normalised durations when pattern edges were relatively intact, Bias = 0.004, p = .012, but not when the edges were phase-scrambled to a larger extent, Bias = 0.21, p = .39. Individual data were presented in S2b.

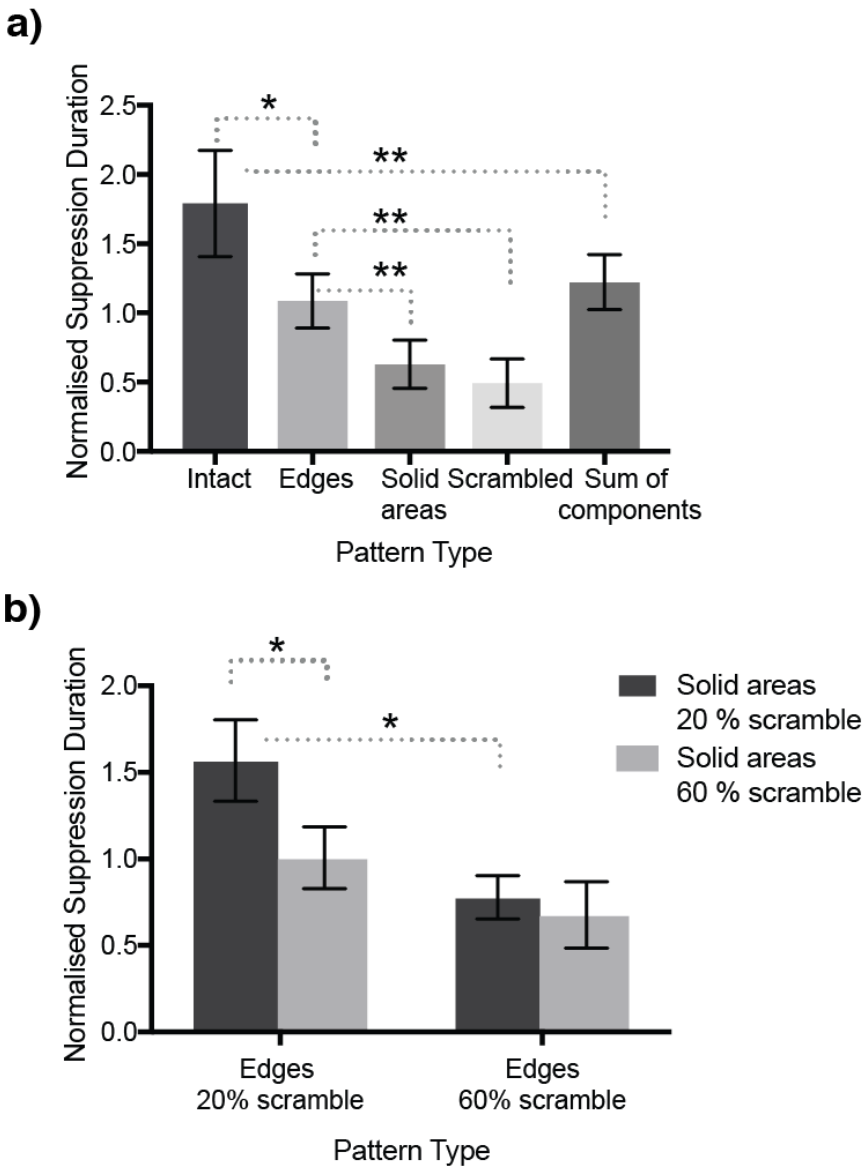

Figure 3.3 (a) Data from Experiment 2 showing the effect of individual Mondrian pattern components on normalised suppression durations. We evaluated the effect of individual pattern components by selectively phase scrambling low (< 3 cpd) and high (≥ 3 cpd) spatial frequency components, giving rise to patterns with preserved edges or solid areas, respectively. This allowed us to vary the structural components of the Mondrian pattern while preserving spatial frequency content. The efficacy of these patterns was evaluated against intact and phase-scrambled patterns, and the results showed that edges had the largest contribution to CFS suppression strength. On the other hand, solid areas were comparable to phase-scrambled patterns. Intact patterns remained the strongest suppressor, producing longer normalised suppression durations than edges. This disparity remained even after considering the collective effect of pattern components (estimated by summing the respective normalised durations and then subtracting that of phase-scrambled patterns). (b) Data from Experiment 2 demonstrating an interaction between pattern edges and solid areas in CFS. Edge and solid-area content were selectively phase-scrambled to a larger or smaller degree (i.e., 60 % or 20 %, respectively) and the effects on normalised suppression durations were examined. Phase scrambling solid areas to a smaller degree resulted in longer normalised suppression durations, but the effect was only

observed when edges were relatively intact. Asterisks denote statistical significance (*: p< .05, **: p< .01) after Holm-Bonferroni correction. Error bars represent 95 % confidence intervals of the mean.

3.3.3 Experiment 3

Experiments 1-2 demonstrated that the effectiveness of dynamic Mondrians as masking patterns was predominantly driven by the abundance of spatial edges in the Mondrian masker. As spatial edges are known to influence both binocular rivalry (Levelt, 1965; Baker and Graf, 2009a; Hunt et al., 2012) and masking (Macknik et al., 2000; Macknik and Martinez-Conde, 2007; Schiller and Smith, 1966), Experiment 3 examined the role of masking in CFS suppression. It is known that masking effectiveness is greater for shorter temporal intervals (Enns and Di Lollo, 2000; Hellige et al., 1979) and for sharp temporal onsets (Macknik et al., 2000). We thus reasoned that if masking were to make a substantial contribution to CFS it would predict longer suppression durations and a greater effect of pattern with increasingly transient maskers. So, we compared the efficacy of temporally low- and high-pass filtered maskers, and then evaluated these maskers against unfiltered maskers, which served as a baseline condition. These measurements were recorded with intact and phase-scrambled patterns because it allowed us to compare the size of pattern effects, defined as the percentage difference in normalised durations between intact and phase-scrambled patterns at each level of temporal frequency content.

Results are illustrated in Figure 3.4 (see also S3a-c). All planned comparisons were conducted with Holm-Bonferroni corrections. Compared to temporally high-pass maskers, we obtained significantly stronger suppression with low-pass maskers, Bias = 0.002, $p = .01$ for intact patterns, but not for phase-scrambled patterns, Bias = 0.20, $p = .11$. When evaluated against unfiltered maskers, low-pass maskers produced comparable normalised durations, and this was true for intact patterns and phase-

scrambled patterns, Bias = 0.21, p = .14 and Bias = 0.49, p = .26 respectively. In contrast, high-pass filtered maskers were consistently weaker than unfiltered maskers, Bias = -0.006, p = .012 for intact patterns and Bias = 0.13, p = .02 for phase-scrambled patterns. We then compared the size of pattern effects for each type of masker. Our results showed a significantly smaller pattern effect in temporally high-pass filtered maskers than unfiltered maskers, Bias = 0.05, p = .009. In contrast, temporally low-pass filtered maskers had a comparable pattern effect to unfiltered maskers, Bias = 0.92, p = .29, and were more dependent on the presence of coherent pattern structures than high-pass maskers, Bias = 0.02, p = .014. Thus, contrary to intuition, transients did not appear to have a major contributory role to the potency of CFS. In fact, they produced less suppression than did low temporal frequencies, and were less reliant on the presence of coherent pattern structures. Similar to Experiment 2, these findings were substantiated by Bayes factors (see Supplementary material for details).

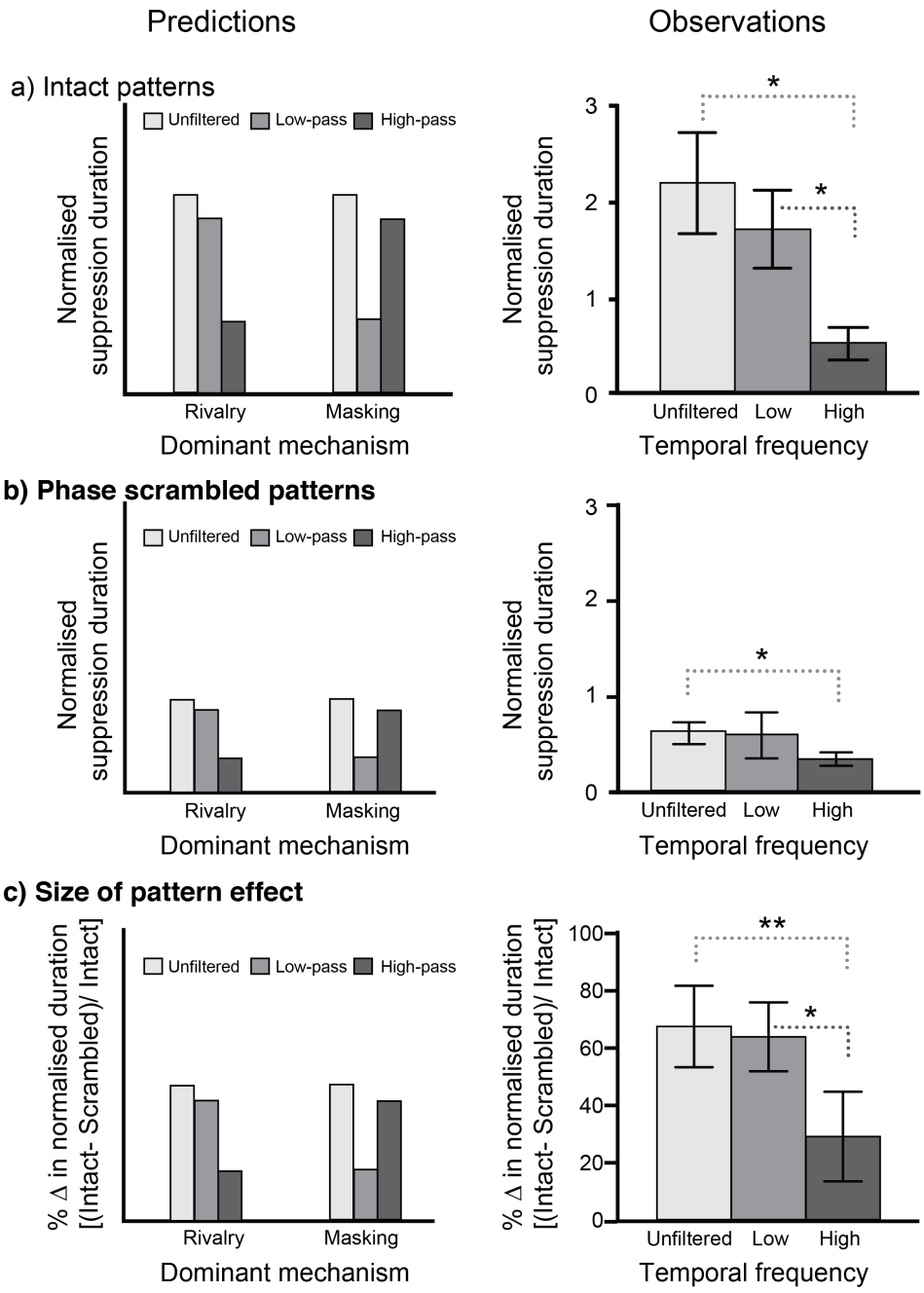

Figure 3.4. (a) Predictions (left panel) and observations (right panel) for temporally unfiltered, low-pass (< 4 Hz) and high-pass (≥ 4 Hz) maskers with intact pattern structures. Because sharp temporal onsets are typical of effective masking stimuli (Macknik et al., 2000), a dominant masking mechanism would produce smaller differences in durations between unfiltered and high-pass maskers (as both contain transients), and significantly weaker suppression for low-pass maskers. The results revealed comparable performances between low-pass and unfiltered maskers, whereas high-pass filtered maskers were significantly weaker than unfiltered maskers. (b) Predictions and observations for phase-scrambled patterns (left and right panels, respectively). Similar predictions were made for phase-scrambled patterns, although lower durations were expected for all masker types. As with intact patterns, we found low-pass filtered maskers to be comparable to unfiltered maskers, whereas high-pass filtered maskers were weaker than unfiltered maskers. (c) Predictions and observations for sizes of pattern effects. We computed the percentage change in normalised

durations between intact and phase-scrambled patterns for each type of temporal frequency content. A dominant masking mechanism would predict smaller percentage changes between high-pass filtered and unfiltered maskers. Against predictions, there were significantly smaller pattern effect sizes in high-pass maskers, and comparable pattern effects between low-pass and unfiltered maskers. Asterisks denote statistical significance (*: $p < .05$, **: $p < .01$) after Holm-Bonferroni correction. Error bars represent 95 % confidence intervals of the mean.

3.4 Discussion

This study was motivated by a simple but important question: why are monocularly viewed, dynamic Mondrian patterns unusually potent at erasing from conscious awareness an otherwise complex monocular image presented to the other eye? Learning the answer to this question is important, because differential effects on suppressed stimuli have been associated with differences in low-level properties such as orientation (Moors et al., 2014; Yang and Blake, 2012) and color (Hong and Blake, 2009). Measuring the temporal frequency tuning of CFS using spatiotemporally controlled noise maskers, Han et al. (2016) obtained a low-temporal-frequency bias in suppression durations, which corresponded with the low-biased temporal frequency spectrum of the typically-used Mondrian masker (C.f. Figure 2.3). Nevertheless, because their filtered-noise maskers were spatially random, they were devoid of the transiently changing coherent form characteristic of the Mondrian masker. Our goal in the present study, then, was to examine the role of Mondrian pattern structure and its relationship with temporal frequency. We were able to replicate and confirm the aforementioned low-frequency bias and to assess the use of filtered noise maskers in CFS studies. Moreover, these manipulations offered a way to separate possible rivalry and masking influences, both of which have been proposed to underlie the effectiveness of CFS suppression (Han et al., 2016; Tsuchiya and Koch, 2005; Tsuchiya et al., 2006).

Spatially intact Mondrian pattern structures produced longer suppression durations for identity and location judgments, showing that coherent pattern structures contributed to suppression and did not selectively impair target recognition. Interestingly, assessments of pattern components showed that the enhancement in suppression strength was predominantly driven by spatial edges. Not only did intact spatial edges produce longer suppression durations than intact solid areas, but varying the structural integrity of solid areas also had no significant influence on suppression durations when spatial edges were scrambled to a larger degree. Since spatial edges influence the effectiveness of rivalry suppression (Alais and Melcher, 2007; Baker and Graf, 2009a) and visual masking (Macknik et al., 2000; Macknik and Martinez-Conde, 2007; Schiller and Smith, 1966), these findings do not differentiate between the two alternatives. To differentiate the putative contributions of these two processes, we extended our investigation to the temporal domain and compared the efficacy of temporally unfiltered, low- and high-pass filtered maskers. Comparable performances were obtained for unfiltered and low-pass filtered maskers, whereas high-pass filtered maskers were significantly weaker. These trends were observed regardless of spatial pattern structures, and there was also a significantly larger effect of pattern structure on low-pass maskers compared to high-pass maskers. Thus, our results point to rivalry being the dominant process in CFS, as a mechanism dominated by masking would likely have been more effective with smaller temporal intervals and transients (Enns and Di Lollo, 2000; Hellige et al., 1979).

There are several important implications of these findings, the most notable relating to the sharp pattern onsets and offsets of the Mondrian masker. Rapid pattern changes could minimize neural adaptation associated with CFS and, thereby, promote longer periods of exclusive dominance (Tsuchiya et al., 2006; Yang and Blake, 2012).

Whilst some CFS studies do report enhanced interocular suppression with very high Mondrian refresh rates, i.e., 85 Hz (Xu et al., 2011), the reasons behind the enhanced effectiveness are unlikely to be straightforward. We say this because interocular suppression peaks at Mondrian refresh rates around 6 Hz (Zhu et al., 2015; Zhu et al., 2016), and computational simulations reveal that reduced neural adaptation does not constitute a major contribution to suppression strength (Moors et al., 2014). Moreover, past research using comparable temporal spectra have consistently found weaker suppression with higher temporal frequency content (Han et al., 2016; Yang and Blake, 2012). Thus, at least for static targets, the poor performance of temporally high-pass maskers accords with previous research and argues against the importance placed on the transients in the dynamic Mondrian masker.

This leaves us with a perplexing observation. If transients do not constitute a large proportion of the Mondrian's temporal frequency spectrum (and they do not: Figure 3.1b and C.f. Figure 2.3) and do not have a major contribution to suppression, then why do these filtered Mondrian maskers appear to be flickering so saliently? A simple explanation would be the over-representation of transient input in the visual system. Termed temporal whitening, this over-representation was studied by Cass, Alais, Spehar and Bex (2009) who found that participants tend to overestimate the proportion of high temporal frequency energy, and at a magnitude that equalises the 1/f temporal amplitude spectrum typical of natural images and flickering Mondrians. This bias results from an asymmetrical inhibition in temporal frequency processing whereby high frequencies (> 4 Hz) inhibit low frequencies (< 4 Hz), but low frequencies do not inhibit high frequencies (Cass and Alais, 2006; Cass et al., 2009). Thus the impression of a rapid flickering Mondrian masker may be an artefact of such biases. High temporal frequencies still appear to contribute to CFS. In fact, given the

evidence demonstrating feature selectivity in CFS suppression (Hong and Blake, 2009; Moors et al., 2014; Yang and Blake, 2012), higher temporal frequencies are likely to be become more important when high frequency targets are used. Indeed, Kaunitz et al. (2014) found stronger masking effects and higher optimal refresh rates (i.e., 28.5 Hz) were obtained when transient targets were used.

Interestingly, Experiment 2 revealed a significant interaction between pattern components with low and high spatial frequencies. Interactions between low and high spatial frequencies have been observed in scene perception studies, and these typically involve feedback signals from late to early visual processing regions (Kveraga, Boshyan and Bar; Peyrin et al., 2010). We speculate that a similar process may occur in CFS, and such a mechanism would accord with multi-level theories of binocular rivalry (Freeman, 2005; Nguyen, Freeman and Alais, 2003; Tong et al., 2006; Wilson, 2003), providing further support for a unified framework between these two paradigms. This parsimonious approach would be instrumental in the study of CFS mechanisms and in the design of CFS experiments. For instance, future research could explore the effects of stimulus size (Kang, 2009) and the perceptual meaning of visual stimuli (Andrews and Lotto, 2004). These have been shown to influence rivalry suppression and it would be interesting to see if similar effects could be observed in CFS. Lastly, the correspondence in results between the current study and Han et al. (2016) not only confirms the low temporal-frequency tuning of CFS, it demonstrates the utility of Fourier filtering techniques and the use of spatiotemporally filtered noise stimuli in CFS studies. Not only is this approach useful in elucidating CFS mechanisms, it is also useful for conducting controlled investigations into unconscious visual processing.

3.5 Conclusion

Until recently, the rapid pattern changes in the Mondrian masker have been widely assumed to drive CFS suppression. Using temporally narrowband filtered noise maskers, Han et al. (2016) demonstrated a strong, low-frequency bias in CFS suppression. Their results corresponded well with the low-biased temporal frequency spectrum of dynamic Mondrian maskers, but the use of filtered noise meant their stimuli modulated smoothly at a given frequency rather than refreshing instantaneously, complicating comparisons with dynamic Mondrians. Here, we used dynamic Mondrians and manipulated their temporal structure and spatial pattern to reveal predominant contributions of spatial edges and low temporal-frequency content in CFS. These findings point to the dominant suppression processes in CFS being very similar to those in binocular rivalry, affording a parsimonious alternative in unifying the two paradigms.

3.6 Chapter review

In Chapter 2, I tested the assumption that CFS is largely driven by the rapid pattern changes in the Mondrian masker. Using narrowband filtered noise maskers, I measured the temporal tuning of CFS suppression and discovered that CFS effectiveness peaked at low temporal frequencies. Given that the noise maskers were void of the contour-rich information present in Mondrian maskers, my goal in Chapter 3 was to verify the low temporal frequency bias with Mondrian pattern structures. As predicted, I observed stronger suppression for temporally low-pass filtered Mondrian maskers than high-pass filtered maskers. Similar to Chapter 2, CFS was also enhanced by high spatial frequency content, producing longer suppression durations when low temporal frequency maskers contained coherent pattern edges. Thus, the collective findings of Chapters 2-3 demonstrated three important points. Firstly, transients do not contribute to the bulk CFS's effectiveness and experimenters should avoid relying on transients to provide effective CFS suppression. Secondly, varying the number of patterns per second is not equivalent to the periodic change in pixel luminance over time, and I would argue that the latter provides a better control of temporal frequency content. Thirdly, in contrast to earlier theories (e.g., Tsuchiya et al., 2006), CFS seems to have a parvocellular bias that is akin to BR. In the following chapter, I tested the extent of the low temporal frequency bias in CFS with slow and rapid modulating targets. Given that static targets were used in Chapters 2-3, it was unclear if the results reflected a general bias towards low temporal frequencies, or a consequence of temporal frequency selectivity.

Chapter 4

Strength of continuous flash suppression is optimal when target and masker modulation rates are matched.

The work in this chapter is published as:
Han, S, & Alais, D. (2017). Strength of continuous flash suppression is optimal when target and masker modulation rates are matched. Journal of Vision, 18(3), 1-14.

Individual data are accessible at: https://doi.org/10.17605/OSF.IO/DPWSE

Abstract

Continuous flash suppression (CFS) is a popular technique whereby a dynamic sequence of Mondrian patterns is presented to one eye in order to suppress a static target presented to the other eye. Although the effectiveness of CFS is generally assumed to increase with the flicker rate of the Mondrian masker, a recent study shows that suppression is optimal at very low masker rates for sustained targets but higher rates may be necessary for transient targets. Here we vary the modulation rates of the masker and target using temporally filtered dynamic noise, which allowed us to examine the relationship between target and masker frequency and its effect on suppression strength. Using these carefully controlled, temporally narrowband stimuli, we demonstrate a pattern of results showing that suppression is greatest when target and masker modulate at similar frequencies. This finding indicates the involvement of early temporal-frequency-tuned filters underlying CFS and is consistent with many existing findings in the CFS literature. We also find these temporally-selective processes are orientation selective, which points to an early cortical substrate such as neurons in primary visual cortex. Overall, our study reveals that CFS suppression can be maximised by carefully matching the masker and target

in temporal frequency and orientation. More generally, we show the importance of using carefully controlled stimuli for elucidating the underlying mechanisms of CFS. This approach is important at a theoretical level as it will enable comparison of CFS with existing models of binocular rivalry and interocular suppression and facilitate a unified explanatory framework.

4.1 Introduction

Our sensory system is flooded with information from the external environment, yet only a small proportion constitutes our conscious experience. Several techniques have been developed to render visual images invisible to allow investigation of the functional and processing status of nonperceived input (Breitmeyer, Ogmen, and Chen, 2004; Kim and Blake, 2005; Tsuchiya and Koch, 2005). Continuous flash suppression (CFS) is one of the most widely used of these techniques. In the CFS paradigm, a dynamic sequence of random Mondrian patterns is viewed in one eye while a static target is presented to the other eye. This generally produces effective and long-lasting suppression, especially when low-contrast targets are used—which is generally the case (Tsuchiya and Koch, 2005; Tsuchiya, et al., 2006). Unlike in binocular rivalry, the first visual percept in CFS is reliably that of the dynamic Mondrian sequence, meaning the suppressed target can be conveniently studied from the outset (Yang et al., 2014). This, coupled with long suppression times, has seen CFS become a widely adopted technique (e.g., Fang and He, 2005; Moors, Wagemans, van Ee, de-Wit, 2015c; Yang et al., 2007).

Mondrian refresh rates of 10 Hz or higher are typically adopted in CFS studies (e.g., Xu et al., 2011; Yuval-Greenberg and Heeger, 2013), as it is widely assumed that one of the keys to CFS's strong suppression is the rapid pattern changes in the masking eye (Tsuchiya et al., 2006; Tsuchiya and Koch, 2005). Existing evidence,

however, suggests that the optimal refresh rate for the masker may differ depending on the nature of the target to be suppressed. One study using brief static targets found that the optimal masker required a flicker rate of up to 28.5 Hz (Kaunitz et al., 2014), while another using prolonged static targets found that suppression peaked at around 6 Hz (Zhu et al., 2015; Zhu et al., 2016). Both of these studies varied the update rate of independent static images, meaning the luminance changes were abrupt and the temporal frequency content was therefore broadband.

A recent study was the first to control the temporal frequency of the masking stimulus in narrow passbands (Han et al., 2016). In this study, where the image undergoes smooth and continuous modulation rather than discrete transient changes, the masking frequency giving greatest suppression of prolonged static targets was very low, at ~1 Hz. Although it may not be obvious at first glance, using the image update rate to manipulate temporal frequency produces broadband temporal content with a strong bias to very low temporal frequencies. This is best exemplified by the pixel timeline, where the 100-ms presentation time of each pattern and the central tendency of luminance changes jointly produce a slow-modulating, stepped waveform (for more details, see Supplementary Text S1, Supplementary Figure S1 and Han et al., 2016). Increasing the update rate does not change the low temporal bias; however, the proportion of high temporal-frequency energy increases (Figure 4.1a). Therefore, one consistent interpretation of these studies, despite their different temporal manipulations, is that prolonged static targets are best produced by very low temporal frequencies.

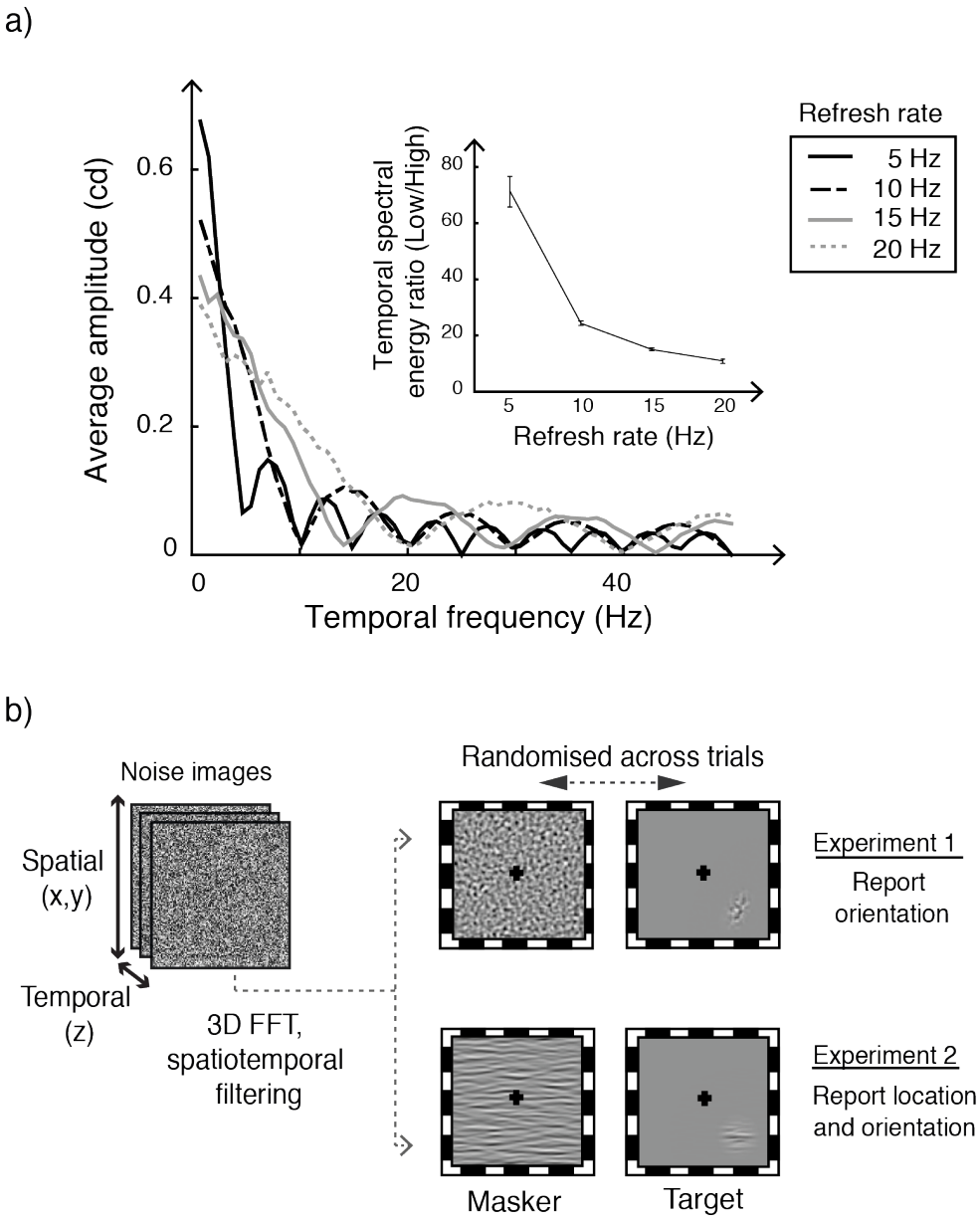

Figure 4.1. (a) Effect of Mondrian refresh rate on temporal-frequency content. Two-dimensional Fourier analyses show that the Mondrian masker has a strongly low-biased temporal-frequency amplitude spectrum across different refresh rates. Although the trend becomes more broadband with faster flicker rates, the low-frequency bias remains. These differences were quantified by comparing the power spectral densities of low (<4 Hz) and high (≥4 Hz) temporal frequencies for Mondrian maskers at 5, 10, 15, and 20 Hz (inset). Five maskers were independently generated for each masker refresh rate. Twenty-five pixels were then randomly sampled from each of these five maskers and their timelines analyzed. (b) Stimuli used in the current experiments. To generate masker and target stimuli, a three-dimensional Fourier transform was first performed on a stack of 205 randomly generated noise images, before narrowband log-Gaussian filters were applied to the temporal (2, 3, 5, 7.5, and 10 Hz) and spatial dimensions (3 c/°). Targets were also spatially windowed with an elliptical Gaussian mask in Experiment 1 and a circular Gaussian mask in Experiment 2. To reduce retinotopic adaptation, the presentation of maskers and targets were randomized between the eyes across trials. Checkerboard frames were used to enclose both maskers and targets to ensure stable fusion. Participants were instructed to report the target's orientation in Experiment 1 (tilted left or right) and its location (which quadrant) and orientation (horizontal or vertical) in Experiment 2.

Psychophysical studies of temporal processing conclude that the entire temporal dimension in vision is encoded by a broad low-pass channel with a cutoff around 4 Hz (Anderson and Burr, 1985; Cass and Alais, 2006; Snowden, Hess, and Waught, 1995) and one or perhaps two higher, bandpass channels (Cass and Alais, 2006; Hess and Snowden, 1992; Johnston and Clifford, 1995). By this account, stimuli that are static or slowly modulating will activate the low-pass temporal-frequency channel, whereas rapidly modulating, transient stimuli would stimulate the high-frequency, bandpass channel. Detection of a static target thus becomes more difficult with low masker modulation or update rates (Han et al., 2016; Zhu et al., 2016), as target and masker will both activate the same channel. Likewise, higher Mondrian update rates are better suppressors of transient targets (Kaunitz et al., 2014) because the increased high-temporal-frequency content drives the same channel as the transient target. Physiologically, these channels may correspond to parvocellular and magnocellular neurons, which are, respectively, more responsive to slower modulating and transient visual stimuli (Derrington and Lennie, 1984).

Several studies have shown that CFS is feature selective. For instance, similarities in target and masker spatial frequency (Maehara et al., 2009; Yang and Blake, 2012) and speeds (Moors et al., 2014) have been shown to enhance suppression. It is therefore likely that CFS would involve suppression processes that are selective in the temporal dimension. However, because Mondrian maskers are temporally broadband and CFS studies typically use static targets (but see Ananyev, Penney, and Hsieh, 2017; Kaunitz et al., 2014; Moors et al., 2014), the proposition has not been specifically addressed. In this study, we measured the temporal selectivity of CFS by comparing 2- and 10-Hz narrowband noise maskers on targets modulating at a range of temporal frequencies. We predict that, regardless of masker

temporal frequency, enhanced suppression will be observed when target and masker frequencies are similar. In contrast, suppression will be reduced for any target–masker combination that activates different channels. We quantify this using two dependent measures: suppression duration and contrast sensitivity threshold. Measured using the commonly used breaking-CFS (b-CFS) paradigm, suppression durations reflect the time to visibility and are more susceptible to nonperceptual factors such as participant decisional criteria in determining target visibility (Yang et al., 2014). Including a more objective measure such as contrast sensitivity threshold allows us to compare both measures and better understand the general trend. In addition, measuring contrast sensitivity will facilitate comparisons with binocular-rivalry studies, which often measure contrast sensitivity in suppression (Alais, 2012; Stuit et al., 2009).

4.2 Experiment 1

4.2.1 Materials and methods

4.2.1.1 Masker stimuli

Spatiotemporally narrowband maskers were generated by filtering 205 randomly generated noise images (each 128 × 128 pixels, approximately 5.4° × 5.4°, 15% RMS contrast and normalized to mean luminance). These noise images were first converted to the frequency domain using a three-dimensional fast Fourier transform and then filtered spatially and temporally using narrowband, log-Gaussian filters. The spatial filter had a center frequency of 3 c/° and the temporal filter had a center frequency of 2 or 10 Hz. All filters had a full bandwidth at half height of one octave. Masker images were then back-transformed and normalized to maximum contrast (15% RMS) and to space-averaged mean luminance. Maskers were then

presented at 95% of maximum contrast (see examples of masker stimuli in Figure 4.1b and Supplementary Movies S1 and S2).

4.2.1.2 Target stimuli

Targets were dynamic filtered noise images made from the same spatiotemporal filtering process as the masker images but using independent noise images. They were generated with the same RMS contrast and center spatial frequency, could take a range of temporal frequencies (2, 3, 5, 7.5, or 10 Hz), and were windowed in the space domain by a small Gaussian mask of either SDxy = 10 pixels for monocular threshold measurements or SDx = 4.5 pixels and SDy = 7.5 pixels for all CFS tasks. Targets thus measured approximately 1° × 1° at half height for monocular threshold measurements and 0.5° × 1° at half height for all CFS tasks.

Both targets and maskers were enclosed by a 0.5°-thick checkerboard frame (5.9° × 5.9° externally and 5.4° × 5.4° internally; see Figure 4.1) to encourage stable fusion. All visual stimuli were presented on a Mitsubishi Diamond Pro 2070SB CRT monitor (screen refresh rate of 100 Hz) connected to a DATAPixx data-acquisition system (Vpixx Technologies, Saint-Bruno, Canada), which allowed millisecond precision and a 16-bit contrast resolution. The presentation order of the target and masker between the eyes was randomized between dominant and nondominant eyes to mitigate adaptation effects.

4.2.1.3 Participants

In Experiment 1, suppression durations and visual contrast thresholds were recorded for five participants who were unaware of the purposes of the experiment (four women, one man; age range: 19–24 years, SD = 1.82). Another three participants who were unaware of the purposes of the experiment (two women, one man; age range: 21–30 years, SD = 5.2) completed only the b-CFS task, whereas

threshold measurements were conducted for author SH and four participants (four women; age range: 20–29 years, SD = 4.93). All participants had normal or corrected-to-normal visual acuity. Participants also had normal stereovision, assessed using the Fly Stereo Acuity test. All experiments were performed with the approval of the institutional review board at the University of Sydney and according to the principles of the Declaration of Helsinki. Informed consent was obtained for all participants and participants were reimbursed 20 AUD per hour for their participation.

4.2.1.4 Eye-dominance assessment

Eye dominance was determined using the "hole in the hand" test, a variation on the Miles test (Miles, 1930). Participants were first seated a distance away (~150 cm) from an object placed at eye level. They were instructed to view the object through a small hole created by both hands, first with both eyes and then alternately with each eye. The eye with less displacement in perceived object location was designated as the dominant eye.

4.2.1.5 Procedure for b-CFS

Targets were first subjectively equated by measuring contrast detection thresholds for each target frequency. To do this, a two-alternative forced-choice (2AFC) QUEST adaptive procedure was adopted for each target frequency, and each staircase consisted of 24 trials. No maskers were presented in the threshold-determination task. Participants judged the location of the target, situated 1.3° to the left or right of a central fixation cross. Each trial lasted for 2 s, followed by 300 ms of dynamic visual white noise. Thresholds were defined at 75% accuracy and were estimated by fitting a cumulative Gaussian psychometric function with the maximum-likelihood estimation procedure. Targets were then presented five times above the respective thresholds for the b-CFS task. To avoid abrupt onsets, maskers and targets

were also ramped in contrast during the initial 1,000 ms of each trial, with the masker leading 50 ms (five frames) before the target to accumulate suppressive effects (Tsuchiya et al., 2006). Predictability and local adaptation were reduced by randomly presenting targets at different points from trial to trial chosen from a circle with a radius of ~1.2° around the fixation cross. Targets were oriented ±45° and participants indicated the orientation of the target (tilted left or right) as soon as it became visible. The time required for each response was recorded, followed by 5 s of dynamic visual white noise. Ten trials per target frequency were collected, the order of which was presented in randomized blocks for each participant. Only trials with correctly located targets and suppression durations that were not more than three times the median absolute deviation were included for analysis. These trials were then sorted according to the dominant eye and averaged for each target temporal frequency. Each participant's data were then normalized to their respective average suppression durations across the 2- and 10-Hz conditions.

4.2.1.6 Procedure for CFS threshold measurements

Separate 2AFC QUEST adaptive staircases were adopted for each target frequency and each eye. Similar to the b-CFS task, participants were asked to judge the orientation of targets, which were oriented ±45° at random positions along a circle of radius ~1.2° centered on the fixation cross. Each trial lasted for 2 s, followed by 300 ms of dynamic visual white noise. Similar to the b-CFS task, target temporal frequencies were blocked in a randomized order, whereas the order of masker frequency was presented in counterbalanced blocks. Similar to Experiment 1, the eye of origin was randomized within each block. Each staircase consisted of 22 trials, resulting in a total of 220 trials per masker frequency. Thresholds were estimated by fitting a cumulative Gaussian psychometric with the maximum-likelihood estimation

procedure. Each participant's estimated thresholds were then normalized to the participant's individual average threshold across the 2- and 10-Hz conditions.

4.2.2 Results

4.2.2.1 Normalized suppression durations

The effects of masker and target temporal frequencies on suppression durations are summarized in Figure 4.2a. We first tested the effect of eye dominance on suppression durations using separate 2 × 5 (eye dominance × target temporal frequency) repeated-measures ANOVAs for each masker temporal frequency. There was no evidence of eye-dominance effects for either masker frequency—2 Hz: $F(1, 7) < 1$; 10 Hz: $F(1, 7) = 1.53$, $p = 0.26$, $\eta p^2 = 0.18$. Eye dominance also did not interact with target temporal frequency—2 Hz: $F(4, 28) < 1$; 10 Hz: $F(4, 28) = 1.46$, $p = 0.27$ (Greenhouse–Geisser corrected), $\eta p2 = 0.17$. In contrast, target temporal frequency had a significant main effect with both types of maskers—2 Hz: $F(1, 7) = 9.55$, $p < 0.001$, $\eta p^2 = 0.57$; 10 Hz: $F(1, 7) = 2.72$, $p < 0.05$, $\eta p^2 = 0.28$. Having established that there were no eye-dominance effects, we pooled the raw suppression-duration data and recompiled a normalized data set without sorting the data according to the dominant eye. This increased the number of data points per target temporal frequency, and allowed us to better estimate individual means for each target frequency. Responses that were inaccurate or more than three times the median absolute deviation were excluded.

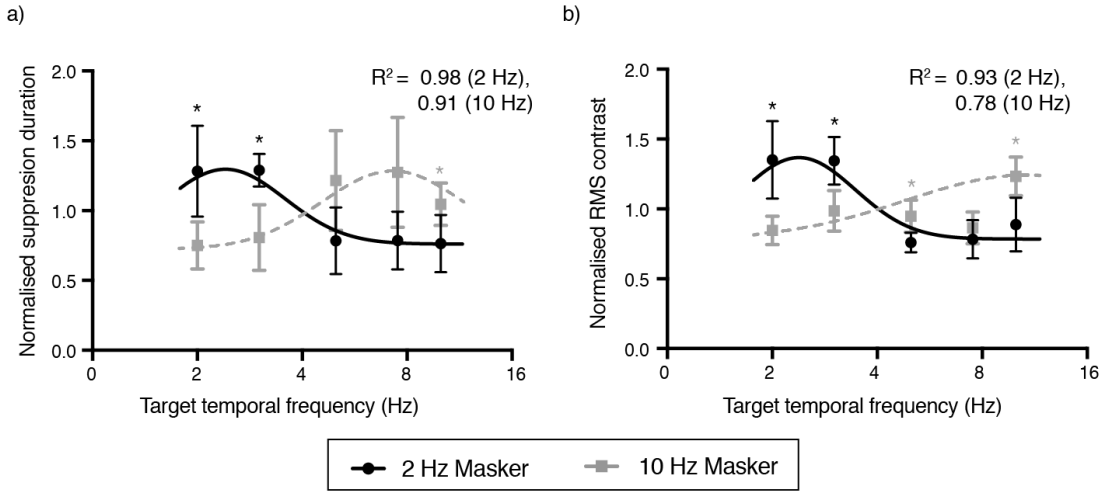

Figure 4.2. (a) Data from Experiment 1 showing the effect of masker and target rates on normalized suppression durations, with target frequency plotted as a logarithmic scale. The data show that CFS suppression duration is strongly dependent on masker–target similarity, increasing with target temporal frequency when the 10-Hz masker was presented and showing a reverse trend when the 2-Hz masker was presented. Group means were described by normal Gaussian functions centered at 1.27 octaves for the 2-Hz masker and 3.25 octaves for the 10-Hz masker. (b) Data from Experiment 1 showing the effect of masker and target rates on contrast thresholds, with target frequency plotted on a logarithmic scale. Gaussian functions were fitted to the group averages and revealed a very similar pattern to the suppression-duration data: a mean frequency of 1.25 octaves for the 2-Hz masker and 3.39 octaves for the 10-Hz masker. All error bars represent 95% confidence intervals, and asterisks indicate significant pairwise comparisons after Holm–Bonferroni correction. Black asterisks indicate that the 2-Hz masker performed better than the 10-Hz masker, and gray asterisks indicate that the 10-Hz masker performed better than the 2-Hz masker.

Using the pooled data, we conducted a 2 × 5 (masker × target temporal frequency) repeated-measures ANOVA. Due to violations of sphericity, statistical significance was assessed with Greenhouse–Geisser correction. Neither masker frequency, $F(1, 7) < 1$, nor target frequency, $F(4, 28) < 1$, had a significant effect on suppression duration, but they interacted significantly, $F(4, 28) = 9.32$, $p < 0.01$, $\eta_p^2 = 0.57$. Shorter normalized durations were produced at higher target frequencies when the 2-Hz masker was presented, and the reverse was true when the masker modulated at 10 Hz. These differences between the two masker frequencies were verified by Holm–Bonferroni-corrected paired-samples *t* tests. Specifically, as plotted in Figure 4.2a, the 2-Hz masker produced significantly longer normalized durations than the 10-Hz masker when the targets modulated at 2 Hz, $t(7) = 3.65$, $p < 0.05$, and 3 Hz, $t(7) = 4.13$, $p < 0.05$. In contrast, the 10-Hz masker produced significantly longer

normalized durations than the 2-Hz masker when the target modulated at 10 Hz, $t(7) = 3.56$, $p < 0.05$.

To further characterize the trends observed, we fitted normal Gaussian functions to each individual's data, with target temporal frequency plotted on a binary logarithmic scale as in Figure 4.2. Using Holm–Bonferroni-corrected paired-samples *t* tests to compare the group mean fit parameters, we determined that normalized durations peaked at 1.41 octaves ($SD = 0.48$) when the 2-Hz masker was presented—significantly lower than the peak duration obtained with the 10-Hz masker, which was located at 2.96 octaves ($SD = 0.35$), $t(7) = 7.56$, $p < 0.001$. Although estimated standard deviations were on average wider with the 10-Hz masker than the 2-Hz masker—1.79 octaves ($SD = 0.82$) and 1.46 octaves ($SD = 0.238$), respectively—this difference did not reach statistical significance, $t(7) = 1.25$, $p = 0.25$. There was no significant difference between the amplitudes of the 2- and 10-Hz maskers, $t(7) = 0.12$ $p = 0.91$. These results for the estimated parameters were not driven by the quality of function fits, as R^2 values were comparable between the two masker frequencies, $R_2^2 = 0.78$ ($SD = 0.07$) and $R_{10}^2 = 0.74$ ($SD = 0.17$).

4.2.2.2 Normalized contrast thresholds

The threshold results for Experiment 1 are summarized in Figure 4.2b. The effect of eye dominance on thresholds was first examined using separate 2 × 5 repeated-measures ANOVAs (eye dominance × target temporal frequency) for each masker frequency. Target temporal frequency had a significant main effect in both instances—2 Hz: $F(4, 36) = 12.16$, $p < 0.01$ (Greenhouse–Geisser corrected), $\eta_p^2 = 0.58$; 10 Hz: $F(4, 36) = 8.03$, $p < 0.001$, $\eta_p^2 = 0.47$. These results were not influenced by eye-specific trends, as eye dominance had no significant effect on thresholds—2 Hz: $F(1, 9) = 3.10$, $p = 0.11$, $\eta_p^2 = 0.26$; 10 Hz: $F(1, 9) < 1$—and did not interact

significantly with target temporal frequency—2 Hz: $F(4, 36) < 1$; 10 Hz: $F(4, 36) = 1.87$, $p = 0.14$, $\eta_p^2 = 0.17$. The data were therefore collapsed across both eyes and reanalyzed with a 2 × 5 repeated-measures ANOVA (masker × target temporal frequency). Our results showed that target temporal frequency had a significant effect on thresholds, $F(4, 36) = 8.22$, $p < 0.001$, $\eta_p^2 = 0.48$, but masker frequency did not, $F(1, 9) < 1$. Similar to the suppression-duration data, both factors interacted strongly, $F(4, 36) = 14.32$, $p < 0.001$, $\eta_p^2 = 0.61$, increasing in magnitude as the difference between target and masker frequencies decreases. These differences were verified by Holm–Bonferroni-corrected paired-samples *t*tests. This showed that the 2-Hz masker produced significantly higher thresholds than the 10-Hz masker when the target modulated at 2 and 3 Hz—t(9) = 3.60, $p < 0.05$, and $t(9) = 3.23$, $p < 0.05$, respectively—and that the 10-Hz masker produced significantly higher thresholds when the target modulated at 5 and 10 Hz—$t(9) = 3.93$, $p < 0.05$, and $t(9) = 3.07$, $p < 0.05$, respectively.

As with normalized durations, normal Gaussian functions were fitted to each individual's threshold data. Fits for two participants were excluded from the group analysis due to poor-quality fits (e.g., R^2 value of 0.15). Estimated parameters from the remaining individual's fits were compared using Holm–Bonferroni-corrected paired-samples *t* tests. Similar to normalized durations, peak threshold elevation produced by the 2-Hz masker occurred at 1.36 octaves ($SD = 0.74$), significantly lower than the 10-Hz masker's 3.02 octaves ($SD = 0.74$), $t(7) = 22.1$, $p < 0.001$. There were no significant differences in estimated amplitude, $t(7) = 2.20$, $p = 0.19$, or standard deviation, $t(7) = 0.06$, $p = 0.95$. Similar to normalized durations, both the 2- and 10-Hz masker frequencies had comparable quality of fit, $R_2^2 = 0.70$ ($SD = 0.18$) and $R_{10}^2 = 0.71$ ($SD = 0.10$), $t(7) = 0.22$, $p = 0.83$.

4.2.3 Discussion

Experiment 1 asked if CFS suppression strength depended on the temporal-frequency difference between target and masker. Using temporally narrowband filtered-noise maskers, we measured the effect of masker temporal frequency at 2 and 10 Hz on the suppression durations and contrast sensitivity thresholds of targets modulating at 2, 3, 5, 7.5, and 10 Hz. Although the suppression-duration data were more variable than contrast thresholds (see confidence intervals in Figure 4.2a and 4.2b), in general, greater suppression durations and contrast thresholds were obtained with increasingly similar target and masker temporal frequencies. This was true regardless of masker frequency, and suggested a strong effect of temporal-frequency selectivity in CFS suppression for both dependent measures. Similar conclusions are supported by analyses of data from individual participants. Specifically, normal Gaussian functions fitted to individual data showed significantly lower estimated means for the 2-Hz masker, but there were no differences in estimated standard deviations and amplitudes. Thus, neither masker frequency was more sensitive to differences in target temporal frequency than the other, nor had a suppressive advantage as has been previously suggested from studies using static targets (Han et al., 2016; Kaunitz et al., 2014; Zhu et al., 2016). What counted in the present experiment, regardless of masker frequency, was the relative difference between target and masker temporal frequency, with maximum suppression occurring for small frequency differences. These results were also not linked to eye dominance, as it neither had an effect on contrast thresholds nor interacted significantly with target temporal frequency.

These observations offer an explanation of the different optimal Mondrian update rates reported in the literature. Nevertheless, the findings are not entirely

surprising. As mentioned earlier, high and low temporal frequencies have been shown to elicit responses in different neuronal populations. Specifically, greater parvocellular responses are recorded at low temporal frequencies and greater magnocellular responses are recorded at higher frequencies (Alitto, Moore, Rathbun, and Usrey, 2011; Derrington and Lennie, 1984; Livingstone and Hubel, 1988). Although the magnocellular and parvocellular pathways are reported to interact (Ferrera, Nealey and Maunsell, 1994; Nealey and Maunsell, 1994; Sawatari and Callaway, 1996), we would expect greater interference, and thereby longer suppression of the target, when targets and maskers engage similar neuronal populations, as the masker is effectively noise in the same channel as the target, with the masker dominating the output because of its much higher contrast.

Neurophysiological studies have shown that activity triggered by higher temporal frequencies is capable of suppressing lower frequencies in the lateral geniculate nucleus, whereas lower frequencies have not been found to inhibit higher frequencies (Fawcett, Barnes, Hillebrand, and Singh, 2004; Freeman, Durand, Kiper, and Carandini, 2002; Hawken, Shapley, and Grosof, 1996; Reid and Alonso, 1996; Shou and Leventhal, 1989; Yen, Fukuda, and Kim, 2012). Similar asymmetrical observations have been reported in a human psychophysical study, with binocularly viewed high-temporal-frequency stimuli (>4 Hz) found to mask low frequencies but not vice versa (Cass and Alais, 2006). These trends were not observed in our data, suggesting that the underlying mechanisms might be cortical in origin. Nevertheless, we did not view the lack of asymmetry as precluding precortical contributions, as interocular competition could occur at multiple levels (Pearson and Clifford, 2006). For instance, although monocular inputs to the lateral geniculate nucleus are largely segregated in separate layers (Meissirel, Wikler, Chalupa, and Rakic, 1997), feedback

signals from V1 may produce fluctuations in lateral geniculate nucleus activity that correlate with rivalry alternations (Haynes et al., 2005; Wunderlich, Schneider, and Kastner, 2006).

4.3 Experiment 2

In Experiment 1, normalized suppression durations and target contrast thresholds increased as target and masker temporal frequencies became similar. Neither masker frequency had a suppressive advantage over the other, producing comparable amplitudes and spreads of normalized durations and thresholds. These results suggested dominant cortical influences, and the goal of Experiment 2 was to evaluate this idea. To do so, we asked if the effect of target orientation on suppression durations and contrast thresholds differs between 2- and 10-Hz maskers. The reasoning behind this approach is as follows. Precortical regions are poorly tuned to orientation (Reid and Alonso, 1996; Shou and Leventhal, 1989) and are more responsive to higher temporal frequencies (Hawken et al., 1996). These properties have been linked to cross-oriented masking in V1 (Freeman et al., 2002), where effective target suppression is produced by fast-modulating, orthogonally oriented maskers (Alitto et al., 2011; Cass and Alais, 2006). Comparing the effect of orientation between 2- and 10-Hz maskers thus allows us to infer the relative contributions of precortical and cortical influences. If CFS suppression were underpinned by substantial precortical influences, the 10-Hz masker would produce a less orientation-specific effect than the 2-Hz masker. In contrast, a more dominant cortical influence in CFS would produce comparable orientation effects on target suppression for both masker frequencies and suppression.

4.3.1 Materials and methods

4.3.1.1 Visual stimuli

All targets and masker stimuli were generated with the same spatiotemporal filtering technique as in Experiment 1 (3 c/° spatially and 2 or 10 Hz temporally), with the addition that these stimuli were also spatially filtered in frequency space using a Gaussian orientation filter with an orientation bandwidth of ±10°. See examples of masker stimuli in Figure 4.1b and Supplementary Movies S3 and S4. Targets and maskers always had the same temporal frequency in this experiment—either both 2 Hz or both 10 Hz—and were either iso- or cross-oriented, making a 2 × 2 factorial combination. Targets and maskers were normalized to maximum contrast (15% RMS) and set to mean luminance. Maskers were approximately 5.4° × 5.4° in dimensions (128 × 128 pixels), whereas targets, measuring 1.5° × 1.5° in diameter, were generated by windowing the spatiotemporally filtered noise images with a small Gaussian mask (SD_{xy} = 8.8 pixels). Both targets and maskers were enclosed in a 0.5°-thick checkerboard frame (5.9° × 5.9° externally and 5.4° × 5.4° internally). Maskers were presented at 95% of maximum contrast and spanned the entire 5.4° × 5.4° area.

4.3.1.2 Participants

Suppression durations and thresholds were measured for two participants (both female; age range: 19–20 years). Another eight participants (six women, two men; age range: 19–24 years, SD = 1.64) completed the b-CFS task, and threshold measurements were recorded for another six participants (two women, four men; age range: 19–30 years, SD = 3.9). All participants had normal or corrected-to-normal visual acuity. Participants also had normal stereovision, assessed using the Fly Stereo Acuity test. All experiments were performed with the approval of the institutional review board of the University of Sydney, and according to the principles of the

Declaration of Helsinki. Informed consent was obtained from all participants. Participants were reimbursed 20 AUD per hour for their participation.

4.3.1.3 Eye-dominance assessment

Eye dominance was assessed with the same test from Experiment 1.

4.3.1.4 Procedure for b-CFS

Targets were presented at a fixed contrast of 5% RMS, modulating at the same rate as the masker temporal frequency. The order of temporal frequency was blocked in a counterbalanced manner. Orientation was also randomized within each block, such that the difference in orientation between targets and maskers in a given trial was either 0° or 90°. This gave rise to a total of four conditions per eye: 2 Hz iso-oriented, 2 Hz cross-oriented, 10 Hz iso-oriented, and 10 Hz cross-oriented. Participants were asked to report, as accurately as possible, the location (which quadrant) and orientation (horizontal or vertical) of the target as soon as it became visible. As in Experiment 1, maskers and targets were ramped in contrast during the initial 1,000 ms of each trial, with the masker presented 50 ms (five frames) before the target. Local adaptation was also reduced by presenting each target in one of four quadrants, with its location randomly chosen from a circle with a radius of 1° around the fixation cross. After each response, 5 s of dynamic white noise was presented to both eyes and the time required for the target to reach visibility was recorded. Twenty trials were recorded for each condition, giving rise to 10 trials per eye and a total of 80 trials per participant. Accurate trials were sorted according to eye dominance, and durations longer than three times the median absolute deviation from the median were identified and removed from each condition. Suppression durations were then normalized to the average duration for each subject across all conditions.

4.3.1.5 Procedure for CFS threshold measurements

For each participant, masker temporal frequencies were presented in counterbalanced blocks, whereas target orientation and eye of origin were randomized within each block. The stimuli were presented on the screen for a total of 2,000 ms, immediately followed by 1,000 ms of dynamic visual white noise. Participants then judged the location of the target, which was presented in one of the four quadrants. The target contrast was varied with a 4AFC QUEST adaptive staircase procedure, and separate staircases were used for each eye and each orientation. These were interleaved within each block and consisted of 25 trials each. Thresholds were estimated by fitting the resulting experimental data with a cumulative Gaussian psychometric function using the maximum-likelihood estimation procedure. As this was a 4AFC task, thresholds were defined as the level of RMS contrast at which accuracy was 62.5%. The estimated thresholds for each participant were then normalized to the participant's average threshold across all conditions (i.e., masker temporal frequency, eye of origin, and orientation).

4.3.2 Results

4.3.2.1 Normalized suppression durations

Prior to comparing the size of orientation effects between the 2- and 10-Hz maskers, we determined whether there were eye-dominance effects by conducting separate 2 × 5 repeated-measures ANOVAs (eye dominance × orientation) for each masker frequency. Orientation had a strong effect on normalized durations produced by 2- and 10-Hz maskers—$F(1, 9) = 30.2, p < 0.001, \eta_p^2 = 0.77$, and $F(1, 9) = 28.8, p < 0.001, \eta_p^2 = 0.76$, respectively. Performance of neither masker was affected by eye dominance—2 Hz: $F(1, 9) = 1.56, p = 0.24, \eta_p^2 = 0.15$; 10 Hz: $F(1, 9) < 1$.

Similarly, the effect of orientation was not dependent on eye dominance—2 Hz: $F(1, 9) = 1.50$, $p = 0.25$, $\eta_p^2 = 0.14$; 10 Hz: $F(1, 9) < 1$.

Having established that there was no effect of eye dominance, we pooled across both eyes and processed raw suppression-duration data with the same exclusion criteria (i.e., accurate trial, no more than three times the median absolute deviation). We then conducted a 2 × 2 (masker temporal frequency × orientation) repeated-measures ANOVA. The results are plotted in Figure 4.3a. There were significant main effects of masker temporal frequency, $F(1, 9) = 9.91$, $p < 0.05$, $\eta_p^2 = 0.52$, and target orientation, $F(1, 9) = 53.86$, $p < 0.0001$, $\eta_p^2 = 0.86$. These factors interacted significantly, $F(1, 9) = 8.08$, $p < 0.05$, $\eta_p^2 = 0.47$, and we examined this interaction more closely with Holm–Bonferroni-corrected paired-samples *t* tests. In general, iso-oriented target–masker combinations produced significantly longer normalized durations—2 Hz: $t(9) = 5.24$, $p < 0.01$; 10 Hz: $t(9) = 5.32$, $p < 0.01$. As shown in Figure 4.3b, this difference was significantly larger for the 2-Hz masker, $t(9) = 2.84$, $p < 0.05$, and was driven by the significantly longer durations for the 2-Hz iso-orientation condition, $t(9) = 3.01$, $p < 0.05$.

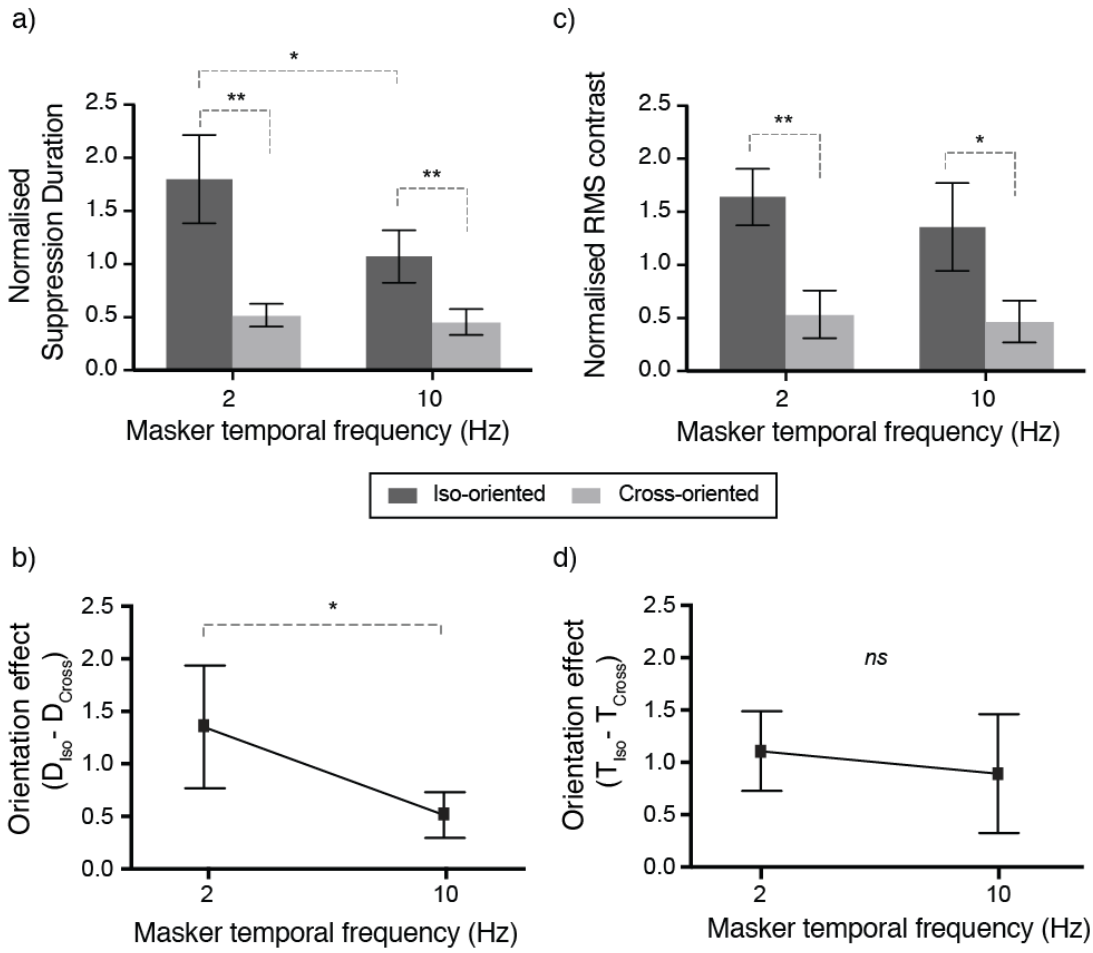

Figure 4.3. (a) Data from Experiment 2 showing the effect of orientation and masker rates on target suppression durations. Suppressed targets were narrowband spatially filtered noise temporally modulating at either 2 or 10 Hz and were orientationally filtered to have the same or orthogonal orientation as the masker (i.e., iso-oriented and cross-oriented). Iso-oriented targets remained suppressed for longer durations, and this increase was larger with the 2-Hz masker than the 10-Hz masker. (b) Data from the same experiment showing the effect of masker rates on the size of orientation effects in normalized durations. Changes in normalized durations were larger for the 2-Hz masker compared to the 10-Hz masker, demonstrating a stronger orientation selectivity in the 2-Hz maskers. (c) Data from the same experiment showing the effect of orientation and masker rates on target contrast sensitivity thresholds. Similar to target suppression durations, thresholds were raised when the target and masker shared the same orientation, and this was true regardless of masker temporal frequency. However, we do not observe the same suppressive advantage in the 2-Hz iso-orientation condition. (d) Data from the same experiment showing the effect of masker rates on the size of orientation effects in normalized thresholds. Unlike suppression durations, orientation had a comparable effect on normalized thresholds for 2- and 10-Hz maskers. Asterisks denote statistical significance after Holm–Bonferroni-corrected paired-samples *t* tests (*$p < 0.05$, **$p < 0.01$, ***$p < 0.001$), and all error bars represent 95% confidence intervals.

4.3.2.2 Normalized contrast thresholds

To examine the effect of eye dominance, the data were first analyzed with separate 2 × 2 repeated-measures ANOVAs (eye dominance × orientation) for each masker temporal frequency. Similar to Experiment 1, eye dominance did not

influence thresholds—2 Hz: $F(1, 7) < 1$; 10 Hz: $F(1, 7) = 1.2$, $p = 0.31$, $\eta_p^2 = 0.15$—nor interact significantly with orientation at either frequency—2 Hz: $F(1, 7) < 1$; 10 Hz: $F(1, 7) = 2.08$, $p = 0.19$, $\eta_p^2 = 0.23$. In contrast, orientation strongly affected thresholds—2 Hz: $F(1, 7) = 47.4$, $p < 0.001$, $\eta_p^2 = 0.87$; 10 Hz: $F(1, 7) = 13.8$, $p < 0.01$, $\eta_p^2 = 0.66$. The data were therefore collapsed across both eyes and analyzed in a 2 × 2 repeated-measures ANOVA, with masker frequency and orientation as independent variables. The results are summarized in Figure 4.3c. Holm–Bonferroni-corrected paired-samples *t* tests were also conducted to evaluate the results of the ANOVA. Similar to the b-CFS results, there was a strong effect of orientation, $F(1, 7) = 36$, $p < 0.001$, $\eta_p^2 = 0.84$. There was, however, no effect of masker frequency, $F(1, 7) = 1.75$, $p = 0.23$, $\eta_p^2 = 0.20$, and no significant interaction between masker frequency and orientation, $F(1, 7) < 1$. As with suppression durations, we found significantly higher thresholds for the 2- and 10-Hz iso-orientation conditions—$t(7) = 6.89$, $p < 0.001$, and $t(7) = 3.71$, $p < 0.05$, respectively. However, there was no significant difference between the change in normalized thresholds for 2 and 10 Hz, $t(7) = 0.91$, $p = 0.40$.

4.4 General Discussion

Despite the widespread use of CFS in studies of unconscious processing and awareness, work elucidating its underlying mechanisms is still incomplete. For example, faster masker refresh rates have generally been associated with greater interocular suppression (e.g., Xu et al., 2011), but recent studies show that this view is simplistic. Prolonged, static target presentations are more effectively suppressed by slower Mondrian update rates, for example, ~6 Hz (Zhu et al., 2015; Zhu et al., 2016), whereas rates up to 28.5 Hz are required for brief target presentation times (Kaunitz et al., 2014). The disparity in trends could be attributed to temporal-frequency

selectivity, as the Mondrian masker contains more low-frequency energy at slow refresh rates and more high-frequency energy at faster update rates (Figure 4.1a). To test this idea, we presented a range of combinations of target and masker temporal frequency (i.e., 2- and 10-Hz maskers; targets at 2, 3, 5, 7.5, and 10 Hz). Two dependent measures were recorded—suppression duration and target contrast thresholds—as this allowed us to verify results obtained with the b-CFS paradigm. Since the b-CFS paradigm relies on subjective reports of visibility, measuring contrast thresholds provides a second, more objective dependent measure that allows us to rule out nonperceptual effects such as differences in participant criteria (Yang et al., 2014).

Consistent with our hypothesis, Experiment 1 showed that suppression in CFS is temporal-frequency selective. Normalized durations and thresholds increased as the difference between target and masker temporal frequencies decreased, regardless of masker frequency. Gaussian approximations of the tuning functions also revealed that, apart from differences in estimated mean frequency, no significant differences in the estimated amplitudes and bandwidth were obtained for either dependent measure. In Experiment 2, clear increases were obtained in both dependent measures when iso-oriented targets and maskers were presented, regardless of masker frequency. We also compared the sizes of orientation effects between the 2- and 10-Hz maskers, and found a significantly larger orientation effect with the 2-Hz masker when suppression durations were recorded, although this effect was not replicated with contrast thresholds. Presenting the masker in the dominant eye has been shown to produce greater interocular suppression (Yang, Blake, and McDonald, 2010), but this was not observed in our study. No significant effect of eye dominance was obtained, regardless of dependent measure. This might be related to the use of sighting

dominance as an eye-dominance assessment, as the current evidence linking sighting dominance and interocular suppression is mixed (Bosten et al., 2015; Dieter, Sy, and Blake, 2017). Nevertheless, the results did consistently reveal strong selectivity for orientation and temporal frequency in both dependent measures, suggesting that any effect of eye dominance would not have resulted in a drastic change in trend.

We discuss the implications of the findings as follows. First, the b-CFS paradigm is often criticized for its susceptibility to non-perceptual effects such as participant decisional criteria (Yang et al., 2014). To account for these influences, a control where the target stimulus is presented in the masking eye is typically included and compared with the CFS condition (e.g., Jiang et al., 2007). Unfortunately, this comparison has been shown to be inappropriate (Stein et al., 2011), leading to the proposal that results obtained from this comparison method are better interpreted as evidence for differences in mere stimulus detectability (Stein and Sterzer, 2014). Similar trends between suppression durations and contrast thresholds were obtained in this study, suggesting that normalized duration could provide an excellent proxy for the more objective measure of contrast elevation, at least for investigations into CFS mechanisms. One exception was the size of orientation effects for the 2- and 10-Hz conditions; the suppression-duration data revealed a significantly larger effect of orientation in the 2-Hz condition, but this was not replicated with contrast thresholds. We do not have a firm understanding of this result, though given the inconsistent results and variability in the data (Figure 4.3b through 4.3d), it might be driven by differences in stimulus detectability and participant decisional criteria in the b-CFS task. The longer exposure period in b-CFS might also have a stronger adaptation effect on the 10-Hz masker (see Solomon, Peirce, Dhruv, and Lennie, 2004), thereby weakening its orientation effect. Note that these results contrast with those of Cass

and Alais (2006), who observed clear asymmetric inhibition of low frequencies and cross-oriented masking by high temporal frequencies. Obtaining these differences might be dependent on the type of visual presentation, as Cass and Alais (2006) used binocularly viewed maskers and targets.

Second, by demonstrating that the suppression of temporal information is frequency selective and sensitive to orientation, we extend the work of previous CFS studies (Moors et al., 2014; Yang and Blake, 2012), contributing to an emerging theme that CFS suppression may be inherently feature specific. Contradictory evidence does exist in the literature, but our view is that in the absence of spatiotemporal control with narrowband stimuli, it is difficult to determine the extent to which feature selectivity influences CFS suppression. For example, Ananyev et al. (2017) found that regardless of target speed, slow-moving Mondrian patterns (1°/s–2°/s) were most effective in suppressing a moving circular disk. Barring more complicated processes, basic spatiotemporal attributes of the stimuli could offer an explanation. As both the target and the masker patterns were composed of shapes with sharp spatial edges and uniform luminance, the spatial profiles would be broadband and $1/f^n$. Mathematically, temporal frequency is the product of spatial frequency and velocity, meaning that the stimuli would be biased toward low temporal frequencies. It therefore seems probable that the low-pass tuning observed in the study by Ananyev et al. might be a consequence of temporal-frequency selectivity. Such specificity is reminiscent of early visual cortical regions such as V1, where neurons exhibit narrow tuning functions to stimulus dimensions such as orientation, spatial frequency, and temporal frequency. Indeed, studies interested in the neural substrates of CFS suppression have implicated early visual areas (Maier et al., 2008; Watanabe et al., 2011; Yuval-Greenberg and Heeger, 2013). Robust activity reduction in higher

visual areas has also been reported (Fang and He, 2005; Hesselmann and Malach, 2011; Jiang and He, 2006), and it is possible that the use of spatiotemporally controlled stimuli like the ones used in the current study might shed some light on how these areas influence each other during CFS suppression.

Third, temporal-frequency selectivity could offer possible explanations for phenomena such as stimulus fractionation in CFS (Moors, Hesselmann, Wagemans, and van Ee, 2017; Zadbood, Lee, and Blake, 2011). Bearing resemblance to independent form- and motion-suppressive processes in rivalry (Alais and Parker, 2006), CFS suppression was reportedly more effective on the form of the target than its temporal information. Visibility of temporal modulations increases with temporal rate but not target form, which remained suppressed (Zadbood et al., 2011). Since the Mondrian masker is biased toward low frequencies (Figure 4.1), temporally selective processes cannot exert substantial suppression on higher target frequencies. This is important, as it explains the increased dissociation between form and temporal information at higher target-modulation rates. Similarly, the low temporal dominance of the Mondrian masker could explain the preservation of dorsal-stream activity in CFS (Fang and He, 2005). Low temporal frequencies are more likely to elicit parvocellular responses (Derrington and Lennie, 1984) that feed into the ventral stream (Merigan and Maunsell, 1993). As a result, dorsal activity that is elicited by target attributes such as high temporal frequencies (Derrington and Lennie, 1984; Merigan and Maunsell, 1993) and elongated shapes (Sakuraba et al., 2012) is inevitably spared. As pointed out by Ludwig and Hesselmann (2015), differences in the extent of dorsal preservation (see Fogelson, Kohler, Miller, Granger, and Tse, 2014; Hesselmann and Malach, 2011) would then depend on the low-level

characteristics of the target and masker presented and the method of presentation used.

Last, our findings can be distinguished from those of Alais and Parker (2012), who used spatiotemporally filtered stimuli similar to ours in a binocular-rivalry paradigm. Their competing stimuli were matched for size, contrast, spatial frequency, and orientation content, so that the only difference between them was temporal frequency, which was carefully manipulated. Rivalry alternations were only reliably reported when modulation rates differed by about two octaves (a fourfold difference), proving that interocular suppression can arise from temporal-frequency differences alone. This result differs from the temporally selective suppression observed in the present CFS study, but so too do the stimulus conditions. Here, spatially similar stimuli differ interocularly in size and contrast, whereas in the rivalry example only the temporal frequency differed (without which the images would fuse). Therefore, the two studies and their conclusions are not directly comparable. However, because rivalry and CFS paradigms both involve interocular suppression, we speculate that differences between the two studies may be related to the size disparity between masker and target in CFS. It is known in binocular rivalry that surrounding one rival image with a spatially similar annulus (e.g., same orientation) enhances suppression of the competing image—regardless of which eye receives the surround (Paffen et al., 2006; Paffen et al., 2004)—and thus the use of the large maskers and spatially similar targets in our study may contribute additional suppression in CFS.

The feature-selective nature of CFS suppression has very important consequences. In particular, care should be taken when pairing targets and maskers to ensure that their stimulus properties overlap, to make sure the stimulus attributes of the target are appropriately suppressed by the masker. Spatiotemporally controlled

stimuli like the ones we have used here and elsewhere (Han et al., 2016) afford a high degree of stimulus control so that targets and maskers can be well matched. This is difficult with the commonly used dynamic Mondrian masker, as its amplitude spectrum, both temporally and spatially, is pink—that is, low frequencies dominate and high frequencies are only weakly present (Han et al., 2016; Yang and Blake, 2012). This means that there is the potential for some target attributes to escape interocular suppression, and this may lead to misleading reports of targets being processed in the absence of awareness. Our view is that careful matching of masker and target properties is very important in CFS research, both for elucidating the specific underlying mechanisms and for providing a more rigorous test for claims of processing without awareness.

4.6 Conclusions

This study mapped the temporal tuning of CFS suppression with temporally narrowband maskers and targets and found strong evidence of feature selectivity for temporal frequency. Two dependent measures, target suppression duration and target contrast threshold, both increased as the temporal-frequency difference between target and masker decreased. This pattern held for low- and high-frequency maskers, with consistent patterns for both measures showing that the two dependent variables are highly correlated. These findings add to evidence demonstrating feature selectivity in both binocular rivalry and CFS (Maehara et al., 2009; Moors et al., 2014; Yang and Blake, 2012) and suggest that a single model of interocular suppression could explain both paradigms. Finally, feature specificity has important implications for choosing CFS stimuli, as poorly matched maskers and targets may lead to particular target attributes escaping significant suppression and leading to spurious claims of processing without awareness.

Chapter 5
General Discussion

In CFS, a dynamic Mondrian sequence is presented to one eye while a static target is being presented to the other eye. It is widely used in studies of unconscious visual processing (e.g., Faivre et al., 2012), but investigations into its underlying mechanisms remain underway. Comparisons between CFS and more well documented dichoptic stimulation techniques such as BR and FS are common (e.g., Tsuchiya and Koch, 2005; Tsuchiya et al., 2006; Yang and Blake, 2012), but the extent of shared processes among these paradigms remains unclear. Nevertheless, studies generally attribute the effectiveness of CFS to the rapid pattern changes (or transients) in the dynamic Mondrian (e.g., Tsuchiya and Koch, 2005; Tsuchiya et al., 2006; Yang and Blake, 2012). This assumption has not been properly tested, and my goal in this work was to evaluate the importance of transients in CFS. To do so, I examined the role of temporal frequency in CFS, as it was a straightforward approach of varying the amount of transients presented.

Temporal frequency was also studied because the seeming importance of transients in CFS contrasted with BR, which did not appear to rely strongly on temporal modulations. For example, motion stimuli were typically used to introduce temporal modulations in BR, but rivalry was only possible between dichoptically presented motion if there were also some form of spatial conflict, such as a difference in motion direction or speed (Nguyen et al., 2003; Alais and Parker, 2006). In addition, BR has been shown to occur less with higher temporal frequencies (Carlson and He, 2000). Hence, studying the role of temporal frequency in CFS would provide further insight on the relationship between CFS and BR. In the following section, I present the main findings of this thesis and discuss their implications in Section 6.3.

The future directions of this research are presented in Section 6.4, and the thesis concludes in Section 6.5.

5.1 Summary of main findings

I studied the role of temporal frequency by measuring the temporal frequency tuning function of CFS (Chapter 2). This approach tested two main assumptions of CFS research, namely, the method of manipulating temporal frequency by varying the number of patterns per second and the importance of transients in CFS suppression. I opted for the more precise manipulation of periodic changes in pixel luminance over time (cycles per second), because the more common method of manipulation (i.e., patterns per second) neglects the pixel luminance changes between each pattern update (see Figure 2.1 in Chapter 2). A Fourier transform analysis was first conducted on the Mondrian masker, revealing a low-pass temporal frequency spectrum. If the two methods of manipulating temporal frequency were equivalent, I would replicate the broad tuning functions obtained by previous studies (Tsuchiya and Koch, 2005; Zhu et al., 2016). Using temporally narrowband maskers, I measured a narrow, low frequency peak around 1 Hz that became more pronounced with higher spatial frequency and visual contrast. These observations argued against the importance of transients in CFS and were in favour of low temporal frequencies. However, as the temporally narrowband noise maskers were devoid of spatial edges and contours, it was possible that relevant mechanisms such as pattern masking were not considered. It was also possible that the tuning observed with noise maskers was not reflective of that in CFS, which is typically conducted with dynamic Mondrian sequences.

The second study (Chapter 3) addressed these issues. I re-assessed the low frequency bias and examined the relationship between temporal frequency and the Mondrian pattern. Consistent with Study 1, slower maskers (< 4 Hz) were more

effective than faster maskers, but they also worked better with coherent edge structure. Since pattern masking is more likely to be effective with shorter temporal intervals (Enns and Di Lollo, 2000), this suggests that the results of the first study were not a consequence of excluding spatial edges and contours. The second study also revealed an interaction between low and high spatial frequency pattern components (i.e., solid areas and pattern edges respectively). Specifically, reducing the structural integrity of solid areas weakened suppression strength when pattern edges were relatively intact, but not when the edges were phase-scrambled to a larger extent. These results may have an underlying mechanism similar to that of scene perception, where interactions between low and high spatial frequency image components were attributed to interactions between early and late visual processing regions (e.g., Peyrin et al., 2010).

The final study of this thesis (Chapter 4) addressed the conflicting tuning functions obtained in the CFS literature. For example, tuning functions measured with static targets tended to peak broadly around pattern update rates of 3-10 Hz (Tsuchiya and Koch, 2005; Zhu et al., 2015; but see Xu et al., 2011), whereas rapid update rates were likely to be more effective when masking transient targets (Kaunitz et al., 2014). Since increasing the number of patterns presented per second broadens the temporal frequency spectrum (Figure 4.1), the low temporal frequency tuning observed in the first two studies might be a consequence of temporal selectivity. Thus, I tested the hypothesis that CFS is temporal-frequency selective in the final study of this thesis. As in the first study, temporally narrowband filtered-noise maskers were used, as these provide finer spatiotemporal control. As expected, the results showed that CFS was more effective when targets were of a similar frequency as the masker. Interestingly, the strength of the temporal frequency selectivity did not differ between

low (2 Hz) and high (10 Hz) frequency maskers, and there was no conclusive evidence that the magnitude of orientation selectivity varied between the two types of maskers. Binocularly viewed, high and low temporal frequency stimuli have been shown to have an asymmetrical relationship, with high frequencies (> 4 Hz) being capable of masking lower frequencies but not vice versa (Cass and Alais, 2006). This asymmetrical relationship resembles interactions between high and low frequencies in the LGN (e.g., Fawcett et al., 2004), which is also less orientation selective than cortical regions. Thus the comparable magnitudes of temporal frequency and orientation selectivity obtained with the low and high frequency maskers in the final study suggest predominant cortical influences in CFS.

5.2 Implications

The results of this thesis have three main implications, to be discussed in detail in the sections below. The first is the need to consider an alternative method of manipulating temporal frequency when assessing CFS. That is, instead of construing temporal frequency as the number of pattern changes per second, cycles per second could be a useful alternative. The second is the relationship between BR and CFS. The third implication pertains to the effective use of CFS and the factors to be considered.

5.2.1 Manipulating temporal frequency

I adopted an alternative method of manipulating temporal frequency, varying the number of periodic changes in pixel luminance per second instead of number of pattern updates per second. The results showed that the two methods of manipulation were not functionally equivalent, and they also argued against the importance placed on transients (e.g., Tsuchiya and Koch, 2005). A contrarian sceptic might contend that, instead of providing insight into CFS mechanisms, my findings reveal an

alternative dichoptic stimulation method. Given that the low frequency narrowband noise maskers were as effective as the standard Mondrian masker (Chapter 2, Figure 2.3c), this new dichoptic stimulation technique also has the advantage of better spatiotemporal control than the regular Mondrian sequence. However, as there was no evidence pointing to a different mechanism, I defaulted to a simpler position: manipulate temporal frequency with more precision.

Apart from simplicity, the main benefit of the parsimonious approach lies in its explanatory power. For example, studies found that CFS suppression peaked broadly around pattern refresh rates of 3-10 Hz when static targets were used (Tsuchiya and Koch, 2005; Zhu et al., 2016), but increased with refresh rates when transients targets were presented (Kaunitz et al., 2014). By manipulating temporal frequency with more precision, I found that the broad tuning function obtained with static targets was an inevitable consequence of the temporal content of the traditional flickering masker, which remained low-biased across refresh rates (Figure 2.1d of Chapter 2). As described by Figure 2.1c of Chapter 2, I learnt that pixel luminance timelines tended to modulate approximately three times slower than the nominal rate, at ~3 Hz for a 10 Hz refresh rate. Refresh rates of 3 to 10 Hz should produce luminance modulations of around 1 to 3 Hz, which are frequencies that fall within the same frequency channel as the 1 Hz peak (Anderson and Burr, 1985; Cass and Alais, 2006; Snowden et al., 1995). Since the peak refresh rates of 3 to 10 Hz were observed with static targets (e.g., Tsuchiya and Koch, 2005), the correspondence to the low temporal frequency channel suggested that CFS suppression was temporal frequency selective. This could explain the positive relationship observed between pattern refresh rates and CFS suppression strength when transient targets were used in previous research (Kaunitz et al., 2014). Consistent with this idea, I found evidence of

temporal frequency selectivity in CFS in the final study (see trends in Figure 4.2 of Chapter 4).

Manipulating temporal frequency by varying the number of periodic changes in pixel luminance per second also provides a better explanation for stimulus fractionation. As discussed in Chapter 4, stimulus fractionation is a phenomenon where CFS is more effective on some low-level properties of a target than others. For example, CFS was found to be more effective on the spatial form of a target than its temporal information, and this dissociation increased when the temporal rate of the target increased (Zadbood et al., 2011). Assuming that the number of pattern changes were a valid measure of temporal content, then based on the feature-selective nature of CFS (e.g., Moors et al., 2014; Yang and Blake, 2012), we would predict greater dissociation between form and temporal information at low target-modulation rates. Empirically, however, greater dissociation was reported for higher target rates (Zadbood et al., 2011). These observations could be explained by the Mondrian's 1/f distribution of temporal luminance modulations (Figure 2.1d of Chapter 2) and the temporal-selective nature of CFS (Figure 4.2 of Chapter 4), which were observations obtained with a more precise manipulation of temporal frequency.

A second benefit is the provision of new predictions and new insights. The finding of a 1/f temporal frequency spectrum for the Mondrian masker demonstrated how temporal whitening could be involved in our perception of CFS. As aforementioned in Chapter 3, temporal whitening is a phenomenon where participants consistently overestimate the proportion of high spatial and temporal frequency energy across different spatiotemporal profiles of broadband noise stimuli (Cass et al., 2009). This overestimation could explain the salience of transients in the Mondrian masker, even though the stimulus is biased towards low temporal frequencies. With

regard to the mechanism underlying temporal whitening, previous studies have suggested that it could involve asymmetrical inhibition in temporal frequency processing, i.e., high frequencies (> 4 Hz) inhibit low frequencies but not vice versa (Cass and Alais, 2006; Cass et al., 2009). Such asymmetrical interactions have been observed in pre-cortical regions (Fawcett et al., 2004), raising questions regarding the involvement of these regions in CFS.

The Mondrian's 1/f distribution of temporal luminance modulations (Figure 2.1d of Chapter 2) also showed that Mondrian masker was more temporally predictable than its stochastic impression. This contrasted with the spatial layout of the Mondrian's pattern edges, which was randomly sampled per pattern update and was not strongly correlated among the different pattern updates (Figures 5.1a-b). If the predictability of Mondrian sequences were to have any effect on CFS effectiveness, one would expect spatial uncertainty to have a larger contribution than temporal uncertainty. Indeed, in work conducted outside the scope of this thesis, I found a modest effect of spatial entropy on the predominance of the Mondrian masker and no convincing effect of temporal entropy on the Mondrian's predominance (Figure 5.1c). As illustrated in Figure 5.1d, this trend remained when two Mondrians of varying spatiotemporal predictability but equal RMS contrast were pitted against each other.

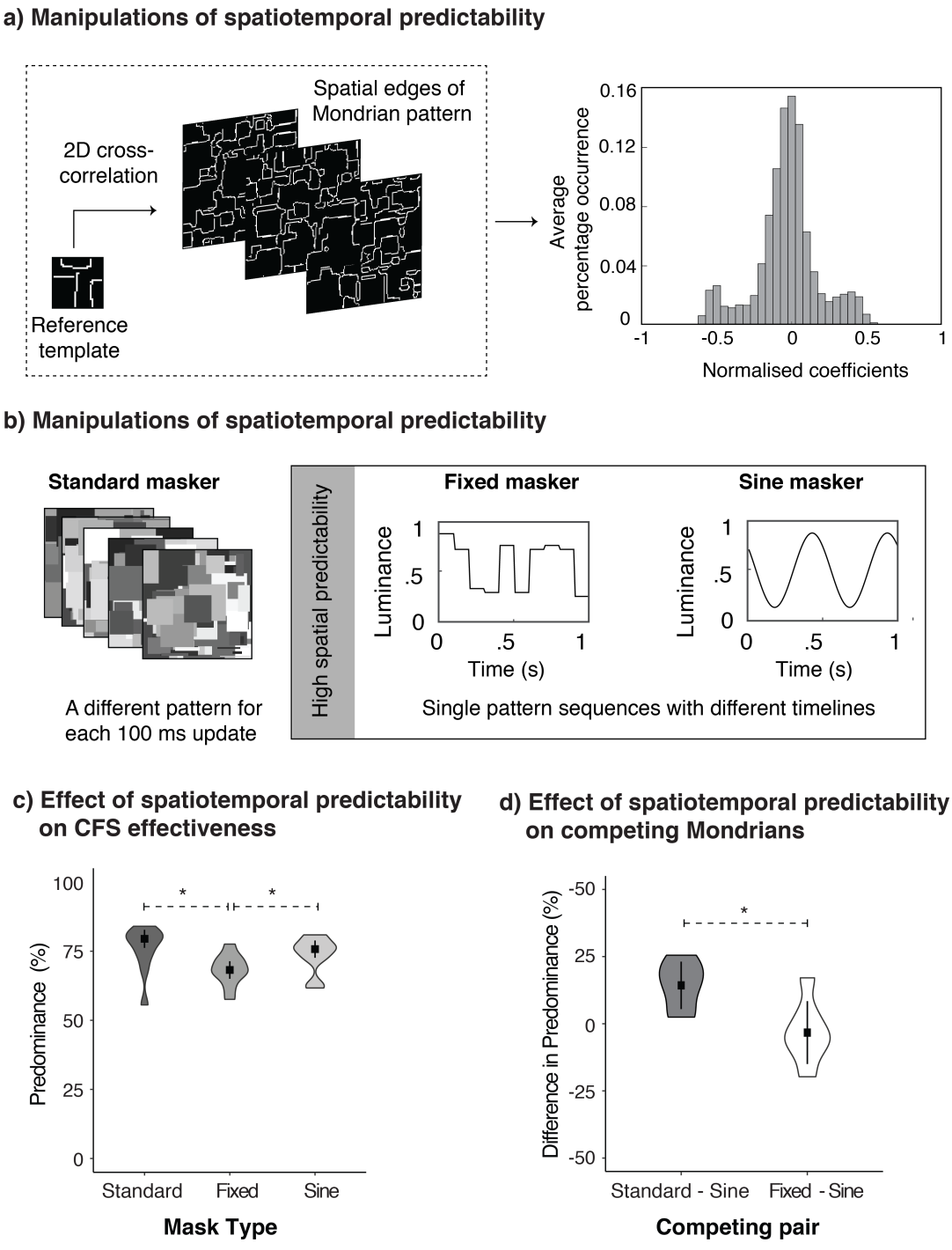

Figure 5.1 Effect of spatiotemporal predictability. (a) Spatial correlations among different pattern updates of the Mondrian sequence. Spatial edges of each pattern (128 by 128 pixels) were first extracted using the Canny method (Canny, 1986). Then, using a reference template (30 by 30 pixels) extracted from the first pattern of the sequence, I performed a two-dimensional cross-correlation on the pattern edges of the remaining patterns. The resultant histogram of the normalised cross-correlation coefficients peaked around zero, revealing a weak correlation among spatial patterns. (b) Manipulations of spatiotemporal predictability of the Mondrian sequence. The Standard Mondrian masker had the highest spatiotemporal unpredictability. It was updated with a random pattern every 100 ms, resulting in random changes in luminance and spatial pattern profiles. Generating single pattern sequences increased spatial predictability, and two generated sequences were the Fixed and Sine maskers. The Fixed masker had the same temporal timeline as the Standard masker whereas the Sine masker modulated regularly (and more

predictably than the Fixed masker) at 2 Hz. The temporal frequency content was comparable across all three maskers as the Standard and Fixed Mondrian sequences were temporally 1/f (Cf. Figure 2.1d of Chapter 2). (c) The effectiveness of the three sequences as CFS maskers were assessed in a tracking paradigm, in which participants tracked the visibility of a 0.125 Hz contrast-modulating bullseye target. The violin plots represent the distributions of data points, the median and the median absolute deviation (denoted by error bars). Each data point represented the percentage of viewing time in which the Mondrian sequence was dominant (predominance). Demonstrating the importance of spatial unpredictability, Fixed maskers had a significantly lower predominance than Standard maskers. However, this effect was limited to the stepped timeline of the Fixed maskers, as Sine maskers were as effective as Standard maskers and performed better than Fixed maskers. (d) Matched in RMS contrast, the different Mondrian sequences were pitted against each other in a rivalry paradigm. To compare their respective effectiveness, I computed the subtracted the predominance of the Sine masker from the Standard and Fixed masker respectively. The results showed that spatial unpredictability (Standard–Sine) produced a larger effect on Mondrian predominance than temporal unpredictability. All pairwise comparisons were conducted with the Wilcoxon signed-rank test in R (R Core Team, 2017) and subjected to Holm-Bonferroni corrections where applicable. Error bars represent the median absolute deviation of individual data points.

Finally, a third benefit of manipulating temporal frequency more precisely is that it is now possible to conduct CFS studies with more spatiotemporal control. Given the inconsistent conclusions on the unconscious processing of threat-related stimuli (Hedger et al., 2016), greater spatiotemporal control can only provide more clarity about observed effects and allay doubts that an observed effect is a mere product of confounding spatiotemporal factors. Moreover, adopting a different method of manipulation does not mean that the stepped transients of the Mondrian have no role in CFS suppression. They probably do, though my findings would suggest that they play a smaller role than previously assumed (Chapters 3-5). One speculation is that the transients provide dichoptic masking, and having a stepped presentation schedule in the Mondrian masker is a convenient way to simultaneously generate transients with a preponderance of a low temporal frequencies. Understanding how transients contribute to CFS would therefore be a question for future investigation, as it would inform us how to best generate CFS, and when to use the Mondrian masker.

5.2.2 Relationship to BR

As discussed in the Introduction, the similarities between CFS and BR provided an opportunity to evaluate my empirical findings against a BR framework. Both paradigms exhibit qualities that resemble a P/ventral pathway bias, such as the suppressive advantage provided by edges and high visual contrast (Maehara et al., 2009; Tsuchiya and Koch, 2005; Baker and Graf, 2009a; see also Table 3 in Section 1.6 of Chapter 1). However, temporal frequency appeared to affect each paradigm differently, as the nominal 10 Hz Mondrian refresh rate in CFS was too high for a P/ventral pathway biased mechanism (Derrington and Lennie, 1984). By re-defining temporal frequency in terms of luminance, I showed that the nominal refresh rate was actually characterised by slow rates of luminance changes in the temporal frequency spectrum (Chapter 3). The low-biased temporal frequency content was also related to suppression strength, which was further enhanced by spatial edges (Chapters 3-4). Consistent with previous research (Tsuchiya and Koch, 2005), suppression was enhanced by higher masker contrasts. Raising masker contrast also did not plateau beyond the saturation of M neurons, i.e., 30 % and above (Green et al., 2009; Chapter 3). These properties were reminiscent of the P/ventral pathway bias in BR, resolving the discrepancy observed with the conventional method of manipulating temporal frequency. Table 6 presents the updated comparisons between BR and CFS, and shows how similar they are on several relevant stimulus dimensions.

Table 6: Some factors that influence BR and CFS suppression (updated)

Factors	BR	CFS
Spatial frequency	Enhanced by phase-aligned high spatial frequency, e.g., images with naturalistic edges have a greater predominance (e.g., Baker and Graf, 2009a).	Image contours are capable of cross-channel suppression (Maehara et al. 2009). Longer suppression durations when maskers contain intact pattern edges (Han et al., 2018; Chapter 3)
Temporal frequency	Lower incidence of rivalry at high frequencies (Wolfe, 1983), but transients reset perceptual dominance temporarily (Blake et al., 1990).	Longer suppression durations with lower temporal frequencies (Han et al., 2016; Chapter 2). Faster rates are required for transient targets (Kaunitz et al., 2014; Han and Alais, 2018; Chapter 4).
Relative visual contrast	Enhanced by higher contrast, e.g., average dominance durations increase with contrast when the stimuli are small (Kang, 2009).	Suppressions durations tend to increase with contrast (Tsuchiya and Koch, 2005), especially when maskers are of lower temporal frequency content (Han et al., 2016; Chapter 2)
Feature selectivity	Enhanced when rivalling stimuli share similar features e.g., higher contrast thresholds when rivalling stimuli share similar orientations (Stuit et al., 2009).	Stronger suppression with similar spatial frequencies (Yang and Blake, 2012) and speeds (Moors et al., 2014).

Understanding that CFS may have a P/ventral pathway bias and is very similar to BR opens up the possibility of using BR as a reference for understanding the differences between the two paradigms. For example in Chapter 4, I found evidence of temporal frequency selectivity in CFS, but reliable BR alternations were only reported for frequencies that were about two octaves apart (Alais and Parker, 2012). Since the targets used in Chapter 4 were spatially matched to the larger-sized masker, the difference might be explained by surround suppression. In surround suppression, the suppression of a rival image could be enhanced by adding a spatially similar annulus (Paffen et al., 2006), and this effect can operate in interocular (dichoptic surrounds), monocular or binocular presentations (Chubb, Sperling and Solomon, 1989; Paffen et al., 2004; Paffen et al., 2005). Consistent with this idea, I found evidence of surround suppression in another collaborative study conducted beyond the scope of this thesis. In that study, I measured the effectiveness of Mondrian

maskers made of 1-dimensional spatial noise and compared the effects of collinear and non-collinear surrounds. As expected, when the maskers were enlarged with collinear surrounds, suppression was less effective than maskers with non-collinear surrounds and maskers without surrounds (see Figure 5.2 below). Given that the Mondrian patterns are randomly sampled and are less likely to have a high degree of collinearity between the central and surrounding portions of the masker, it made sense why CFS seems to immune to changes in masker size. Larger BR stimuli tend to have more incidences of piecemeal rivalry (Blake et al., 1992) and tend to conform to Levelt's original second proposition (Kang, 2009), presumably because the stimulus contours are not stochastically updated like CFS.

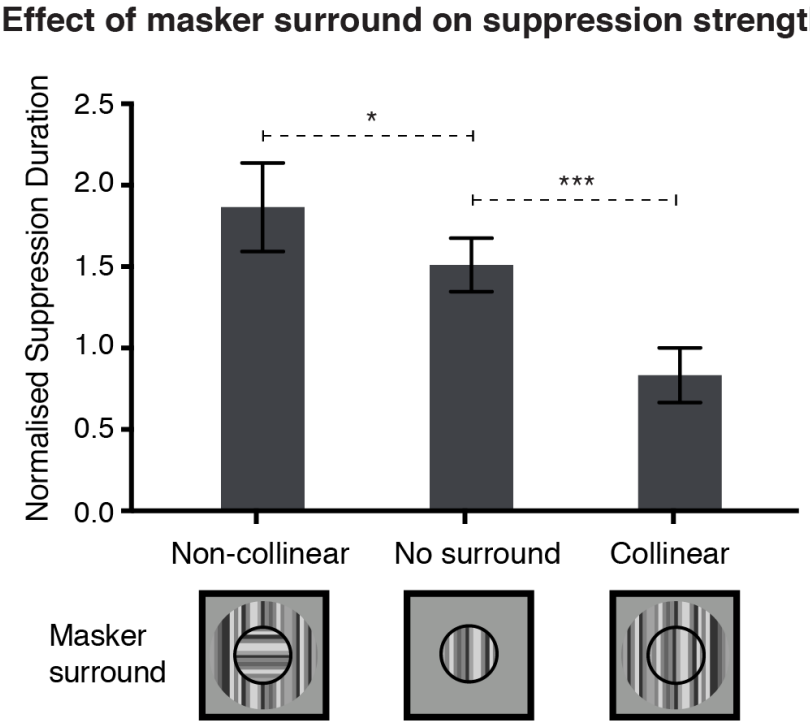

Figure 5.2 Effect of level of masker contour collinearity on CFS suppression. The performance of a central masker (radius of 1.29°) was recorded in the presence or absence of surrounds (external radius of 3.2° and internal radius of 1.38°, 9° gap between surround and central mask) that were either collinear to the central mask or orthogonal to the central mask. All maskers were presented at high contrast (RMS = 20 %) and were used to suppress a 3 cpd sinusoidal grating (radius of 1°) tilted 5° to the left or right. Performance was measured using the b-CFS paradigm. In general, suppression durations were significantly lower when the

central mask is enlarged by a collinear surround, and significantly higher when a non-collinear surround is used.

Another advantage of using BR as a reference is that it provides alternative insights into why CFS suppression durations peak around 1 Hz in Chapter 3. Studies posit that rivalry alternations are dependent on the balance of neural activity between the two eyes, switching to the less dominant image once neural activity associated with the contralateral eye adapts and falls below a certain level (e.g., McDougall, 1901; Carter and Cavanagh, 2007; Alais et al., 2010; see also Chapter 2 for details). Assuming that a similar mechanism underlies CFS target breakthroughs, we would expect any masker that adapts slowly to provide a greater amount of suppression. Having a preponderance of low temporal frequencies in the Mondrian masker fits the bill, since these stimuli are more likely to elicit P neural responses (Merigan and Maunsell, 1993). As P neural responses are more sustained than M neural responses, they are more likely to maintain the difference in neural activity between the two eyes, enhancing CFS suppression as a result. Note, however, that any advantage from the Mondrian's low temporal frequency content is contingent on the temporal rate of the target. As shown in Chapter 4, high frequency targets (≥ 4 Hz) are best paired with high frequency maskers.

The lack of eye-specific effects in Chapter 4 is another discrepancy between BR and CFS. If BR is used as a reference, it quickly becomes clear that a reason is the weak relationship between sighting dominance and interocular suppression (Bosten et al., 2015; Dieter et al., 2017). In fact, studies do report eye-specific effects in CFS (Yang et al., 2010). One possible reason for the lack of eye specific effects in Chapter 5 is that the eye of origin was randomised across trials. Moors et al. (2015a) previously reported that serial correlations observed with variable-eye presentations were weaker and reversed in sign compared to fixed-eye presentations in CFS.

Similar correlations have also been reported in BR (Mamassian and Goutcher, 2005; Pastukhov and Braun, 2011; van Ee, 2009). Thus, while randomising the eye of origin across trials may be useful in reducing the effects of neural adaptation, the procedure might have inadvertently reduced the magnitude of any eye-specific effects.

Perceptually, the Mondrian masker is characterised by rapid pattern onsets and offsets. It thus follows that these features are expected to contribute to suppression in a significant way. Studies have proposed alternative explanations such as the accumulation of FS processes (Tsuchiya et al., 2006) and dichoptic masking (Maehara et al., 2009), both which placed emphasis on the presence of transients. The empirical evidence presented in this thesis did not support the dominance of transient-driven mechanisms, suggesting instead a P-bias for static targets and temporal frequency selectivity for contrast-modulating targets. I postulate, however, that the pattern changes in the Mondrian might serve other purposes in CFS. For example, the sharp luminance onsets and offsets generate broadband temporal frequency content. This could allow the Mondrian to remain effective for a larger range of targets compared to narrowband maskers. In addition, the pattern changes produce unpredictable spatial information that could reduce adaptation incurred from the stepped presentation schedule of the Mondrian (Alais et al., 2010). The unpredictable pattern changes could also raise noise levels through dichoptic pattern masking (Agaoglu, Agaoglu, Breitmeyer, and Ogmen, 2015). Studies have suggested similar mechanisms between BR and dichoptic masking (Baker and Graf, 2009b; Boxtel et al., 2008), thus there is no reason to assume that these two processes cannot act in tandem.

5.2.3. Some guidelines on choosing a CFS masker

An effective CFS masker must be able to accomplish two main goals. Firstly, it must be able to provide sufficiently long suppression durations that can last for more than a couple of block of trials in an experiment. This is a genuine concern as Kim, Kim and Blake (2017) showed that suppression with the regular, 10 Hz Mondrian masker decreases in effectiveness after extended periods of exposure to CFS. As illustrated in Figures 4.2 and 5.1c, one way to prolong the effectiveness of the masker is to use continuously varying maskers that match the temporal frequency content of the target. Maskers with stepped pixel timelines would suffice, but only if the spatial patterns are updated unpredictably to compensate for the neural adaptation incurred from periods of constant luminance (Figure 5.1 c-d; see also Alais et al., 2010). Secondly, an effective CFS masker must be able to able to suppress the target's contents. Partial suppression of neural activity elicited by the physical properties of the target would produce highly inconsistent results, such as findings obtained with threat-related stimuli (Hedger et al., 2016). Based on the results presented thus far, it is apparent that the low-level properties of the CFS masker have to be compatible with the target for optimal suppression. I have thus summarised a few principles regarding the effective use of CFS as a flowchart in Figure 5.3 below. Given the scope of this thesis, these pointers are focused on the temporal aspects of CFS, but future and ongoing research will only refine and add to these preliminary guidelines.

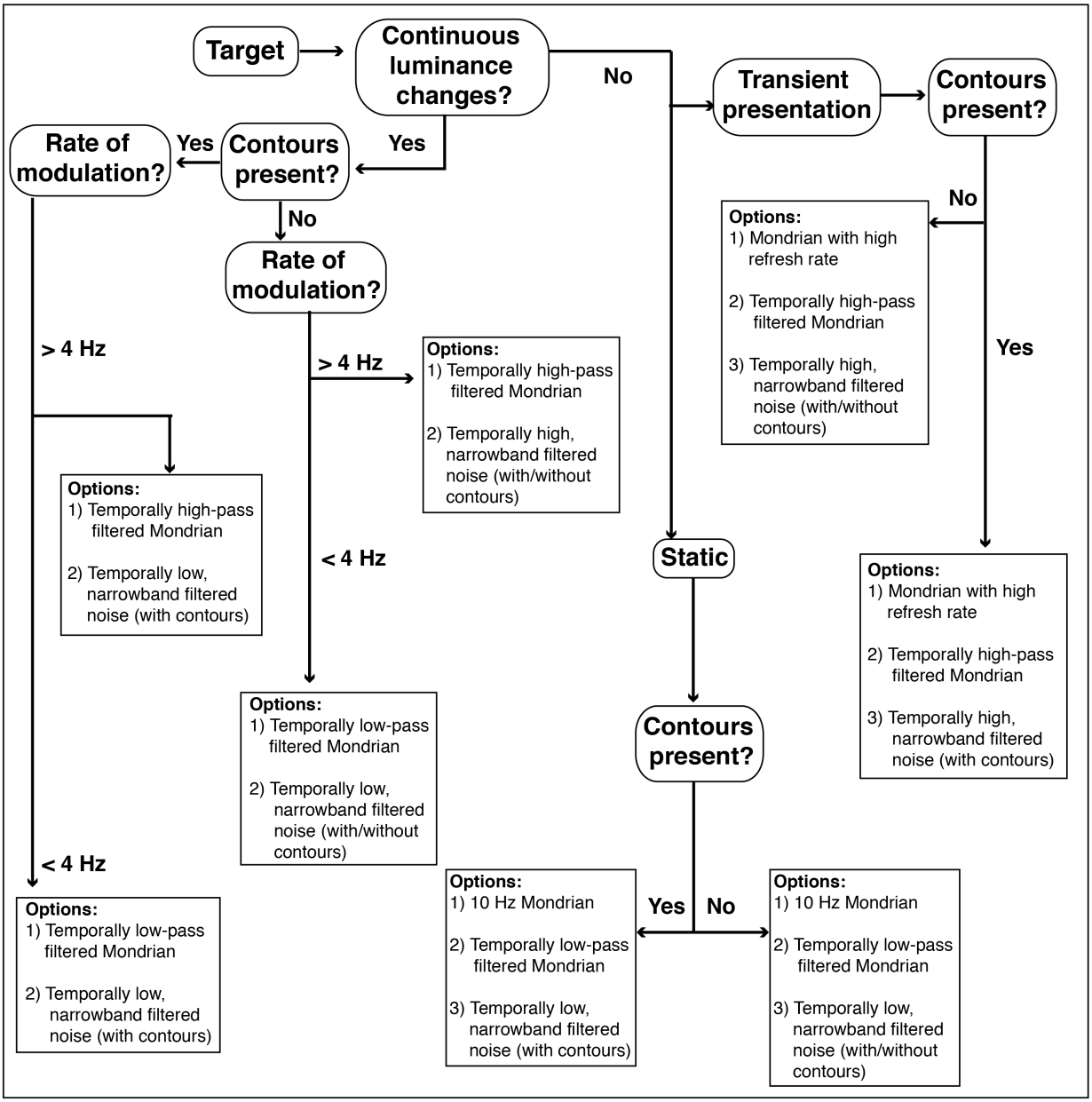

Figure 5.3. Temporal factors in choosing a CFS masker. To avoid partial suppression and to maintain CFS effectiveness, continuously varying targets are best paired with continuously varying maskers, and targets with contours are best paired with maskers with contours. Note that recommended maskers are predicted to provide optimal suppression; maskers not in the list may provide sufficient suppression, but perhaps with less effectiveness over time. For example, the contour-free, 1 Hz narrowband noise maskers in Chapter 2 were effective suppressors of low contrast, natural image targets.

5.3 Future directions

In Chapter 3, suppression was enhanced when high spatial frequency, static targets were used. Although a preference for higher spatial frequency content was also found in Chapter 4, the reverse has been reported by previous studies (e.g., Yang and Blake, 2012; Tsuchiya and Koch, 2005). Citing the 1/f spatial frequency profile of the Mondrian, Yang and Blake (2012) attributed the greater suppressive efficacy of lower spatial frequency content to spatial frequency selectivity. This does not necessarily preclude the possibility of a P-bias in CFS, but the inconsistency in findings warrants further thought and investigation. The maskers used in Chapters 3-4 had similar spatial frequency profiles to those used in previous studies, differing only in the phase structure of the masker (i.e., patterns composed of circles instead of squares in Chapter 4 and completely random phase structures in Chapter 3). In addition, the targets used in Chapters 3-4 were natural images instead of Gabors, meaning that the degree of similarity between the phase structures of the target and masker was also different from previous studies. Given that binocular fusion tends to take precedence over rivalry (Blake and Boothroyd, 1985), and that rivalry dynamics are influenced by the perceptual meaning of dichoptic stimuli (Andrews and Lotto, 2004), it is plausible that the difference in results might be contributed by the differences in target/masker pattern similarity. It would be interesting to see if we could still observe a preference for high spatial frequencies *after* ruling out the effect of pattern similarity. Another way to test the idea of a P-bias in CFS would be to present isoluminant, chromatic stimuli. Unlike the P/ventral pathway, the M/dorsal pathway is colour blind and is more sensitive to differences in luminance (Howard and Rogers, 1995). Comparing the suppressive performance of isoluminant, chromatic stimuli and grey-scale stimuli could give us a clearer idea of the extent of P-biased processes in CFS.

Another possible future direction is to measure the time course of CFS. Despite the similarities between CFS and BR, it remains unclear if target sensitivity varies in a similar manner in CFS. Given the imbalance in stimulus strength between the two eyes, the rate of growth in target sensitivity is likely to be slower. Alternatively, target sensitivity might remain constant for the initial suppression period, growing rapidly in the later phases of suppression. In addition, it would be interesting to compare the time courses obtained with target identity and target location judgments. As aforementioned, the rapid pattern onsets and offsets may serve as a form of pattern masking. In pattern masking, target visibility might be impaired by confusion or 'misbinding' of the masker's features with that of the target (Agaoglu et al., 2015). Assuming that CFS does involve pattern masking processes, then we would expect to see a dissociation between identity and location judgments, particularly at the later phases of the time course. If so, pattern masking might explain some of the inconsistencies regarding unconscious processing of threat-related stimuli (Hedger et al., 2016). For example, fearful faces tend to have wide-open mouths and/or eyes (Yang et al., 2007). These features create regions of high contrast that are salient and more recognizable than the features of neutral faces. These salient features would affect participant decisional criteria, an inevitable issue in the b-CFS paradigm (Yang et al., 2014).

Lastly, apart from BR, other forms of bi-stable phenomena have been used to render a target invisible (e.g., Bonneh et al., 2001; Wilke, Logothetis, and Leopold, 2003; O'Shea et al., 2009). A common oscillator has been proposed to underlie the different forms of perceptual rivalries (Carter and Pettigrew, 2003; see also Chapter 1), and it would be interesting to test this proposition by evaluating CFS against other forms of perceptual bi-stability. For example, monocular rivalry (MR) was produced

when orthogonally oriented red and green gratings were optically superimposed and presented to one eye (Breese, 1899; O'Shea et al., 2009). Similar to BR, the dominance durations in MR were stochastic and followed a gamma distribution (O'Shea et al., 2009). Supplementary analyses on this thesis' dataset showed that the distribution of CFS suppression durations was skewed to the right (see Figure S8), indicating the possible involvement of similar mechanisms. As suggested in this thesis, similarities among the different paradigms could be useful in refining CFS use.

5.4 Conclusions

CFS is form of visual presentation where a rapidly changing Mondrian sequence presented to one eye suppresses a static target in the other eye for several seconds at a time. Although closely related to other dichoptic stimulation techniques like BR and FS, the evidence linking CFS to either paradigm is mixed. As a start, this thesis examined the role of temporal frequency in CFS. This is because CFS's effectiveness is typically attributed to the rapid pattern onsets and offsets of the Mondrian. Here, I adopted an alternative method of varying temporal frequency, interpreting more conventionally as the number of periodic changes in pixel luminance instead of number of pattern changes per second. The results revealed that the Mondrian had a low-biased temporal frequency spectrum, and this bias was corroborated in suppression durations (Chapters 3-4). There was also a preference for high spatial frequency and high contrast stimuli, demonstrating a P/ventral pathway bias that is reminiscent of BR. Further investigation in Chapter 5 revealed temporal frequency and orientation selectivity in CFS, suggesting an early locus of suppression and drawing closer links between BR and CFS. These similarities pointed to a unified framework, which was found to be instrumental in interpreting documented CFS findings and guiding future work with the technique.

Chapter 6

Supplementary

The following provides supplementary information and analyses for Chapters 2-4.

6.1 Chapter 2

6.1.1 Figure S1

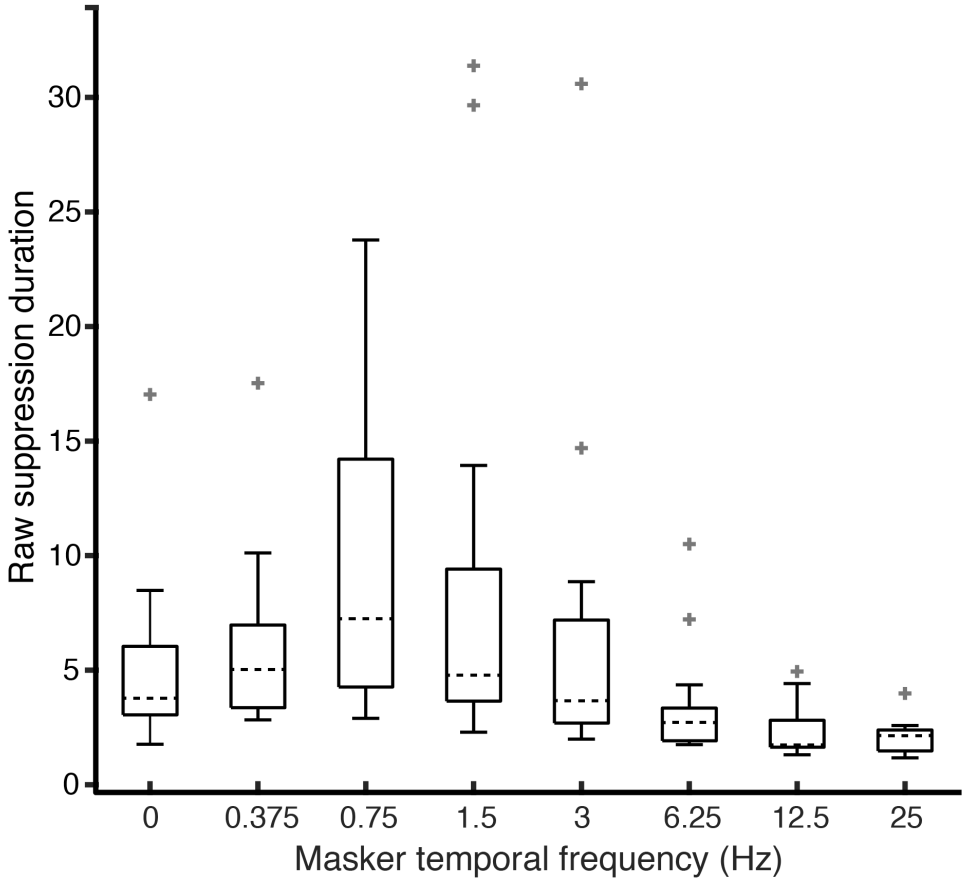

Figure S1. Boxplot describing the distributions of raw suppression durations obtained for each level of masker temporal frequency in Experiment 1. Median suppression durations were represented by dotted lines, and the interquartile ranges were represented by the box limits. Whiskers represented the maximum and minimum suppression durations and outliers were represented by the plus sign (+). The 0.75 Hz to 1.5 Hz maskers were the most effective, producing maximum suppression durations of around 15 to 25s in those conditions. The least effective suppressors were 12.5 and 25 Hz maskers, as these produced maximum suppression durations of 4-5s, a 3 to 5-fold decrease from that obtained with the lower temporal frequency maskers.

6.1.2 Figure S2

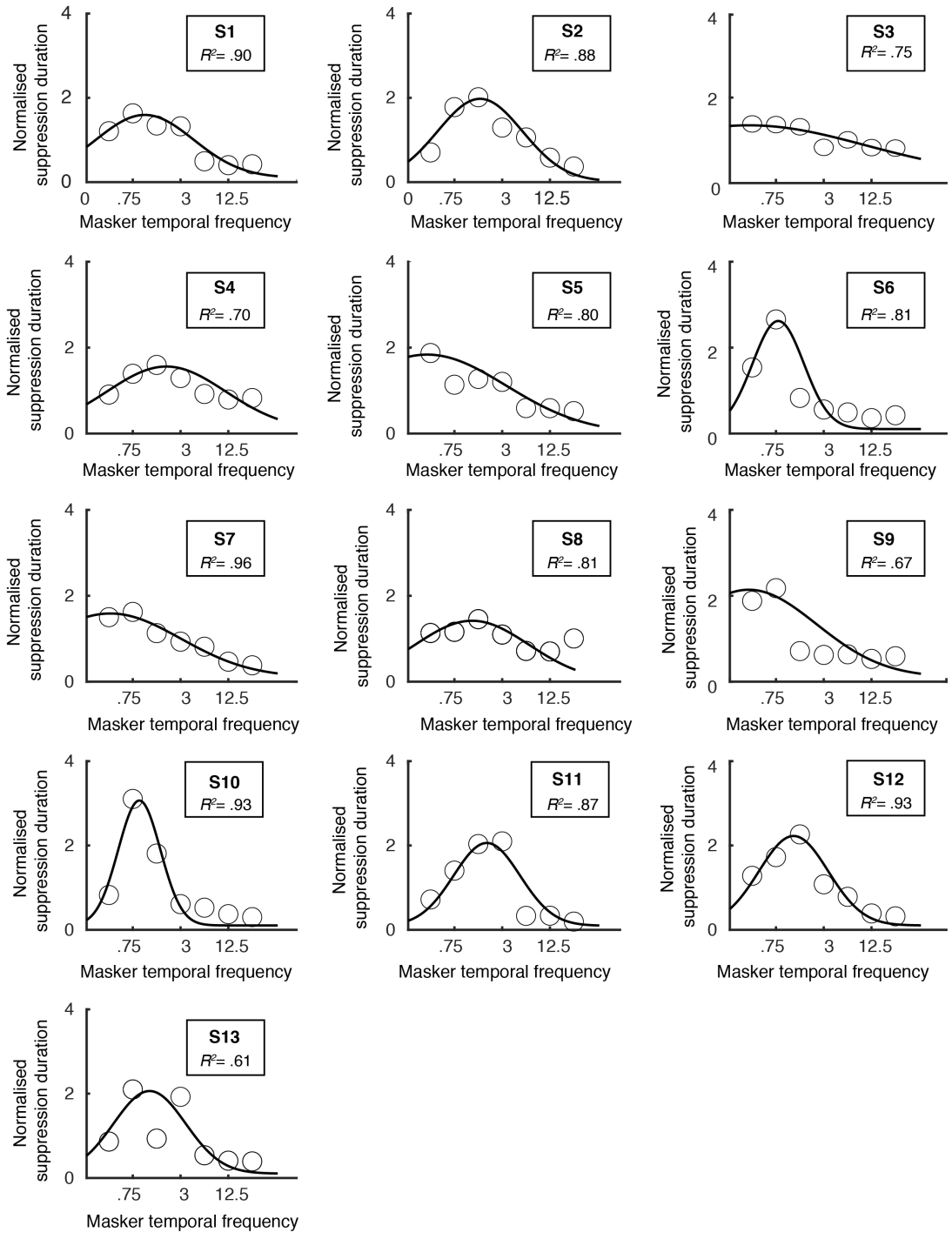

Figure S2. Gaussian functions were fitted to individual data. Consistent with the raw suppression duration data, normalised suppression durations were consistently higher at lower masker temporal frequencies, peaking around 0.75 Hz to 3 Hz across participants.

6.2 Chapter 3

6.2.1 Figure S3

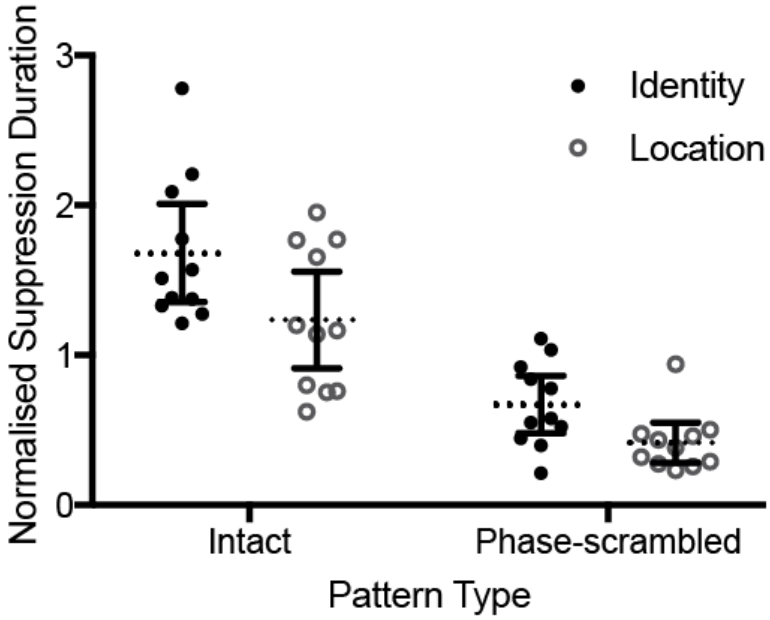

Figure S3. Distributions of average normalised suppression durations for Experiment 1, demonstrating the effect of judgment type at each level of pattern structure type. Dotted lines represent mean normalised durations whereas solid error bars are 95 % confidence intervals. In general, longer normalised durations were required for identity judgments when phase-scrambled patterns were presented. In contrast, individual trends for location and identity judgments were more variable when intact patterns were used.

6.2.2 Figure S4

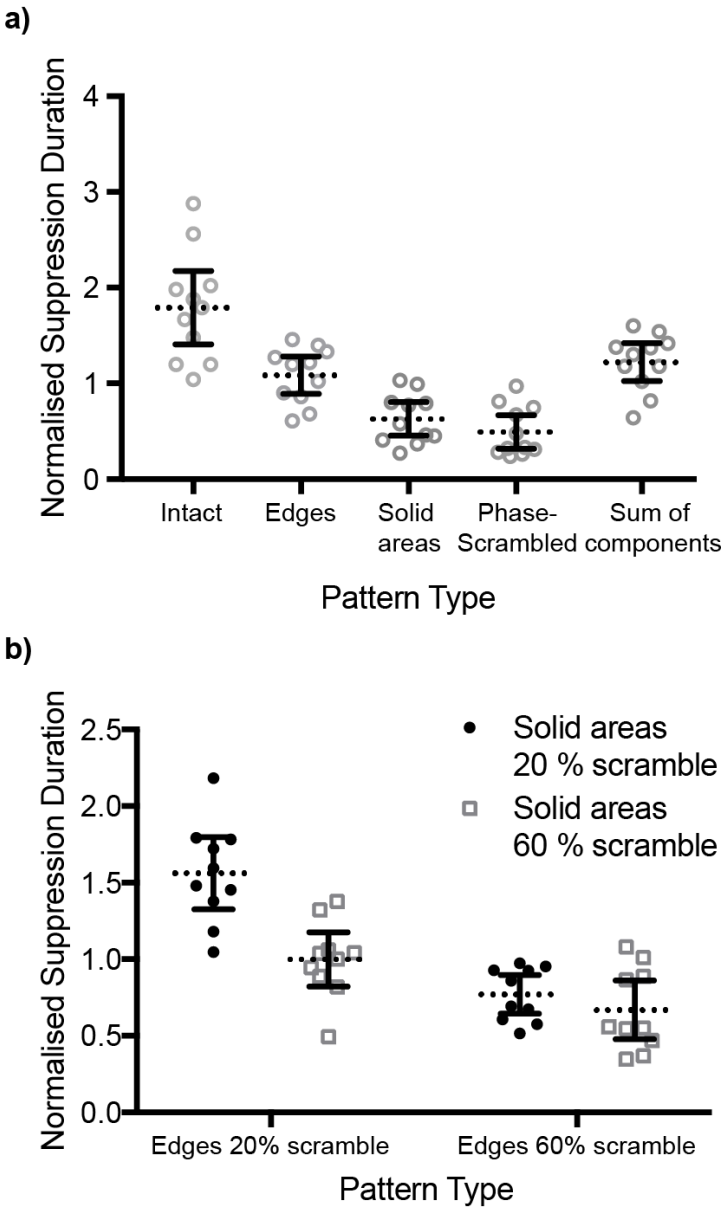

Figure S4. Normalised individual data for Experiment 2. Dotted lines denote mean durations whereas solid error bars represent 95 % confidence intervals. The effect of individual pattern components is described in (a). In general, patterns were most effective in the order: intact, edges and solid areas. Individual data were comparable between solid areas and phase-scrambled patterns, and the sum of components remained less effective than intact patterns. As described in (b), normalised durations were longer when solid areas were intact, however this effect was more pronounced when edges were relatively more intact.

6.2.3 Figure S5

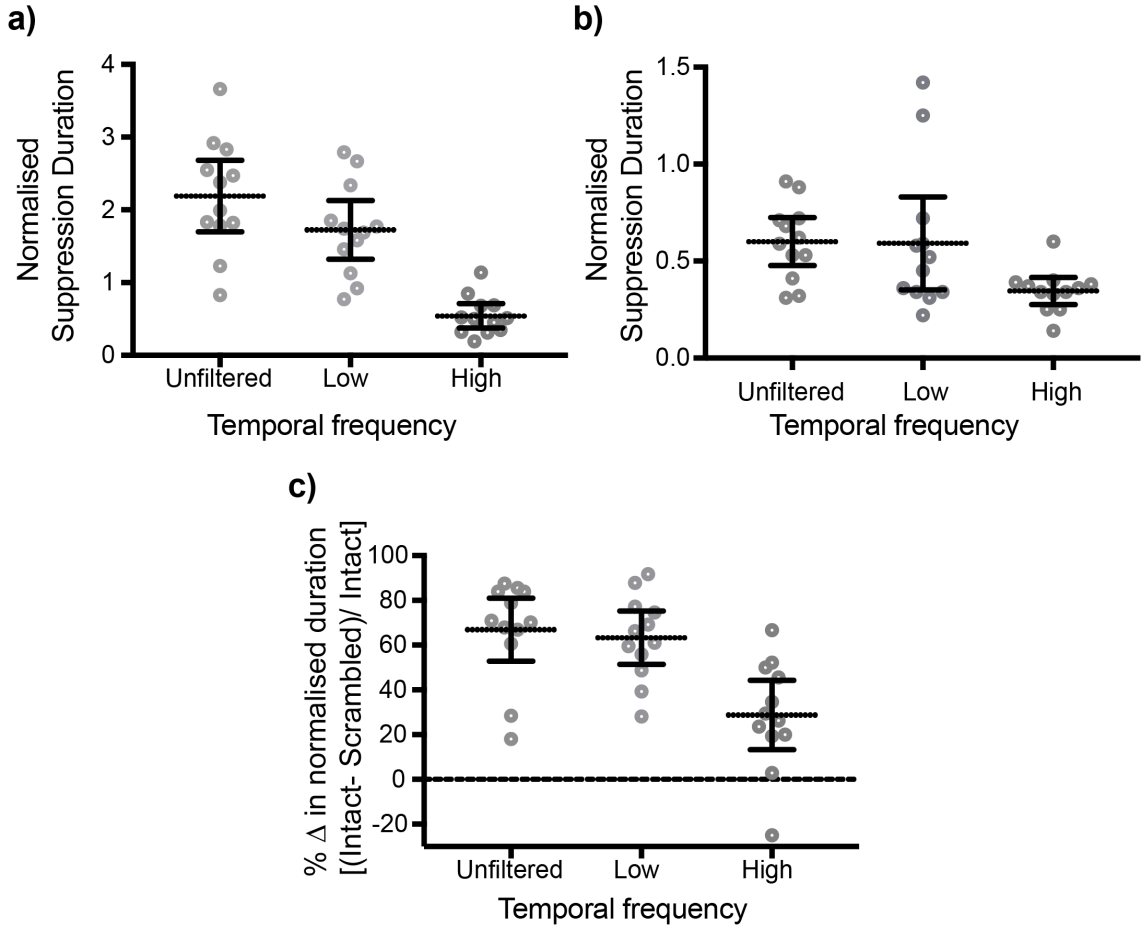

Figure S5. Normalised individual data for Experiment 3, demonstrating the effect of pattern structure and temporal frequency content. In (a), participant responses were consistently faster when intact Mondrian patterns were temporally high-pass filtered. In contrast, temporally unfiltered intact patterns were comparable with low-pass filtered patterns. As described in (b), similar observations were made for phase-scrambled patterns. Although phase-scrambled patterns were in general weaker than intact patterns, normalised durations were slightly but consistently lower when high-pass filtered patterns were used. (c) Effect of temporal frequency on the effect of pattern structure: Percentage changes in normalised durations between intact and phase-scrambled patterns were lower when the patterns were temporally high-pass. In contrast, percentage changes were comparable between temporally unfiltered and low-pass filtered patterns.

6.2.4 Figure S6

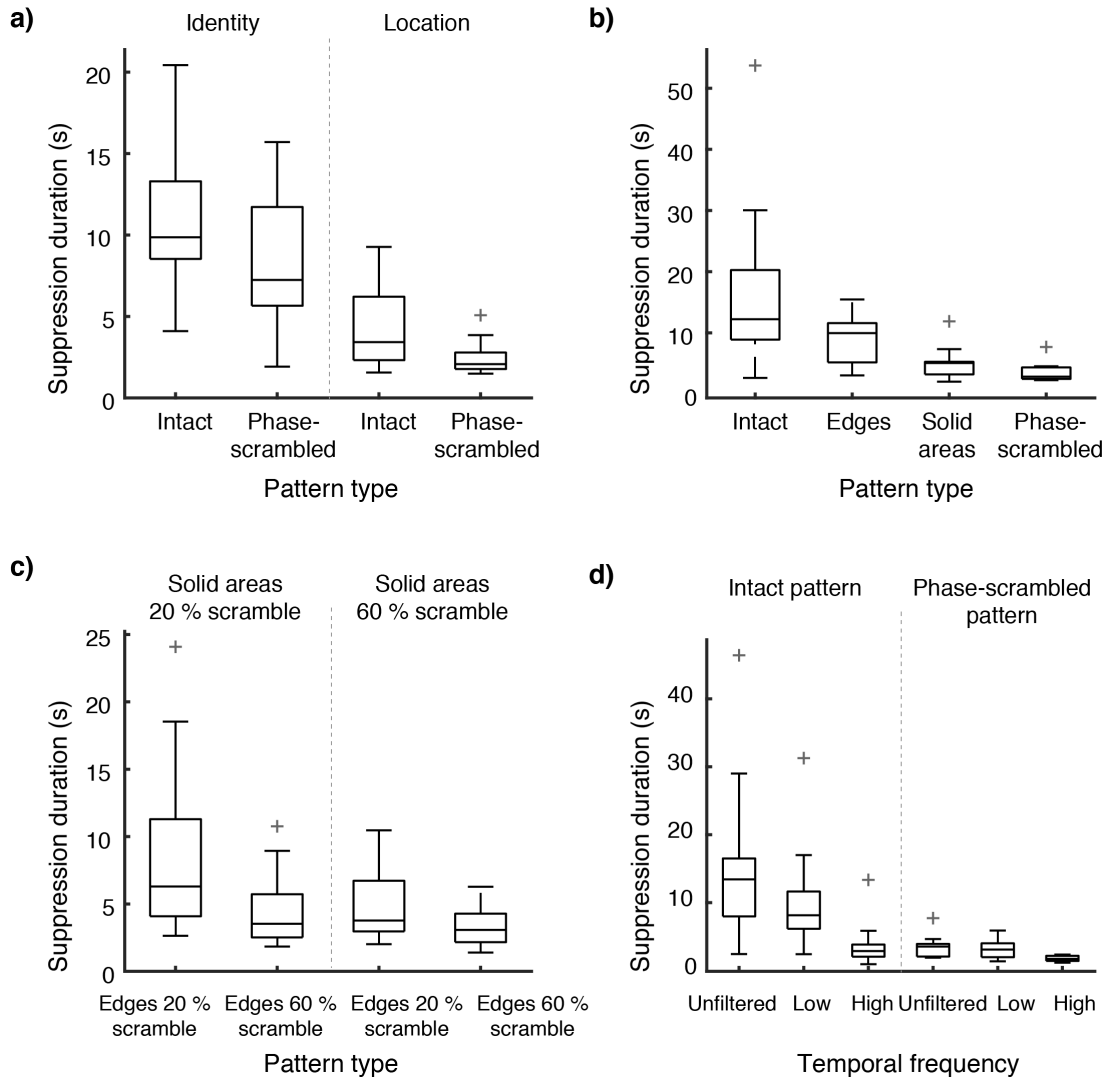

Figure S6. Boxplots described the distributions of raw suppression durations for Experiments 1 (a), 2a (b, Cf. Figure S4a), 2b (c, Cf. Figure S4b) and 3 (d) of Chapter 3. The median suppression durations were represented by dotted lines, and the interquartile ranges were represented by the box limits. Whiskers represented the maximum and minimum suppression durations and outliers were represented by the plus sign (+).

6.2.5 Text S1

In Experiment 2, we decomposed the Mondrian pattern and found a predominant effect of pattern edges. Since edges have been implicated in both rivalry and masking, obtaining a predominant edge effect allowed us to compare the roles of either process in Experiment 3. These results are especially relevant to the understanding and effective use of CFS, and it would be helpful to have a measure of the evidence supporting these conclusions. However, given the nature of the permutation test and hypothesis testing (Morey, Romeijin, and Rouder, 2016), this was not possible. We thus conducted two-sided Bayesian t-tests (with a default Cauchy prior width of r =0.707) for each key finding using the web-based program developed by Rouder, Speckman, Sun, Morey and Iverson (2009). The Bayes factors reported in the following express the relative likelihood of the data being in favour of the alternative hypothesis (H1). Using suggested conventional cut-offs suggested by Jeffreys (1961, as cited in Dienes, 2014), factors greater than 3 represent substantial evidence for H1 whereas a factor less than 0.33 provides substantial support for the null hypothesis (H0). Any value that fell between 0.33 and 3 was regarded as providing weak evidence. Bayes factors for the key findings in Experiments 2 and 3 are provided in the following sections (7.1.5 and 7.1.6), and they mirrored the conclusions of the permutation test.

6.2.6 Table S1

Bayes Factors were computed for the key findings of Experiment 2:

1. Pattern edges were more effective than solid areas.
2. Solid areas are comparable to phase-scrambled (PS) patterns.
3. Relatively intact edges performed better when solid areas were more intact.
4. Phase-scrambling edges to a larger extent eliminated the effect of solid areas.

Conditions compared (C_1, C_2)	Mean (M_1, M_2)	*SD* (SD_1, SD_2)	Bayes Factor favouring H1	Corrected *p* values	Strength of evidence
Edges, Solid areas	1.09, 0.62	0.29, 0.26	159.81	.005	Substantial
Solid areas, PS	0.63, 0.49	0.26, 0.26	1.26	.30	Weak
Edges, PS	1.09, 0.49	0.29, 0.26	167.48	.004	Substantial
20%, 60% edges (at 20% solid areas)	1.56,1.00	0.33, 0.25	10.58	.012	Substantial
20%, 60% solid areas (at 60% edges)	0.77, 0.67	0.18, 0.27	0.47	.39	Weak

6.2.7 Table S2

Bayes Factors were computed for the key findings of Experiment 3:

1. Comparisons involving intact (I) patterns
    a. Low-pass maskers were more effective than high-pass maskers.
    b. High-pass maskers were weaker than unfiltered maskers.
    c. Low-pass maskers were comparable to unfiltered maskers.
2. Comparisons involving phase-scrambled patterns (PS)
    a. Low-pass maskers were comparable to high-pass maskers.
    b. High-pass maskers were weaker than unfiltered maskers.
    c. Low-pass maskers were comparable to unfiltered maskers.
3. Comparison examining the magnitude of the effect of the pattern structure (P)
    a. Low-pass maskers had a larger pattern effect than high-pass maskers.
    b. High-pass maskers had a smaller pattern effect than unfiltered maskers.
    c. High-pass maskers had a comparable pattern effect with unfiltered maskers

Conditions compared (C_1, C_2)	Mean (M_1, M_2)	*SD* (SD_1, SD_2)	Bayes Factor favouring H1	Corrected *p* values	Strength of evidence
Low- and high-pass (I)	1.73, 0.54	0.63, 0.26	127.58	.01	Substantial
Low-pass, unfiltered (I)	1.73, 2.19	0.63, 0.77	0.56	.14	Weak
High-pass, unfiltered (I)	0.54, 2.19	0.26, 0.77	708.12	.012	Substantial
Low- and high-pass (PS)	0.60, 0.35	0.38, 0.11	2.2	.11	Weak
Low-pass, unfiltered (PS)	0.59, 0.60	0.38, 0.19	0.29	.26	Weak
High-pass,unfiltered (PS)	0.35, 0.60	0.11, 0.19	56.95	.02	Substantial
Low- and high-pass (P)	63.3, 28.8	18.8, 24.3	51.06	.014	Substantial
Low-pass, unfiltered (P)	63.3, 66.9	18.8, 22.2	0.38	.29	Weak
High-pass, unfiltered (P)	28.8, 66.9	24.3, 18.8	76.06	.009	Substantial

6.3 Chapter 4

6.3.1 Figure S7

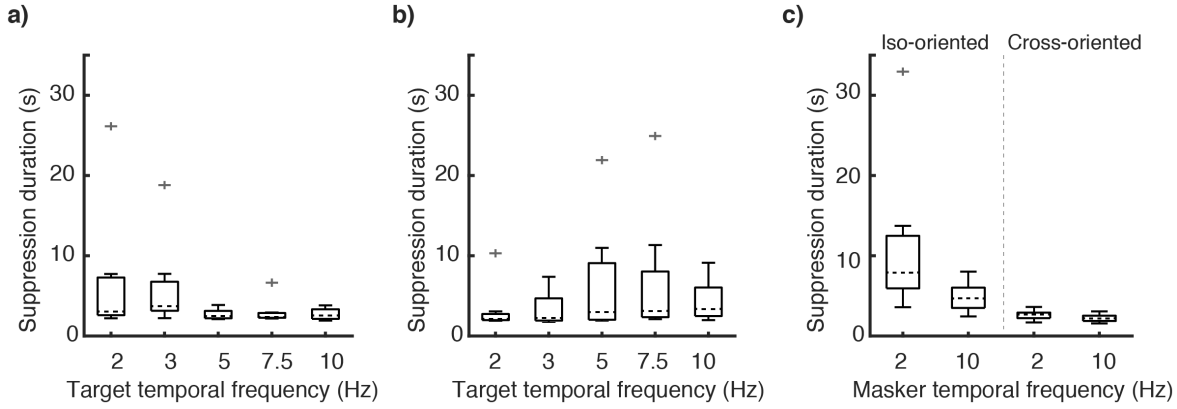

Figure S7. Boxplots described the distributions of raw suppression durations for Experiments 1-2 of Chapter 4. Median suppression durations were represented by dotted lines, and the interquartile ranges were represented by the box limits. Whiskers represented the maximum and minimum suppression durations and outliers were represented by the plus sign (+). (a) The distributions of suppression durations obtained with a 2 Hz masker. When a 2 Hz masker was presented, higher suppression durations were obtained at lower target temporal frequencies. (b) The distributions of suppression durations obtained with a 2 Hz masker. Unlike the 2 Hz masker, presenting a 10 Hz masker produced higher suppression durations at higher target temporal frequencies. (c) The effect of orientation and temporal frequency on CFS suppression durations. Higher raw durations were obtained for both 2 and 10 Hz maskers when the target was of the same orientation as the masker. However, the difference between iso-orientation and cross-orientation was larger for the 2 Hz masker than the 10 Hz masker.

6.3.2 Text S2

We describe the factors that contribute to the low temporal dominancy of the Mondrian masker. By convention, the masker is composed of a series of patterns sampled at a rate of 10 Hz. For a monitor refresh rate of 100 Hz, this would mean that each pattern would be presented for 100 ms, thereby producing 10 consecutive values of the same pixel luminance. Assuming that each pattern change would produce maximum change in luminance, we would obtain a 5 Hz square wave (see Figure S4 in the next section). This is considerably lower than the nominal 10 Hz, and is the first clue that there is a low temporal dominancy in the Mondrian masker. The second clue is apparent when we consider the way in which pixel luminance is distributed for each pattern. Pattern elements are generally assigned a random grey level and a random spatial location. Hence, the resulting pixel time line is rarely a 5 Hz square due to central tendency. Between patterns, the change in pixel luminance could range from maximum (black to white) to zero (static pixel). This would slow down luminance transitions further, contributing to a low temporal dominancy in the Mondrian masker.

6.3.3 Figure S8

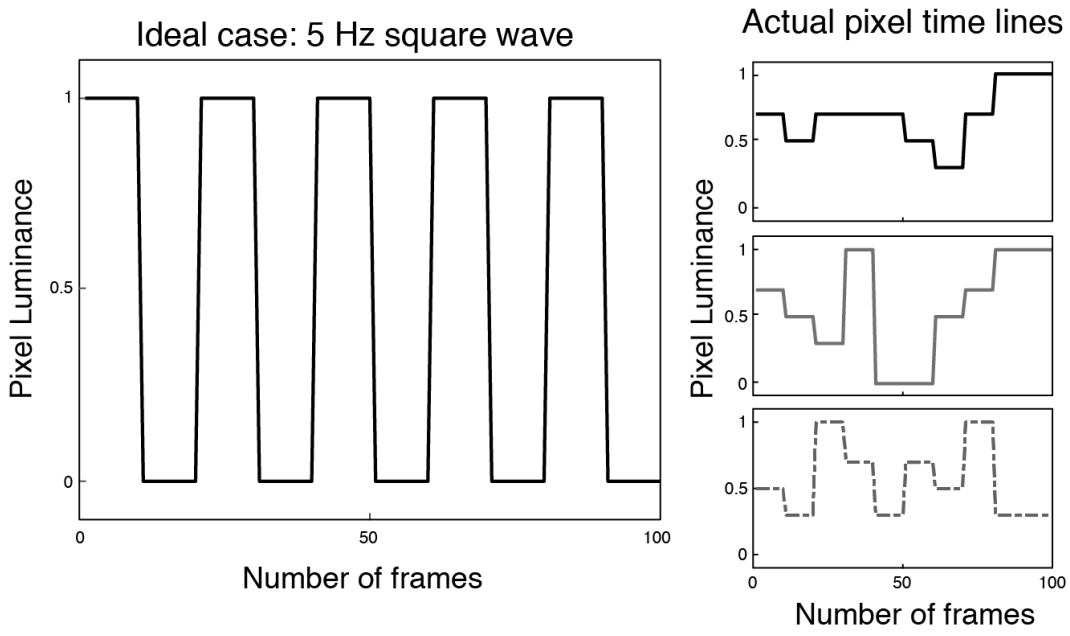

Figure S8. Changes in the pixel luminance of the Mondrian masker plotted against the number of frames. Due to the stepped presentation schedule of the Mondrian masker, a 5 Hz square wave would be obtained if all pixels alternated between black and white with each pattern change (see left panel). However, due to the random sampling of grey levels and central tendency, extracted pixel time lines typically modulate at a lower temporal rate (see right panel).

6.4 Chapter 5

6.4.1 Figure S9

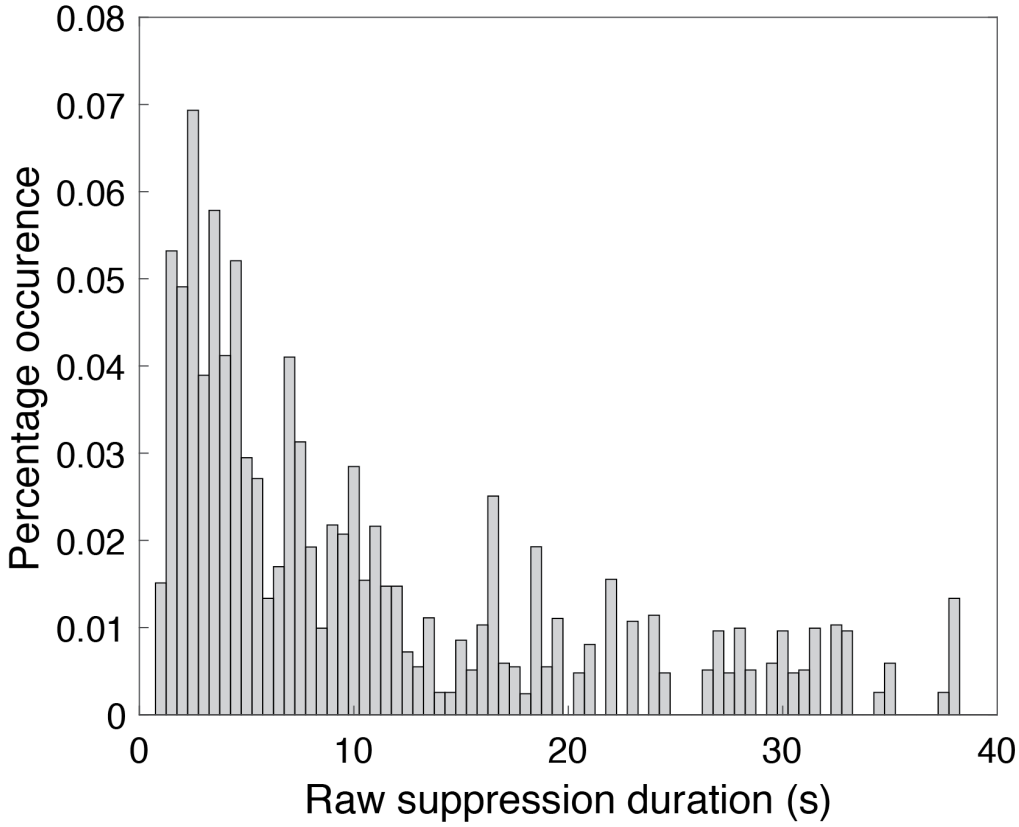

Figure S9. The distribution of CFS suppression durations compiled from Experiment 1 of Chapter 2, averaged across participants. To provide an accurate representation of the distribution of suppression durations, outliers were not removed in this analysis. Similar to binocular rivalry, the distribution of suppression durations in CFS was skewed to the right.

References

Adams, J.K. (1957). Laboratory studies of behavior without awareness. *Psychological Bulletin*, 54(*5*), 383-405. http://dx.doi.org/10.1037/h0043350

Agaoglu, S., Agaoglu, M. N., Breitmeyer, B. G., & Ogmen, H. (2015). A statistical perspective to visual masking. *Vision Research*, 115, 23–39. https://doi.org/10.1016/j.visres.2015.07.003

Alais, D. (2012). Binocular rivalry: Competition and inhibition in visual perception. *Wiley Interdisciplinary Reviews: Cognitive Science*, 3 (1), 87–103, https://doi.org/10.1002/wcs.151

Alais, D., & Blake, R. (2005). *Binocular Rivalry* (D. Alais & R. Blake, Eds.). Cambridge, Massachusetts: The MIT Press.

Alais, D., & Melcher, D. (2007). Strength and coherence of binocular rivalry depends on shared stimulus complexity. *Vision Research*, 47(*2*), 269–279. https://doi.org/10.1016/j.visres.2006.09.003

Alais, D., & Parker, A. (2006). Independent binocular rivalry processes for motion and form. *Neuron*, 52(*5*), 911–920. https://doi.org/10.1016/j.neuron.2006.10.027

Alais, D., & Parker, A. (2012). Binocular rivalry produced by temporal frequency differences. *Frontiers in Human Neuroscience*, 6, 227, https://doi.org/10.3389/fnhum.2012.00227

Alais, D., Cass, J., O'Shea, R.P., & Blake, R. (2010). Visual Sensitivity Underlying Changes in Visual Consciousness. *Current Biology*, 20(*15*), 1362–1367. https://doi.org/10.1016/j.cub.2010.06.015

Alais, D., Lorenceau, J., Arrighi, R., & Cass, J. (2006). Contour interactions between pairs of Gabors engaged in binocular rivalry reveal a map of the association. *Vision Research,* 46, 1473–1487. https://doi.org/10.1016/j.visres.2005.09.029

Alais, D., O'Shea, R. P., Mesana-Alais, C., & Wilson, I. G. (2000). On binocular alternation. *Perception,* 29*,* 1437-1445. https://doi.org/10.1068/p3017

Alitto, H. J., Moore, B. D., Rathbun, D. L., & Usrey, W. M. (2011). A comparison of visual responses in the lateral geniculate nucleus of alert and anaesthetized macaque monkeys. *The Journal of Physiology*, 589 (1), 87–99. https://doi.org/10.1113/jphysiol.2010.190538

Alpers, G. W., & Gerdes, A. B. M. (2007). Here Is Looking at You: Emotional Faces Predominate in Binocular Rivalry. *Emotion*, 7(*3*), 495–506. https://doi.org/10.1037/1528-3542.7.3.495

Alpers, G. W., & Pauli, P. (2006). Emotional pictures predominate in binocular rivalry. *Cognition and Emotion*, 20(*5*), 596–607. https://doi.org/10.1080/02699930500282249

Alpers, G. W., Ruhleder, M., Walz, N., Muhlberger, A., & Pauli, P. (2005). Binocular rivalry between emotional and neutral stimuli: A validation using fear conditioning and EEG. *International Journal of Psychophysiology*, 57, 25–32. https://doi.org/10.1016/j.ijpsycho.2005.01.008

Ananyev, E., Penney, T. B., & Hsieh, P. B. (2017). Separate requirements for detection and perceptual stability of motion in interocular suppression. *Scientific Reports*, 7(7230), 1–10, https://doi.org/10.1038/s41598-017-07805-5

Anderson, S. J., & Burr, D. C. (1985). Spatial and temporal selectivity of the motion detection system. *Vision Research*, 25(*8*), 1147–1154.

Andrews, T. J., & Blakemore, C. (2002). Integration of motion information during binocular rivalry. *Vision Research*, 42(*3*), 301–309. https://10.1016/S0042-6989(01)00286-3

Andrews, T. J., & Lotto, R. B. (2004). Fusion and rivalry are dependent on the perceptual meaning of visual stimuli. *Current Biology*, 14(*5*), 418–423. https://doi.org/10.1016/j.cub.2004.02.030

Arnold, D.H, & Quinn, H. (2010). Binocular rivalry and multi-stable perception: independence and monocular channels, *Journal of Vision*, 10(*10*), 1-9. https://doi.org/10.1167/10.10.8

Audet, T., Bub, D., & Lecours, A. (1991). Visual neglect and left-sided context effects. *Brain Cognition*, 16, 11–28.

Baker, D. H., & Graf, E. W. (2009a). Natural images dominate in binocular rivalry. *PNAS*, 106(*13*), 5436–5441. https://doi.org/10.1073/pnas.0812860106

Baker, D. H., & Graf, E. W. (2009b). On the relation between dichoptic masking and binocular rivalry. *Vision Research*, *49*(4), 451–9. https://doi.org/10.1016/j.visres.2008.12.002

Blake, R. (1977). Threshold conditions for binocular rivalry. *Journal of Experimental Psychology Human Perception and Performance*, 3(*2*), 251–257.

Blake, R. (1989). A neural theory of binocular rivalry. *Psychological Review*, 96(*1*), 145–167. https://doi.org/10.1037/0033-295X.96.1.145

Blake, R. (1995). Visual suppression of one eye's view with dichoptic stimulation. *Journal of the Society for Information Display,* 3(*4*), 215-217. https://doi.org/10.1889/1.1984972

Blake, R. (2001). A Primer on Binocular Rivalry, Including Current Controversies. *Brain and Mind*, 2, 5–38. https://doi.org/10.1023/A:1017925416289

Blake, R. (2005). Landmarks in the history of binocular rivalry. In D. Alais & R. Blake (Eds.), *Binocular Rivalry* (1-28). Cambridge, Massachusetts: The MIT Press.

Blake, R., & Logothetis, N. K. (2002). Visual Competition. *Nature Reviews Neuroscience*, 3(*1*), 13–21. https://doi.org/10.1038/nrn701

Blake, R., & Boothroyd, K. (1985). The precedence of binocular fusion over binocular rivalry. *Perception & Psychophysics*, 37(*2*), 114-124.

Blake, R., & Wilson, H. (2011). Binocular vision. *Vision Research,* 51(*7*), 754-770. https://doi.org/10.1016/j.visres.2010.10.009

Blake, R., Brascamp, J., Heeger, D.J. (2014). Can binocular rivalry reveal neural correlates of consciousness? *Philosophical transaction of the royal society B,* 369(*1641*), 1-9. https://doi.org/10/1098/rstb.2013/0211

Blake, R., O'Shea, R.P., & Mueller, T.J. (1992). Spatial zones of binocular rivalry in central and peripheral vision. *Visual Neuroscience,* 8(*5*), 469-478.

Blake, R., Westendorf, D. H., & Overton, R. (1980). What is suppressed during binocular rivalry? *Perception,* 9(*2*), 223-231. https://doi.org/10.1068/p090223

Blake, R., Westendorf, D., & Fox, R. (1990). Temporal perturbations of binocular rivalry. *Perception & Psychophysics*, 48(*6*), 593–602. https://doi.org/10.3758/BF03211605

Bonneh, Y., & Sagi, D. (1999). Configuration saliency in short duration binocular rivalry. *Vision Research*, 39, 271–281.

Bonneh, Y., Sagi, D., Kami, A. (2001). A transition between eye and object rivalry determined by stimulus coherence. *Vision Research,* 41(*8*), 981-989. https://doi.org/10.1016/S0042-6989(01)00013-X

Bonneh, Y.S., Cooperman, A., & Sagi, D. (2001). Motion-induced blindness in normal observers. *Letters to Nature,* 411, 798-801.

Bossink, C. J. H., Stalmeier, P. F. M., & de Weert, C. M. M. (1993). A test of Levelt's second proposition for binocular rivalry. *Vision Research*, 33(*10*), 1413–1419. https://doi.org/10.1016/0042-6989(93)90047-Z

Bosten, J. M., Goodbourn, P. T., Lawrance-Owen, A. J., Bargary, G., Hogg, R. E., & Mollon, J. D. (2015). A population study of binocular function. *Vision Research*, 110 (*Part A*), 34–50, https://doi.org/10.1016/j.visres.2015.02.017

Bower, T.G.R., & Haley, L.J. (1964). Temporal effects in binocular vision. *Psychonomic Science,* 1, 409-420.

Boxtel, J. J. A. Van, Alais, D., Erkelens, C. J., & Ee, R. Van. (2008). The Role of Temporally Coarse Form Processing during Binocular Rivalry. *PloS ONE*, 3(*1*): e1429. https://doi.org/10.1371/journal.pone.0001429

Brascamp, J. W., Klink, P. C., & Levelt, J. M. (2015). The " laws " of binocular rivalry : 50 years of Levelt ' s propositions, 109, 20–37. https://doi.org/10.1016/j.visres.2015.02.019

Brascamp, J., van Ee, R., Noest, A., Jacobs, R., & van den Berg, A. (2006). The time course of binocular rivalry reveals a fundamental role of noise. Journal of Vision, 6(11), 1244–1256.

Breese, B.B. (1899). On inhibition. *The Psychological Review: Monograph Supplements,* 3(*1*), 1-65. http://dx.doi.org/10.1037/h0092990

Breitmeyer, B. G., Ogmen, H., & Chen, J. (2004). Unconscious priming by color and form: Different processes and levels. *Consciousness and Cognition*, 13, 138–157,https://doi.org/10.1016/j.concog.2003.07.004.

Breitmeyer, B.G. (1984). Visual masking: An integrative approach. New York, NY: Oxford University Press.

Breitmeyer, B.G. (2014). Psychophysical "blinding" methods reveal a functional hierarchy of unconscious visual processing. *Consciousness and Cognition*, 35, 234-250. https://doi.org/10.1016/j.concog.2015.01.012

Brussell, E. M., & Favreau, O. E. (1977). Backward pattern masking can vary as a nonmonotonic function of target duration: On the influence of intratarget metacontrast. *Journal of Experimental Psychology: Human Perception and Performance, 3*(*3*), 461-472. http://dx.doi.org/10.1037/0096-1523.3.3.461

Buckthought, A., Kim, J., & Wilson, H. R. (2008). Hysteresis effects in stereopsis and binocular rivalry. Vision Research, 48, 819–830. https:/doi.org/10.1016/j.visres.2007.12.013

Burke, D., Alais, D., & Wenderoth, P. (1999). Determinants of fusion of dichoptically presented orthogonal gratings. *Perception,* 28, 73-88. https://doi.org/10.1068/2694

Carlson, T. A., & He, S. (2000). Visible binocular beats from invisible monocular stimuli during binocular rivalry. *Current Biology*, 10(*17*), 1055–1058. https://doi.org/10.1016/S0960-9822(00)00672-2

Carmel, D., Arcaro, M., Kastner, S., & Hasson, U. (2010). How to create and use binocular rivalry. *Journal of visualized experiments,* 45, 1-10. https://doi.org/10.379/2030

Carney, T., Shadlen, M., & Switkes, E. (1987). Parallel processing of motion & colour information. *Nature*, 328(6131), 647–649. https://doi.org/10.1038/328647a0

Carter, O., & Cavanagh, P. (2007). Onset rivalry: Brief presentation isolates an early independent phase of perceptual competition. *PLoS ONE*, 2(*4*), 1–7. https://doi.org/10.1371/journal.pone.0000343

Carter, O., & Pettigrew, J.D. (2003). A common oscillator for perceptual rivalries? *Perception*, 32(*3*), 295–305. https://doi.org/10.1068/p3472

Carter, O., Pettigrew, J.D., Hasler, F., Wallis, G., Liu, G., Hell, D., & Vollenweider, F. (2005). Modulating the rate and rhythmicity of perceptual rivalry alternations with the mixed 5-HT2A and 5-HT1A agonist psilocybin. *Neuropsychopharmacology*, 30(*6*), 1154–62. https://doi.org/10.1038/sj.npp.1300621

Cass, J., & Alais, D. (2006). Evidence for two interacting temporal channels in human visual processing. *Vision Research*, 46(*18*), 2859–2868. https://doi.org/10.1016/j.visres.2006.02.015

Cass, J., Alais, D., Spehar, B., & Bex, P.J. (2009). Temporal whitening: Transient noise perceptually equalizes the 1/f temporal amplitude spectrum, *Journal of Vision*, 9(*10*), 1-19, https://doi.org/10.1167/9.10.12

Cave, C. B., Blake, R., & McNamara, T. P. (1998). Binocular Rivalry Disrupts Visual Priming. *Psychological Science*, 9(*4*), 299–302. https://doi.org/10.1111/1467-9280.00059

Chapman, C., Hoag, R., & Giaschi, D. (2004). The effect of disrupting the human magnocellular pathway on global motion perception. *Vision Research*, 44(*22*), 2551–2557. https://doi.org/10.1016/j.visres.2004.06.003

Chong, H. Y. (2008). *Resampling, a conceptual and procedural introduction*. (J. W. Osborne, Ed.). California, United States of America: SAGE Publications.

Chubb C., Sperling G., & Solomon J. A. (1989). Texture interactions determine perceived contrast. *Proceedings of the National Academy of Sciences*, *USA*, 86, 9631–9635.

Derrington, B.Y.A.M., & Lennie, P. (1984). Spatial and temporal contrast sensitivities of neurones in lateral geniculate nucleus of macaque. *The Journal of Physiology*, 357, 219–240.

DeYoe, E. A., & Van Essen, D. C. (1988). Concurrent processing streams in monkey visual cortex. *Trends in Neurosciences*, 11(*5*), 219–226. https://doi.org/10.1016/0166-2236(88)90130-0

Dienes, Z. (2014). Using Bayes to get the most out of non-significant results. *Frontiers in Psychology*, 5, 1–17. https://doi.org/10.3389/fpsyg.2014.00781

Dieter, K. C., Sy, J.L., & Blake, R. (2017). Individual differences in sensory eye dominance reflected in the dynamics of binocular rivalry. *Vision Research*, 141, 40–50. https://doi.org/10.1016/j.visres.2016.09.014

Drewes, J., Zhu, W., Wutz, A., & Melcher, D. (2015). Dense sampling reveals behavioral oscillations in rapid visual categorization. *Scientific Reports*, 5, 1–9. https://doi.org/10.1038/srep16290

Driver, J., & Mattingley, J. (1998). Parietal neglect and visual awareness. *Nature Neuroscience*, 1, 17–22.

Enns, J., & Di Lollo, V. (2000). What's new in visual masking? *Trends in Cognitive Sciences*, 4(*9*), 345–352. https://doi.org/10.1016/S1364-6613(00)01520-5

Faivre, N., & Koch, C. (2014). Temporal structure coding with & without awareness, *Cognition,* 131(*3*), 404-414. https://doi.org/10.1016/j.cognition.2014.02.008

Fang, F., & He, S. (2005). Cortical responses to invisible objects in the human dorsal and ventral pathways. *Nature Neuroscience*, 8(*10*), 1380-1385. https://doi.org/10.1038/nn1537

Fawcett, I.P., Barnes, G.R., Hillebrand, A., & Singh, K.D. (2004). The temporal frequency tuning of human visual cortex investigated using synthetic aperture

magnetometry. *NeuroImage*, 21, 1542–1553. https://doi.org/10.1016/j.neuroimage.2003.10.045

Ferrera, V.P., Nealey, T.A., & Maunsell, H.R. (1994). Responses in macaque visual area V4 following inactivation of the parvocellular and magnocellular LGN pathways. *The Journal of Neuroscience*, 14(*4*), 2080–2088.

Fogelson, S. V., Kohler, P. J., Miller, K. J., Granger, R., & Tse, P. U. (2014). Unconscious neural processing differs with method used to render stimuli invisible. *Frontiers in Psychology*, *5*, 1-11. https://doi.org/10.3389/fpsyg.2014.00601

Fowler, C., Wolford, G., Slade, R., & Tassinary, L. (1981). Lexical access with and without awareness. *Journal of Experimental Psychology: General*, 110, 341–362.

Fox, R., & Rasche, F. (1969). Binocular rivalry and reciprocal inhibition. Perception & Psychophysics, 5(*4*), 215–217.

Freeman, A. W. (2005). Multistage model for binocular rivalry. *Journal of Neurophysiology*, 94(*6*), 4412–4420. https://doi.org/10.1152/jn.00557.2005

Freeman, T. C. B., Durand, S., Kiper, D. C., & Carandini, M. (2002). Suppression without inhibition in visual cortex. *Neuron*, 35(*4*), 759–771. https://doi.org/10.1016/S0896-6273(02)00819-X.

Gayet, S., Van der Stigchel, S., Paffen, C.L.E. (2014). Breaking continuous flash suppression: Competing for consciousness on the pre-semantic battlefield. *Frontiers in Psychology*, 5, 1-10. https://doi.org/10.3389/fpsyg.2014.00460

Gobbini, M.I., Gors, J.D., Halchenko, Yo, Rogers, C., Guntupalli, J.S., Hughes, H., & Cipolli, C. (2013). Prioritized Detection of Personally Familiar Faces. *PLoS ONE*, 8(6), 1–7. https://doi.org/10.1371/journal.pone.0066620

Green, M.F., et al. (2009). Perception measurement in clinical trials of schizophrenia: promising paradigms from CNTRICS, *Schizophrenia Bulletin*, 35, 163–181.

Han, S., Lunghi, C., Alais, D. (2016). The temporal frequency tuning of continuous flash suppression reveals peak suppression at very low frequencies. *Scientific Reports*, 6, 1-12. https://doi.org/10.1038/srep35723

Hawken, M. J., Shapley, R. M., & Grosof, D. H. (1996). Temporal-frequency selectivity in monkey visual cortex. *Visual Neuroscience*, 13, 477–492, https://doi.org/10.1017/S0952523800008154

Haynes, J., Deichmann, R., & Rees, G. (2005). Eye-specific suppression in human LGN reflects perceptual dominance during binocular rivalry. *Nature*, 438(*7067*), 496–499. https://doi.org/10.1038/nature04169.

He, S., Carlson, T. A., & Chen, X. (2005). Parallel pathways & temporal dynamics in binocular rivalry in Binocular Rivalry. In D. Alais & R. Blake (Eds.), *Binocular Rivalry* (81-100). Cambridge, Massachusetts: The MIT Press.

Hedger, N., Adams, W.J., & Garner, M. (2015). Autonomic arousal and attentional orienting to visual threat are predicted by awareness. *Journal of Experimental Psychology: Human perception and performance.* 41(*3*), 798-806. https://doi.org/10.1037/xhp0000051

Hedger, N., Gray, K.L.H., Garner, M., & Adams, W.J. (2016). Are visual threats prioritised without awareness? A critical review and meta analysis involving 3 behavioural paradigms and 2696 observers. *Psychological Bulletin*, 142 (*9*), 934-968. https://doi.org/10.1037/bul0000054

Hellige, J. B., Walsh, D. A., Lawrence, V. W., & Prasse, M. (1979). Figural relationship effects and mechanisms of visual masking. *Journal of Experimental Psychology: Human Perception and Performance*, 5(*1*), 88–100.

Helmholtz, H. (1924). Treastise on Physiological Optics. *Nature,* 114, 887-889.

Hess, R. F., & Snowden, R. J. (1992). Temporal properties of human visual filters: Number, shapes and spatial covariation. *Vision Research*, 32(*1*), 47–59.

Hesselmann, G., & Malach, R. (2011). The link between fMRI-BOLD activation and perceptual awareness is "stream-invariant" in the human visual system. *Cerebral Cortex*, 21, 2829–2837. https://doi.org/10.1093/cercor/bhr085

Hesselmann, G., & Moors, P. (2015). Definitely maybe: can unconscious processes perform the same functions as conscious processes? *Consciousness Research*, 584, 1-5. https://doi.org/10.3389/fpsyg.2015.00584

Hesselmann, G., Darcy, N., Sterzer, P., & Knops, A. (2015). Exploring the boundary conditions of unconscious numerical priming effects with continuous flash suppression. *Conscious cognition,* 31, 60-72. https://doi.org/10.1016/j.concog.2014.10.009

Hicks, T., Lee, B., & Vidyasagar, T. (1983). The responses of cells in the macaque lateral geniculate nucleus to sinusoidal gratings. *Journal of Physiology*, 337, 183–200.

Hollins, M. (1980). The effect of contrast on the completeness of binocular rivalry suppression. *Perception & Psychophysics*, 27(*6*), 550–556. https://doi.org/10.3758/BF03198684

Hong, S.W., & Blake, R. (2009). Interocular suppression differentially affects achromatic and chromatic mechanisms. *Attention, Perception, & Psychophysics*, 71(*2*), 403-411. https://doi.org/10.3758/APP.71.2.403

Howard, I.P. and Rogers, B.J. (1995). *Binocular vision and stereopsis*. New York: Oxford University Press.

Hunt, J.L., Mattingley, J.B., & Goodhill, G.J. (2012). Randomly oriented edge arrangements dominate naturalistic arrangements in binocular rivalry. *Vision Research*, 64, 49-55. https://doi.org/10.1016/j.visres.2012.05.007

Jiang, Y., & He, S. (2006). Cortical responses to invisible faces: Dissociating subsystems for facial-information processing. *Current Biology*, 16 (24), 2023–2029, https://doi.org/10.1016/j.cub.2006.08.084

Jiang, Y., Costello, P., & He, S. (2007). Processing of Invisible Stimuli. *Psychological Science*, 18(*4*), 349–355. https://doi.org/10.1111/j.1467-9280.2007.01902.x

Johnston, A., & Clifford, C.W.G. (1995). Perceived motion of contrast-modulated gratings: Predictions of the multi-channel gradient model and the role of full-wave rectification. *Vision Research*, 35(*12*), 1771–1783.

Kang, M.S. (2009). Size matters: A study of binocular rivalry dynamics. *Journal of Vision*, 9(*1*), 1-11. https://doi.org/10.1167/9.1.17

Kang, M.S., Blake, R., & Woodman, G. F. (2012). Semantic analysis does not occur in the absence of awareness induced by interocular suppression. *The Journal of Neuroscience*, 31(*38*), 13535–13545. https://doi.org/10.1523/JNEUROSCI.1691-11.2011

Kaunitz, L. N., Fracasso, A., Skujevskis, M., & Melcher, D. (2014). Waves of visibility: Probing the depth of inter-ocular suppression with transient and sustained targets. *Frontiers in Psychology*, 5, 1-10. https://doi.org/10.3389/fpsyg.2014.00804.

Kelly, D.H. (1979). Motion & vision. II. Stabilized spatio-temporal threshold surface. *Journal of the Optical Society of America*, 69(*10*), 1340-1349.

Kido, K., & Makioka, S. (2013). Priming effects under continuous flash suppression: An examination on subliminal bottom-up processing. *Japanese Psychological Research*, 56(*2*), 126-138. https://doi.org/10.1111/jpr.12034

Kim, C. Y., & Blake, R. (2005). Psychophysical magic: Rendering the visible "invisible." *Trends in Cognitive Sciences*, 9(8), 381–388. https://doi.org/10.1016/j.tics.2005.06.012.

Kim, H., Kim, C., Blake, R. (2017). Monocular perceptual deprivation from interocular suppression temporarily imbalances ocular dominance. *Current Biology,* 27, 884-889. http://dx.doi.org/10.1016.j.cub.2017.01.063

Knapen, T., Pearson, J., Brascamp, J., van Ee, R., & Blake, R. (2008). The role of frontal areas in alternations during perceptual bistability. *Journal of Vision*, 8(*6*), 254. https://doi.org/10.1167/8.6.254

Knill, D.C., & Pouget, A. (2004). The Bayesian brain: the role of uncertainty in neural coding and computation. *Trends in Neurosciences,* 27(*12*), 712-719. https://doi.org/10.1016/j.tins.2004.10.007

Kovács, I., Papathomas, T., Yang, M., & Fehér, A. (1996). When the brain changes its mind: Interocular grouping during binocular rivalry. *PNAS*, 93(26), 15508–15511.

Kreiman, G., Fried, I., & Koch, C. (2002). Single-neuron correlates of subjective vision in the human medial temporal lobe. *PNAS*, 99, 8378–8383. https://doi.org/10.1073/pnas.072194099

Kunst-Wilson, W.R., & Zajonc, R.B. (1980). Affective discrimination of stimuli that cannot be recognized. *Science*, 207, 557–558.

Kveraga, K., Boshyan, J., & Bar, M. (2007). Magnocellular projections as the trigger of top-down facilitation in recognition. *The Journal of Neuroscience*, 27(*48*), 13232-13240. https://doi.org/10.1523/JNEUROSCI.3481-07.2007

Lago-Fernández, L. F., & Deco, G. (2002). A model of binocular rivalry based on competition in IT. *Neurocomputing*, 44–46, 503–507. https://doi.org/10.1016/S0925-2312(02)00408-3

Laing, C.R., & Chow, C.C. (2002). A spiking neuron model for binocular rivalry. *Journal of Computational Neuroscience*, 12(*1*), 39–53. https://doi.org/10.1023/A:1014942129705

Lee, S.H., & Blake, R. (2004). A fresh look at interocular grouping during binocular rivalry. *Vision Research*, 44, 983–991. https://doi.org/10.1016/j.visres.2003.12.007

Legge, G.E. (1979). Spatial frequency masking in human vision: Binocular interactions. *Journal of the Optical Society of America,* 69, 838-847.

Lehky, S.R. (1988). An astable multivibrator model of binocular rivalry. *Perception,* 17(*2*), 215-228.

Leopold, D., & Logothetis, N. (1996). Activity changes in early visual cortex reflect monkeys' percepts during binocular rivalry. *Nature*, 379(*6565*), 549–553.

Levelt, W.J.M. (1965). *On binocular rivalry.* (Doctoral dissertation). Institute for Perception RVO-TNO, Soesterberg, Netherlands.

Ling, S., & Blake, R. (2010). Suppression during binocular rivalry broadens orientation tuning. *Psychological Science*, 20(*11*), 1348-1355. https://doi.org/10.1111/j.1467-9280.2009.02446.x

Liu L., Tyler C.W., & Schor, C.F. (1992). Failure of rivalry at low contrast: Evidence of a suprathreshold binocular summation process. *Vision Research*, 32, 1471-1479.

Liu, C.S., Bryan, R.N., Miki, A., Woo, J.H., Liu, G.T., & Elliot, M.A. (2006). Magnocellular and Parvocellular Visual Pathways Have Different Blood Oxygen Level–Dependent Signal Time Courses in Human Primary Visual Cortex. *American Journal of Neuroradiology*, 27(*8*), 1628-1634.

Livingstone, M., & Hubel, D. (1988). Segregation of form, color, movement, and depth: anatomy, physiology, and perception. *Science*, 240(*4853*), 740–749. https://doi.org/10.1126/science.3283936

Logothetis, N.K., Leopold, D.A., & Sheinberg, D. L. (1996). What is rivalling during binocular rivalry? *Letters to Nature*, 380, 621–624.

Ludwig, K., & Hesselmann, G. (2015). Weighing the evidence for a dorsal processing bias under continuous flash suppression. *Consciousness and Cognition*, 35, 251–259,https://doi.org/10.1016/j.concog.2014.12.010.

Lumer, E.D., Friston, K., & Rees, G. (1998). Neural correlates of perceptual rivalry in the human brain, *Science*, 280, 1930-1934.

Lunghi, C., Lo Verde, L., & Alais, D. (2017). Touch accelerates visual awareness. *i-Perception*, 8(*1*), 1-14. https://doi.org/10.1177/2041669516686986

Lunghi, C., Morrone, M.C., & Alais, D. (2014). Auditory and tactile signals combine to influence vision during binocular rivalry. *The Journal of Neuroscience,* 34(*3*), 784-792. https://doi.org/10.1523/JNEUROSCI.2732-13.2014

Macknik, S.L., & Livingstone, M.S. (1998). Neuronal correlates of visibility and invisibility in the primate visual system. *Nature Neuroscience*, 1(*2*), 144-149. https://doi.org/10.1038/393

Macknik, S.L., Martinez-Conde, & S., Haglund, M.M. (2000). The role of spatiotemporal edges in visibility and visual masking, *PNAS*, 97(*13*), 7556-7560. https://doi.org/10.1073/pnas.110142097

Macknik, S.L., & Martinez-Conde, S. (2007). The role of feedback in visual masking and visual processing. *Advances in Cognitive Psychology*, 3(*1*), 125-152. https://doi.org/10.2478/v10053-008-0020-5

Maehara, G., Huang, P., & Hess, R. F. (2009). Importance of phase alignment for interocular suppression. *Vision Research*, 49(*14*), 1838–1847, https://doi.org/10.1016/j.visres.2009.04.020.

Mamassian, P., & Goutcher, R. (2005). Temporal dynamics in bistable perception. *Journal of Vision*, 5, 361-375. https://doi.org/10.1167/5.4.7

Maier, A., Wilke, M., Aura, C., Zhu, C., Ye, F. Q., & Leopold, A. (2008). Divergence of fMRI and neural signals in V1 during perceptual suppression in the awake monkey. *Nature Neuroscience*, 11(*10*), 1193–1200, https://doi.org/10.1038/nn.2173

McDougall, W. (1901). On the seat of the psycho-physical processes. *Brain*, 24, 579-630. https://doi.org/10.1093/brain/24.4.579

Meissirel, C., Wikler, K. C., Chalupa, L. M., & Rakic, P. (1997). Early divergence of magnocellular and parvocellular functional. *PNAS*, 94, 5900–5905.

Meng, M., & Tong, F. (2004). Can attention selectively bias bistable perception? Differences between binocular rivalry and ambiguous figures. *Journal of Vision*, 4(*7*), 539–551. https://doi.org/10.1167/4.7.2

Merigan, W. H., & Maunsell, J. H. (1993). How parallel are the primate visual pathways? *Annual Review of Neuroscience*, 16, 369–402. https://doi.org/10.1146/annurev.ne.16.030193.002101.

Miles, W. R. (1930). Ocular dominance in human adults. *The Journal of General Psychology*, 3(*3*), 412–430. https://doi.org/10.1080/00221309.1930.9918218.

Milner, A. D., & Goodale, M. A. (2008). Two visual systems re-viewed. *Neuropsychologia*, 46, 774–785. https://doi.org/10.1016/j.neuropsychologia.2007.10.005

Mishkin, M., Ungerleider, L. G., & Macko, K.A. (1983). Object vision & spatial vision: Two central pathways. *Trends in Neurosciences*, 6, 414–417. https://doi.org/10.1016/0166-2236(83)90190-X

Moors, P., Hesselmann, G., Wagemans, J., & van Ee, R. (2017). Continuous flash suppression: Stimulus fractionation rather than integration. *Trends in Cognitive Sciences*, 21(*10*), 719–721. https://doi.org/10.1016/j.tics.2017.06.005.

Moors, P., Stein, T., Wagemans, J., & van Ee, R. (2015a). Serial correlations in Continuous Flash Suppression. *Neuroscience of Consciousness*, 2015(*1*), 1–10. https://doi.org/10.1093/nc/niv010

Moors, P., Huygelier, H., Wagemans, J., De-Wit, L., & Van Ee, R. (2015b). Suppressed visual looming stimuli are not integrated with auditory looming signals: Evidence from continuous flash suppression. *i-Perception*, 6 (*1*), 48-62. https://doi.org/10.1068/i0678

Moors, P., Wagemans, J., van Ee, R., de-Wit, L. (2015c). No evidence for surface organization in Kanizsa configurations during continuous flash suppression. *Attention, Perception, & Psychophysics*, 902–914. https://doi.org/10.3758/s13414-015-1043-x

Moors, P., Wagemans, J., & De-Wit, L. (2014). Moving stimuli are less effectively masked using traditional continuous flash suppression (CFS) compared to a moving Mondrian mask (MMM): A test case for feature-selective suppression and retinotopic adaptation. *PLoS ONE*, 9(*5*), 1-10. https://doi.org/10.1371/journal.pone.0098298

Moors, P., Wagemans, J., & de-Wit, L. (2016). Faces in commonly experienced configurations enter awareness faster due to their curvature relative to fixation. *PeerJ,* 4, 1-14. https://doi.org/10.7717/peerj.1565

Moreno-Bote, R., Shpiro, A., Rinzel, J., & Rubin, N. (2010). Alternation rate in perceptual bistability is maximal at and symmetric around equi-dominance. *Journal of Vision*, 10(*1*). 1–18. https://doi.org/10.1167/10.11.1

Morey, R. D., Romeijn, J., & Rouder, J. N. (2016). The philosophy of Bayes factors and the quantification of statistical evidence. *Journal of Mathematical Psychology*, 72, 6–18. https://doi.org/10.1016/j.jmp/2015/11/001

Mueller, T. J. (1990). A physiological model of binocular rivalry. Visual Neuroscience, 4, 63–73.

Mueller, T. J., & Blake, R. (1989). A fresh look at the temporal dynamics of binocular rivalry. *Biological Cybernetics*, 61(*3*), 223–232. https://doi.org/10.1007/BF00198769

Nealey, T. A., & Maunsell, H. R. (1994). Magnocellular and parvocellular contributions to the responses of the neurons in macaque striate cortex. *The Journal of Neuroscience*, 14 (4), 2069–2079.

Necker, L.A. (1832). Observations on some remarkable optical phaenomena seen in Switzerland; and on an optical phaenomenon which occurs on viewing a figure of a crystal or geometrical solid. *The London and Edinburgh Philosophical Magazine and Journal of Science*, 1(*5*), 329–337. https://doi.org/10.1080/14786443208647909

Nguyen, V.A., Freeman, A.W., & Alais, D. (2003). Increasing depth of binocular rivalry suppression along two visual pathways. *Vision Research*, 43(*19*), 2003-2008. https://doi.org/10.1016/S0042-6989(03)00314-6

O'Shea, R.P., Parker, A., La Rooy, D., & Alais, D. (2009). Monocular rivalry exhibits three hallmarks of binocular rivalry: evidence for common processes. *Vision Research,* 49(2009), 671-681. https://doi.org/10.1016/j.visres.2009.01.020

Paffen, C.L.E., Alais, D., & Verstraten, F.A.J. (2005). Center–surround inhibition deepens binocular rivalry suppression, 45(*20*), 2642–2649. https://doi.org/10.1016/j.visres.2005.04.018.

Paffen, C.L.E., te Pas, S.F., Kanai, R., van der Smagt, M.J., & Verstraten, F.A.J. (2004). Center-surround interactions in visual motion processing during binocular rivalry. *Vision Research,* 44(*14*), 1635-1639. http://dx/doi.org/10.1016/j.visres.2004.02.007

Paffen, C.L.E., Tadin, D., te Pas, S.F., Blake, R., & Verstraten, F.A.J. (2006). Adaptive center-surround interactions in human vision revealed during binocular rivalry. .*Vision Research,* 46(*5*), 599–604. https://doi.org/10.1016/j.visres.2005.05.013

Patel, V., Stuit, S., & Blake, R. (2015). Individual differences in temporal dynamics of binocular rivalry and of stimulus rivalry. *Psychonomic Bulletin & Review*, 22(*2*), 476–482. https://doi.org/10.3758/s13423-014-0695-1

Pastukhov, A., & Braun, J. (2011). Cumulative history quantifies the role of neural adaptation in multistable perception. *Journal of Vision*, 11(*10*), 12–12. https://doi.org/10.1167/11.10.12

Pearson, J., & Clifford, C. W. G. (2006). Suppressed patterns alter vision during binocular rivalry. *Current Biology*, 15 (23), 2142–2148, https://doi.org/10.1016/j.cub.2005.10.066.

Pettigrew, J.D., & Miller, S.M. (1998). A 'sticky' interhemispheric switch in bipolar disorder? *Proc Biol Sci*, 265(1411), 2141-2148. https://doi.org/10.1098/rspb.1998.0551

Pettigrew, J. D. (2001). Searching for the switch: Neural bases for perceptual rivalry alternations. *Brain and Mind*, 2, 85–118.

Peyrin, C., Michel, C.M., Schwartz, S., Thut, G., Seghier, M., Landis, T., ..., Vuilleumier, P. (2010). The neural substrates and timing of top-down processes during coarse-to-fine categorization of visual scenes: A combined fMRI and ERP study. *Journal of Cognitive Neuroscience*, 22(*12*), 2768-2780. https://doi.org/10.1162/jocn.2010.21424

Pillai, R. (1939). A study of the threshold in relation to the investigations on subliminal impressions and allied phenomena. *British Journal Educational Psychology*, 9, 97–98.

Platonov, A., & Goossens, J. (2013). Influence of contrast and coherence on the temporal dynamics of binocular motion rivalry. *PLoS ONE*, 8(8), 1-12. https://doi.org/10.1371/journal.pone.0071931

Polonsky, A., Blake, R., Braun, J., & Heeger, D.J. (2000). Neuronal activity in human primary visual cortex correlates with perception during binocular rivalry. *Nature Neuroscience*, 3(*11*), 1153-1159. https://doi.org/10.1038/80676

Purcell, D., Stewart, A., & Stanovich, K. (1983). Another look at semantic priming without awareness. *Perception & Psychophysics*, 34(*1*), 65–71.

Purpura, K., Kaplan, E., & Shapley, R. M. (1988). Background light and the contrast gain of primate P and M retinal ganglion cells. *PNAS*, 85(*12*), 4534–4537. https://doi.org/10.1073/pnas.85.12.4534

Ramachandran, V. S. (1991). Form, motion, & binocular rivalry. *Science*, 251, 950–951.

Reid, R. C., & Alonso, J. M. (1996). The processing and encoding of information in the visual cortex. *Current Opinion in Neurobiology*, 6, 475–480.

Ritchie, K.L., Bannerman, R.L., & Sahraie, A. (2012). The effect of fear in the periphery in binocular rivalry. *Perception,* 41, 1395-1401. https://doi.org/10.1068/p7157

Rouder, J. N., Speckman, P. L., Sun, D., Morey, R. D., & Iverson, G. (2009). Bayesian t tests for accepting and rejecting the null hypothesis. *Psychonomic Bulletin & Review*, 16(*2*), 225–237. https://doi.org/10.3758/PBR.16.2.225

Sakuraba, S., Sakai, S., Yamanaka, M., Yokosawa, K., & Hirayama, K. (2012). Does the human dorsal stream really process a category for tools? *The Journal of Neuroscience*, 32(*11*), 3949-3953. https://doi.org/10.1523/JNEUROSCI.3973-11.2012

Sawatari, A., & Callaway, E. M. (1996). Convergence of magno- and parvocellular pathways in layer 4B of macaque primary visual cortex. *Nature*, 380(*6573*), 442–446. https://doi.org/10.1038/380442a0.

Schiller, P.H., & Smith, M.C. (1966). Detection in metacontrast. *Journal of Experimental Psychology*, 71(*1*), 32-39. https://doi.org/10.1037/h0022617

Seely, J., & Chow, C. (2011). Role of mutual inhibition in binocular rivalry. *Journal of Neurophysiology*, 106(*5*), 2136–2150. https://doi.org/10.1152/jn.00228.2011

Shapley, R. (1990). Visual sensitivity & parallel retinocortical channels. *Annual Review of Psychology*, 41, 635–658. https://doi.org/10.1146/annurev.psych.41.1.635

Sheinberg, D.L. and Logothetis, N.K., (1997). The role of temporal cortical areas in perceptual organization, *PNAS*, 94, 3408-3413.

Shiraishi, S. (1977). A test of Levelt's model on binocular rivalry. Japanese *Psychological Research*, 19(*3*), 129–135.

Shou, T., & Leventhal, A. G. (1989). Organized arrangement of orientation-sensitive cat's dorsal lateral geniculate nucleus. *The Journal of Neuroscience*, 9(*12*), 4287–4302.

Silver, M.A., & Logothetis, N.K. (2007). Temporal frequency and contrast tagging bias the type of competition in interocular switch rivalry. *Vision Research,* 47(*4*), 532-543. https://doi.org/10.1016/j.visres.2006.10.011

Sklar, A.Y., Levy, N., Goldstein, A., Mandel, R., Maril, A., & Hassin, R.R. (2012). Reading and doing arithmetric nonconsciously. *PNAS*, 109(*48*), 19614-19619. https://doi.org/10.1073/pnas/1211645109

Snowden, R. J., Hess, R. F., & Waught, S. J. (1995). The processing of temporal modulation at different levels of retinal illuminance. *Vision Research*, 35(*6*), 775–789.

Solomon, S. G., White, A. J., & Martin, P. R. (1999). Temporal contrast sensitivity in the lateral geniculate nucleus of a New World monkey, the marmoset Callithrix jacchus. *The Journal of Physiology*, 517, 907–917.

Solomon, S.G., Peirce, J.W., Dhruv, N.T., & Lennie, P. (2004). Profound contrast adaptation early in the visual pathway. *Neuron*, 42, 155–162.

Stein, T., & Sterzer, P. (2014). Unconscious processing under interocular suppression: Getting the right measure. *Frontiers in Psychology*, 5, 1-5. https://doi.org/10.3389/fpsyg.2014.00387.

Stein, T., Hebart, M.N., Sterzer, P. (2011). Breaking continuous flash suppression: A new measure of unconscious processing during interocular suppression? *Frontiers in Human Neuroscience*, 5, 1-17. https://doi.org/10.3389/fnhum.2011.00167

Stein, T., Sterzer, P., & Peelen, M.V. (2012). Privileged detection of conspecifics: evidence from inversion effects during continuous flash suppression, *Cognition*, 125(*1*), 64-79. https://10.1016/j.cognition.2012.06.005

Stuit, S. M., Cass, J., Paffen, C. L. E., & Alais, D. (2009). Orientation-tuned suppression in binocular rivalry reveals general and specific components of rivalry suppression. *Journal of Vision*, 9(*11*): 17, 1–15. https://doi.org/10.1167/9.11.17.

Sugie, N. (1982). Neural models of brightness perception and retinal rivalry in binocular vision. *Biological Cybernetics*, 43, 13-21.

Sweeny, T.D., Grabowecky, M., Suzuki, S. (2011). Awareness becomes necessary between adaptive pattern coding of open and closed curvatures. *Psychological Science*, 22(*7*), 943-950. https://doi.org.10.1177/0956797611413292

Tolhurst, D.J., & Movshon, J.A. (1975). Spatial & contrast sensitivity of striate cortical neurons, *Nature,* 257(*5528*), 674-675.

Tomassini, A., Spinelli, D., Jacono, M., Sandini, G., & Morrone, M. C. (2015). Rhythmic Oscillations of Visual Contrast Sensitivity Synchronized with Action. *The Journal of Neuroscience*, 35(*18*), 7019–7029. https://doi.org/10.1523/JNEUROSCI.4568-14.2015

Tong, F., & Engel, S.A. (2001). Interocular rivalry revealed in the human cortical blind-spot representation. *Nature,* 411, 195-199. https://doi.org/10.1038/35075583

Tong, F., Meng, M., & Blake, R. (2006). Neural bases of binocular rivalry. *Trends in Cognitive Science,* 10(*11*), 502-511. https://doi.org/10.1016/j.tics.2006.09.003

Tsuchiya, N., & Koch, C. (2005). Continuous flash suppression reduces negative afterimages. *Nature Neuroscience*, 8(*8*), 1096–1101. https://doi.org/10.1038/nn1500

Tsuchiya, N., Koch, C., Gilroy, L. A., & Blake, R. (2006). Depth of interocular suppression associated with continuous flash suppression, flash suppression, and binocular rivalry. *Journal of Vision*, 6(*10*), 1068–1078. https://doi.org/10.1167/6.10.6.

Ungerleider, L. G., & Haxby, J. V. (1994). "What" & "where" in the human brain. *Current Opinion in Neurobiology*, 4(*2*), 157–165. https://doi.org/10.1016/0959-4388(94)90066-3

van Ee, R. (2009). Stochastic variations in sensory awareness are driven by noisy neuronal adaptation: Evidence from serial correlations in perceptual bistability. *Journal of the Optical Society of America A, Optics, Image Science and Vision*, 26(*12*), 2612–2622. https://doi.org/10.1364/JOSAA.26.002612

Vuilleumier, P., Armony, J., Clarke, K., Husain, M., Driver, J., & Dolan, R. (2002). Neural response to emotional faces with and without awareness: event-related fMRI in a parietal patient with visual extinction and spatial neglect. *Neuropsychologia*, 40(*12*), 2156–66.

Wade, N.J. (1998) A natural history of vision, Cambridge MA: MIT Press.

Watanabe, M., Cheng, K., Murayama, Y., Ueno, K., Asamizuya, T., Tanaka, K., & Logothetis, N. (2011). Attention but not awareness modulates the BOLD signal in the human V1 during binocular suppression. *Science*, 334 (*6057*), 829–831, https://doi.org/10.1126/science.1203161

Whittle, P., Bloor, D. and Pocock, S. (1968). Some experiments on figural effects in binocular rivalry. *Perception & Psychophysics*, 4, 183-188.

Wilke, M., Logothetis, N. K., & Leopold, D. A. (2003). Generalized Flash Suppression of Salient Visual Targets. *Neuron*, *39*, 1043–1052. https://doi.org/10.1016/j.neuron.2003.08.003

Wilke, M., Logothetis, N. K., & Leopold, D. A. (2006). Local field potential reflects perceptual suppression in monkey visual cortex. *PNAS*, 103(*46*), 17507–17512. https://doi.org/10.1073/pnas.0604673103

Wilson, H.R. (2003). Computational evidence for a rivalry hierarchy in vision. *PNAS*, 100(*24*), 14499-14503. https://doi.org/10.1073/pnas.2333622100

Wilson, H.R., Blake, R., & Lee, S.H. (2001). Dynamics of travelling waves in visual perception. *Nature,* 412, 907-910. https://doi.org/10.1038/35091066

Wolfe, J.M. (1984). Reversing ocular dominance and suppression in a single flash. *Vision Research*, 24(*5*), 471–478.

Wolfe, J.M. (1983). Influence of spatial frequency, luminance and duration on binocular rivalry and abnormal fusion of briefly presented dichoptic stimuli. *Perception*, 12, 447-456.

Wunderlich, K., Schneider, K. A., & Kastner, S. (2006). Neural correlates of binocular rivalry in the human lateral geniculate nucleus. *Nature Neuroscience*, 8(*11*), 1595–1602. https://doi.org/10.1038/nn1554

Xu, S., Zhang, S., & Geng, H. (2011). Gaze-induced joint attention persists under high perceptual load and does not depend on awareness. *Vision Research*, 51(*18*), 2048–2056. https://doi.org/10.1016/j.visres.2011.07.023

Yang, E., & Blake, R. (2012). Deconstructing continuous flash suppression. Journal of Vision, 12(*8*), 1-14. https://doi.org/10.1167/12.3.8

Yang, E., Blake, R., & McDonald, J. E. (2010). A new interocular suppression technique for measuring sensory eye dominance. *Investigative Ophthalmology & Visual Science*, 51(*1*), 588–593. https://doi.org/10.1167/iovs.08-3076

Yang, E., Brascamp, J., Kang, M., & Blake, R. (2014). On the use of continuous flash suppression for the study of visual processing outside of awareness. *Frontiers in Psychology,* 5, 1–17, https://doi.org/10.3389/fpsyg.2014.00724

Yang, E., Zald, D.H., & Blake, R. (2007). Fearful Expressions Gain Preferential Access to Awareness During Continuous Flash Suppression. *Emotion*, 7(*4*), 882–886, https://doi.org/10.1037/1528-3542.7.4.882

Yen, C.C.C., Fukuda, M., & Kim, S.G. (2012). BOLD responses to different temporal frequency stimuli in the lateral geniculate nucleus and visual cortex: Insights into the neural basis of fMRI. *NeuroImage*, 58 (1), 82–90. https://doi.org/10.1016/j.neuroimage.2011.06.022.BOLD

Yuval-Greenberg, S., & Heeger, D. J. (2013). Continuous Flash Suppression Modulates Cortical Activity in Early Visual Cortex. *The Journal of Neuroscience,* 33(*23*), 9635–9643. https://doi.org/10.1523/JNEUROSCI.4612-12.2013

Zadbood, A., Lee, S., & Blake, R. (2011). Stimulus fractionation by interocular suppression. *Frontiers in Human Neuroscience*, 5, 1–9, https://doi.org/10.3389/fnhum.2011.00135

Zhu, W., Drewes, J., & Melcher, D. (2015). Continuous flash suppression effectiveness depends on mask temporal frequency. *Journal of Vision*, 15(*12*), 812, https://doi.org/10.1167/15.12.812

Zhu, W., Drewes, J., & Melcher, D. (2016). Time for awareness: the influence of temporal properties of the mask on continuous flash suppression effectiveness *PLOS ONE, 11(*7*),* 1-15. https://doi.org/10.1371/journal.pone.0159206

Zimba, L. D., & Blake, R. (1983). Binocular rivalry and semantic processing: out of sight, out of mind. *Journal of Experimental Psychology. Human Perception and Performance*, 9(*5*), 807–15.